



Fakultät für Medizin

Institut für Virologie

T cell Re-direction against Glypican-3 for Immunotherapy of Hepatocellular Carcinoma

Christina Dargel

Vollständiger Abdruck der von der Fakultät für Medizin der Technischen Universität München zur Erlangung des akademischen Grades eines

Doktors der Naturwissenschaften (Dr.rer.nat.)

genehmigten Dissertation.

Vorsitzender: Univ.-Prof. Dr. D. Busch

Prüfer der Dissertation:

1. Univ.-Prof. Dr. U. Protzer

2. Univ.-Prof. Dr. J. Durner

Die Dissertation wurde am 10.10.2014 bei der Fakultät für Medizin der Technischen Universität München eingereicht und durch die Fakultät für Medizin am 21.01.2015 angenommen.

Meiner Familie und Nils

Table of contents

I	ABSTRACT	I
II	ZUSAMMENFASSUNG	III
III	ABBREVIATIONS	V
1	INTRODUCTION	1
1.1	Hepatocellular Carcinoma	1
1.1.1	Immunotherapeutic Treatment Approaches for HCC	3
1.1.2	GPC3 as Tumour Associated Antigen.....	3
1.2	Adoptive T-cell therapy for Malignant Diseases	5
1.2.1	Re-direction of T cells towards Tumour Associated Antigens	6
1.2.2	Adoptive T-cell Therapy Using Allogeneic Tumour-specific T cells	7
1.3	Cytotoxic T cells	10
1.3.1	The T-cell Receptor Complex.....	10
1.3.2	Antigen Presentation by MHC I Molecules	13
1.3.3	CD8 ⁺ T cells Undergo Positive and Negative Selection in the Thymus	14
1.3.4	CD8 ⁺ T cell Activation	15
1.3.5	CD8 ⁺ T cell Differentiation	16
1.3.6	CD8 ⁺ T cell Mediated Cytotoxicity	16
1.4	Aim of the Study	17
2	MATERIALS	19
2.1	Reagents and Chemicals	19
2.2	Buffers and Solutions	21
2.3	Kits.....	22
2.4	Enzymes	23
2.5	Synthetic Oligonucleotides (Primers).....	23
2.6	Peptides	25
2.7	Antibodies	26
2.8	Cytokines	27
2.9	Plasmids	27
2.10	Cell lines	28
2.11	Bacteria Strains.....	28
2.12	Cell Culture Media.....	28
2.13	Mouse Strains	29
2.14	Consumables	29
2.15	Technical Devices	30
2.16	Software.....	30

3	METHODS	31
3.1	Molecular Biological Techniques	31
3.2	Cell Culturing Techniques	35
3.3	Western Blot for Protein Analysis	38
3.4	Flow Cytometry	40
3.5	Allorestricted Stimulation of GPC3-specific T cells	43
3.6	Functional Analysis of Peptide-specific T cells	46
3.7	Analysis and Cloning of TCRs from GPC3-specific T-cell clones	47
3.8	Retroviral TCR Transfer into Human T cells or Jurkat cells	55
3.9	Adoptive Transfer of TCR P1-1 ⁺ T cells <i>In Vivo</i>	56
3.10	Statistical Analysis	57
4	RESULTS	59
4.1	Selection of GPC3 Epitopes for T cell Stimulation	59
4.1.1	Identification of Novel HLA-A2 Restricted GPC3 Peptides Presented by Human Hepatoma Cells	61
4.1.2	Analysis of GPC3 Peptide Binding to HLA-A2	62
4.2	Allorestricted Stimulation of GPC3-specific T cells	63
4.3	Stimulation of HLA-A2 Restricted GPC3₅₂₂-specific T cells with HLA-A2 <i>ivt</i>-RNA Pulsed and GPC3₅₂₂ Peptide Loaded moDC	64
4.4	Stimulation of HLA-A2 Restricted GPC3₃₆₇- and GPC3₃₂₆-specific T cells with Peptide Loaded T2 cells	66
4.5	Stimulation of HLA-A2 Restricted GPC3₃₆₇- and GPC3₃₂₆-specific T cells with <i>ivt</i>-RNA Pulsed moDC	69
4.5.1	Expression of GPC3 and HLA-A2 after <i>ivt</i> -RNA pulsing of moDC	70
4.5.1.1	Cloning of a GPC3 Expression Construct	70
4.5.1.2	Expression of GPC3 and HLA-A2 after <i>ivt</i> -RNA Electroporation of K562 cells	71
4.5.1.3	Maturation and GPC3 and HLA-A2 <i>ivt</i> -RNA Electroporation of DC	73
4.5.2	Stimulation of HLA-A2 Restricted GPC3-specific T cells with <i>ivt</i> -RNA Pulsed moDC	74
4.5.2.1	Isolation of Multimer Sorted GPC3-specific T-cell Clones	74
4.5.2.2	Isolation of CD137 Sorted GPC3-specific T-cell Clones	80
4.6	TCR Identification, Cloning, and Expression in Human T cells	83
4.6.1	Expression and Functionality of TCRs Isolated from GPC3 ₃₂₆ - and GPC3 ₃₆₇ -specific T-cell clones	85
4.6.2	Optimization of P1-1 for Expression in Human T cells	88
4.7	Functionality of TCR P1-1 <i>In Vitro</i> and <i>In Vivo</i>	90
4.7.1	Peptide Specificity and Cross-Reactivity of TCR P1-1 Grafted T cells	90

4.7.2	Effective Killing of HLA-A2 ⁺ GPC3 ⁺ Human Hepatoma Cells by TCR P1-1 Grafted CD8 ⁺ T cells	93
4.7.3	TCR P1-1 Can Retarget CD8 ⁺ but not CD4 ⁺ T cells Towards GPC3 ⁺ HLA-A2 ⁺ Tumour Cells	94
4.7.4	Adoptive Transfer of P1-1 ⁺ T cells Suppresses Tumour Growth in an <i>In Vivo</i> HCC Model	96
5	DISCUSSION	99
5.1	Selection of GPC3 as Target for Adoptive T-cell therapy of HCC	99
5.2	Stimulation of Allorestricted GPC3-specific T cells.....	101
5.2.1	Specificity and Functionality of GPC3-specific T-cell clones.....	103
5.3	TCR Identification and Optimization	104
5.4	Re-direction of Donor T cells towards GPC3 by TCR P1-1.....	107
5.4.1	Peptide Specificity, Avidity and Cross-reactivity of TCR P1-1	107
5.4.2	TCR P1-1 Re-directs CD8 ⁺ T cells to Kill Human Hepatoma Cells <i>In Vitro</i>	109
5.4.3	TCR P1-1 in CD8 ⁺ and CD4 ⁺ T cells	109
5.5	Functionality of TCR P1-1 <i>In Vivo</i>	111
5.6	Possible Therapeutic Applications of TCR P1-1	112
5.7	Bypassing HCC Induced Immune Tolerance.....	113
5.8	Conclusion	114
6	REFERENCES.....	117
7	ACKNOWLEDGEMENTS	127
8	APPENDIX.....	129
8.1	Mass spectra of GPC3₃₆₇ and GPC3₃₂₆	129
8.2	Methods for mass spectroscopic analysis of immune-affinity purified HLA-I complexes	131
8.3	Vector maps.....	133
8.4	Curriculum Vitae	135

I Abstract

Hepatocellular carcinoma (HCC) represents the third most common cause of cancer related death worldwide with nearly 800,000 cases per year. Although numerous efforts had been employed during the last years, effective treatments are still not available. A new therapeutic approach is the adoptive T-cell therapy of HCC. Glypican-3 (GPC3) as a tumour associated antigen is expressed in ~75% of all HCC but not in healthy human liver or other organs. Therefore, our goal was to generate cytotoxic T lymphocytes, which are capable of recognizing and eliminating GPC3-expressing tumour cells.

Immunodominant epitopes for GPC3 have not been described sufficiently. In the present study we used mass spectrometric analysis to obtain a comprehensive HLA I peptidome from a GPC3⁺ HLA-A2⁺ hepatoma cell line. Two HLA-A2 bound GPC3 peptides were identified, namely GPC3₃₂₆ and GPC3₃₆₇. These results enabled us to target GPC3 epitopes that are presented on GPC3 positive HCC cells.

To isolate tumour reactive high avidity T cells, an allo-restricted stimulation approach was used. For stimulation of naïve T cells, autologous dendritic cells were co-transfected with GPC3 and HLA-A2 RNA and used as antigen presenting cells. T cells from the naïve T cell repertoire of HLA-A2 negative donors were co-cultured with and expanded on these HLA-A2⁺ GPC3⁺ DC. After two weeks, MHC streptamer-positive CD8⁺ T cells specific for both targeted GPC3 epitopes were detected (<1%). We were able to enrich these cell populations further to 20% A2-GPC3₃₂₆ - and 61% A2-GPC3₃₆₇ multimer positive T-cell lines and grew T-cell clones from them. In a co-culture with GPC3 peptide loaded T2 cells we identified T-cell clones displaying specific effector function by IFN γ secretion. Functional T-cell clones showed strong A2-GPC3 multimer binding.

We have identified and cloned a T-cell receptor sequence from these T-cell clones. The functionality of the isolated TCR P1-1 towards human hepatoma cells was subsequently investigated *in vitro* and *in vivo*. T cells engrafted with the GPC3 specific TCR P1-1 showed strong A2-GPC3 multimer binding. When co-cultured with GPC3 peptide loaded target cells or HLA-A2⁺ GPC3⁺ HepG2 cells, TCR P1-1 transduced T cells secreted IFN γ . Furthermore cytotoxicity was shown by killing of nearly 100% of HepG2 cells. Finally killing of HepG2 cells was confirmed *in vivo* in a murine transplantation model. GPC3-directed T-cell therapy shows great promise for the treatment of HCC.

II Zusammenfassung

Das hepatozelluläre Karzinom (HCC) ist der häufigste primäre Lebertumor und stellt eine der wichtigsten tumorassoziierten Todesursachen dar. HCC ist weltweit die fünfthäufigste Krebsart und die dritthäufigste tumorassoziierte Todesursache mit steigender Inzidenz. Eine Heilung des HCC bietet lediglich die chirurgische Entfernung des Tumors durch eine Leberteilresektion oder die orthotope Lebertransplantation. Diese Ansätze sind jedoch frühen HCC Stadien vorbehalten und bergen das Risiko einer HCC-Rekurrenz.

Ein neuer Therapieansatz, der in der vorliegenden Arbeit untersucht wurde, ist die Immuntherapie durch den adoptiven Transfer von T-Zellen, die in der Lage sind Tumorantigene zu erkennen und maligne Zellen zu eliminieren. Da eine Infiltration von T-Zellen in HCC-Gewebe zu einer verlängerten Lebenszeit der Patienten geführt hat, kann davon ausgegangen werden, dass ein solcher immuntherapeutischer Ansatz, insbesondere der adoptive Transfer von T-Zellen, sehr vielversprechend ist.

Wie viele Tumore exprimiert auch das HCC tumorassoziierte Antigene auf der Oberfläche. Glypican-3 (GPC3) ist ein Tumorantigen, welches sich als Target für die Immuntherapie des HCC anbietet, da es spezifisch in 75% der HCC exprimiert wird, nicht aber in gesundem Lebergewebe oder anderen gesunden Geweben.

Für eine erfolgreiche T-Zell Stimulation ist die Wahl des T-Zell Epitopes, gegen das sich die T-Zellen richten sollen, sehr entscheidend. Wir konnten mittels massenspektrometrischen Analysen zwei GPC3 Epitope - GPC3₃₂₆ und GPC3₃₆₇ - identifizieren, die im Kontext von HLA-A2 auf humanen Hepatomazellen (HepG2) präsentiert wurden.

In dieser Arbeit wurden T-Zellen eines HLA-A2 negativen Spenders mit GPC3 und HLA-A2 transfizierten dendritischen Zellen stimuliert und expandiert, um HLA-A2 restringierte GPC3 spezifische T-Zellen aus dem HLA-A2 naiven Repertoire zu generieren. T-Zell Klone, die aus den Stimulationsansätzen entstanden, wurden auf ihre Spezifität und Reaktivität hin untersucht und die T-Zell Rezeptor Sequenzen der GPC3-spezifischen Klone wurden analysiert. Wir konnten einen GPC3 spezifischen T-Zell Rezeptor (TCR P1-1) identifizieren und haben diesen in ein optimiertes retrovirales Expressionskonstrukt eingebracht. Nach Transfer von TCR P1-1 in Spenderlymphozyten konnte die GPC3-Epitop-Spezifität sowie Abtötungen von GPC3⁺ humanen Hepatomazellen *in vitro* und *in vivo* bewiesen werden.

III Abbreviations

Abbreviation	
(p)APC	(Professional) antigen presenting cell
AA	Amino acid
AFP	Alpha-fetoprotein
AICD	Activation-induced cell death
Amp	Ampicillin resistance gene
bp	Base pair
BSA	Bovine serum albumine
C	Constant
CD	Cluster of differentiation
cDNA	Covalently closed DNA
CDR	Complementary-determining region
D	Diversity
DC	Dendritic cell
E:T	Effector to target
EGFR	Epidermal growth factor receptor
ELISA	Enzyme-linked immunosorbent assay
EMA	Ethidium monoazide
FACS	Fluorescent activated cell sorting
FCS	Fetal calf serum
GPC3	Glypican-3
GPI	Glycosyl-phosphatidylinositol
GvL	Graft versus leukaemia effect
GvT	Graft versus tumour effect
HBV	Hepatitis B Virus
HCC	Hepatocellular carcinoma
HCV	Hepatitis C Virus
HSCT	Hematopeietic stem cell transplantation
hTCM	Human T cell medium
ICOS	Inducible T cell co-stimulator
ICS	Intracellular cytokine staining
IFN	Interferon
IL	Interleukin
IRES	Internal ribosomal entry site
ITAM	Immunoreceptor tyrosine-based activation motifs
IVIS	In Vivo Imaging System
<i>Ivt</i> -RNA	<i>In vitro</i> transcribed RNA
J	Joining

Abbreviations

kD	Kilo Dalton
LAMP-1	Lysosomal-associated membrane protein 1
LT	Lymphotoxin
LTR	Long terminal repeat
MFI	Mean fluorescence intensity
MHC	Major histocompatibility complex
moDC	Monocytic derived mature DC
NEAA	Non-essential amino acids
P/S	Penicillin / Streptomycin
P2A	'self-cleaving' 2A peptide sequence
PBMC	Peripheral blood mononuclear cells
PD-1	Programmed cell death protein 1
PolyA	Polyadenylation
PRE	Post-transcriptional regulatory element
SCID	Severe combined immunodeficiency
SD	Standard deviation
SDS-PAGE	Sodium dodecyl sulfate polyacrylamide gel electrophoresis
TAA	Tumour associated antigen
TAP	Transporters associated with antigen processing
TCR	T-cell receptor
TCR-SCAN	TCR single cell analysis
TIL	Tumour infiltrating lymphocytes
TNF	Tumour necrosis factor
TRAC	T-cell receptor alpha constant
TRAV	T-cell receptor alpha variable
TRBC	T-cell receptor beta constant
TRBV	T-cell receptor beta variable
T _{reg}	Regulatory T cells
TSA	Tumour-specific antigen
V	Variable
w/o	Without
WB	Western Blot

1 Introduction

1.1 Hepatocellular Carcinoma

Liver cancer represents the fifth most commonly diagnosed cancer and second leading cause of cancer related death in adult men worldwide. In adult women HCC is the ninth most frequently diagnosed cancer and the sixth leading cause of cancer related death (1). The number of annual incidences in 2012 was 780,000 (2). With nearly 750,000 estimated deaths worldwide in 2012 (9.1% of all cancer cases), the number of deaths is almost identical to the incidence, emphasizing the poor prognosis and high fatality rate of this disease (2).

Especially in less developed countries as well as in China liver cancer is a large problem. In 2012, 33% of all worldwide estimated liver cancer cases occurred in less developed countries and alone 50% of all cases and deaths were estimated to occur in China (2) (Figure 1).

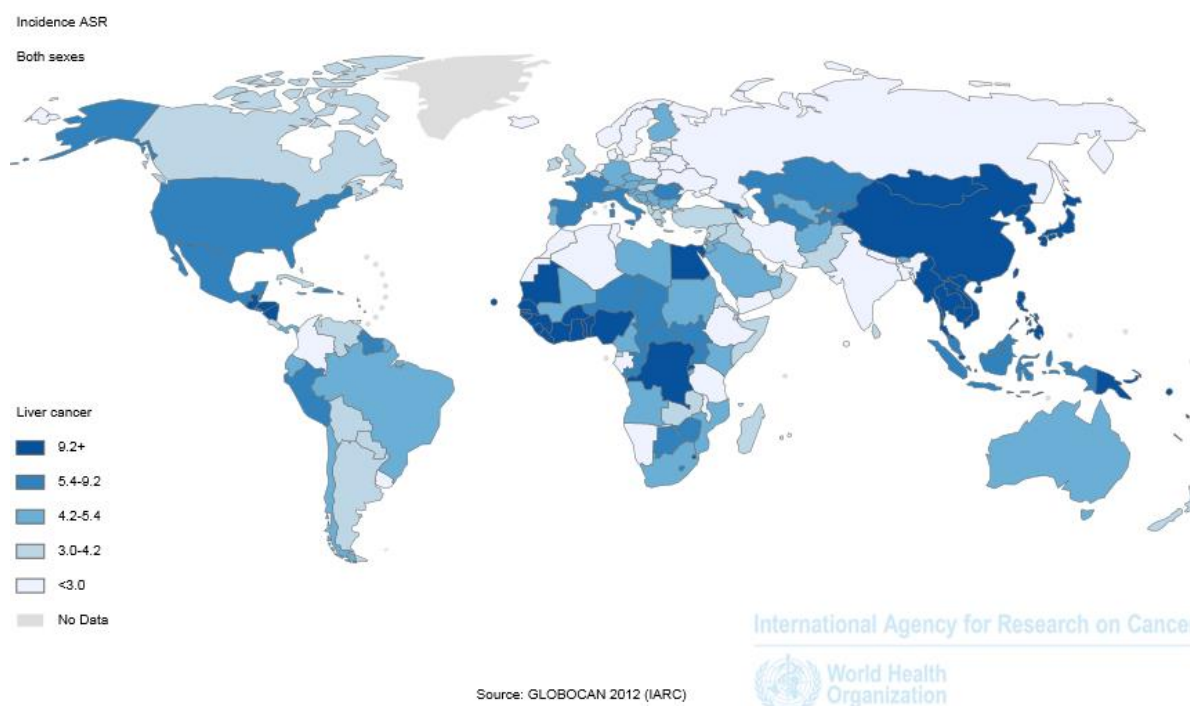


Figure 1 Age standardized worldwide incidence map of live cancer (per 100,000 persons) according to the International Agency for Research on Cancer GLOBOCAN 2012 report (2).

The most frequent histological subtype of liver cancer is hepatocellular carcinoma (HCC), accounting for 70-85% of all primary liver cancers worldwide (1). HCC develops from hepatocytes that become malignant due to mutations causing the cell to replicate at a higher

rate and/or avoid apoptosis. Liver cancer can also develop from other cells within the liver, like for instance cholangiocarcinoma, which is a cancer of the epithelial cells in the bile duct and accounts for approximately 15% of primary liver cancers (3).

Patients with chronic liver diseases such as liver cirrhosis due to chronic hepatitis B virus (HBV) infection and chronic hepatitis C virus (HCV) infection are at high risk to develop HCC. Among patients with liver cirrhosis, HCC remains to be the leading cause of death throughout the world (4). Chronic HBV and HCV infections are estimated to account for 60% and 33% of all HCC cases, respectively (1, 5). In Sub-Saharan Africa and Southeast Asia HCC has become the most common cause for cancer related death due to the high prevalence of HBV and HCV infections in these countries. Over the last years HCC incidences decreased in some of those high-risk areas, due to HBV vaccination programs (6). At the same time HCC incidences in Europe and the USA are on the rise, as a consequence of high numbers of patients with obesity, which leads to high fat diet induced non-alcoholic steatohepatitis (NASH), a form of non-alcoholic fatty liver disease (NAFLD). Today, HCC already is the fastest increasing cancer type in the USA (7). Other risk factors for HCC include alcohol abuse and aflatoxin B1 (AFB) exposure. HCC often is diagnosed only when the patient is already in an advanced stage, adding to the high mortality related to HCC (8).

Although numerous efforts have been employed during the last years, effective treatments are still missing. Common treatment options include tumour resection, liver transplantation, thermal radiofrequency ablation, and transarterial chemoembolization. Up to now, HCC resection and liver transplantation are the most effective therapeutic interventions; however, only feasible for patients with small singular nodules. Chemo- and radiotherapy can only lead to marginal life-span prolongation. The current standard of care for late stage patients is the multi-targeted tyrosin kinase inhibitor sorafenib that inhibits tumour cell proliferation and angiogenesis (7). Nevertheless, sorafenib only leads to a prolonged life time of 3-8 months and therefore must be considered rather a palliative than curative treatment (9, 10). Until today,

the overall 5-year relative survival rate is only 14% (11). Taken together, treatment options for HCC are still very limited and new therapeutic strategies are urgently needed.

1.1.1 Immunotherapeutic Treatment Approaches for HCC

Immunotherapy is considered to be a promising treatment option for HCC. The goal of such a therapy is to induce or boost HCC-specific immune responses. In several previous studies, immune cell infiltration in HCC has been shown to be beneficial for patient survival (12, 13), and especially CD8⁺ T cells have proven crucial for effective anti-tumour responses (14-16). In fact, tumour antigen-specific T cells have been detected in HCC patients. Some of them are directed against tumour associated antigens (TAA) that are expressed in several tumours, such as hTERT (17), MAGE-A1 (18) or NY-ESO-1 (19), but also HCC-specific T cell responses towards alpha-fetoprotein (AFP) (20) or Glypican-3 (GPC3) (21) have been described. However tumour-specific T cells often show only limited functionality as they exhibit an exhausted phenotype (19). In our research group we focused on the development of adoptive T-cell therapy approaches targeting AFP and GPC3, whereby AFP was studied by the former group member Martin Sprinzl and GPC3 was chosen as a target for adoptive T-cell therapy in the present study.

Adoptive T-cell therapy for HCC represents a possible way to boost the anti-tumour immune response and thereby overcome limitations of the patient's immune cells. The therapeutic potential of adoptive T cell transfer has recently been described in a clinical trial, where HCC patients received *in vitro* expanded autologous T cells after HCC resection. HCC recurrence was significantly reduced by 18% after adoptive T-cell therapy has been applied, in comparison to an untreated control group (22).

1.1.2 GPC3 as Tumour Associated Antigen

Like other tumours, HCC express a number of TAA that are potential targets for antigen-specific adoptive T-cell therapy. One of those is GPC3, a 580 amino acid (AA) heparan sulfate proteoglycan that is bound to the cell membrane via a glycosyl-phosphatidylinositol (GPI) anchor (Figure 2 A). The protein is stabilized in its secondary structure by several disulfide

bonds and contains two heparan sulfate chains, located closely to the carboxy-terminus (Figure 2 A). GPC3 is expressed during fetal development, where it facilitates the interaction between growth factors and their receptors (23). In HCC GPC3 stimulates proliferation of hepatoma cells by increasing Wnt signalling (24). The suggested mode of action is that GPC3 increases binding of Wnt to its signalling partner Frizzled, which results in stimulation of β -catenin transcriptional activity and activation of cell cycle proteins such as c-Myc and cyclin D1 (25). It can be hypothesised that HCC cells rely on GPC3 expression in order to continue to grow and therefore loss of GPC3 expression by tumour cells through immunoediting is unlikely, rendering GPC3 a suitable target antigen for adoptive T-cell therapy (21). GPC3 is not expressed in healthy adult tissue, including liver tissue or benign liver lesions, but gets reactivated in ~75% of HCC (26-28) (Figure 2 B). GPC3 expression has been reported to occur in HCC from an early stage on (29). Moreover GPC3 expression in HCC is associated with poor prognosis (30). Altogether we think GPC3 is a very useful candidate TAA to target in adoptive T-cell therapy for HCC. Other TAA expressed in HCC, such as AFP, hTERT or NY-ESO-1 may also be suitable targets for adoptive T-cell therapy of HCC. In a clinical application it is imaginable that T cells recognizing different TAA will be combined according to the TAA expression profile of each individual patient.

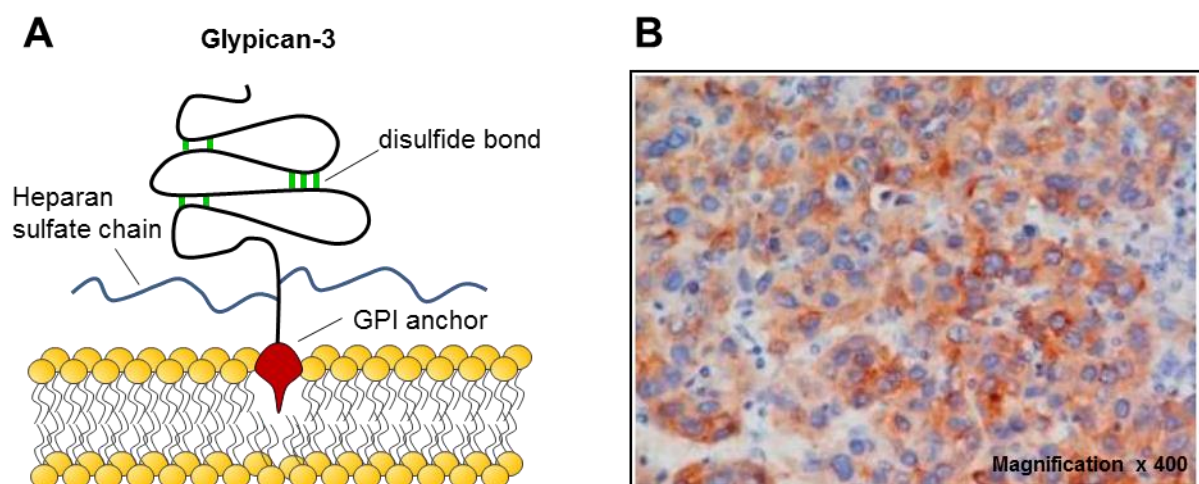


Figure 2 Glypican-3. (A) Schematic illustration of the GPC3 protein bound to the cell membrane by a GPI anchor. Adapted from Filmus et al. (25). (B) Immunohistochemical staining of GPC3 in HCC tissue by Liang et al. (31).

GPC3-targeting immunotherapeutic approaches for HCC that are currently under investigation are peptide vaccination in order to induce cytotoxic T cells (21, 32), a humanized anti-GPC3 monoclonal antibody (33, 34) and a GPC3-specific chimeric antigen receptor (CAR) (35, 36). Usage of anti-GPC3 antibody *in vivo* led to antibody-dependent cell-mediated cytotoxicity (ADCC) in hepatocellular carcinoma cells (34). Phase I clinical studies employing GPC3 peptide vaccinations (37) and the humanized anti-GPC3 monoclonal antibody GC33 (38, 39) have been performed and showed promising outcome, what entailed a currently ongoing phase II study by the same research groups. GPC3-specific T-cell receptors (TCR) as an immunotherapeutic tool for treatment of HCC are not yet described, but may represent a promising therapeutic strategy and are therefore investigated in the present study.

1.2 Adoptive T-cell therapy for Malignant Diseases

An effective immune response is known to play a central role in the control of not only infected but also malignant cells. In the late 19th century William Coley was one of the first to observe a correlation between infection-induced immune responses and patient recovery from cancer by treating patients with a formulation of dead bacteria, called Coley's toxin (40). During the 1960s, Frank Macfarlane Burnet and Lewis Thomas devolved the theory of immune surveillance and cancer control. The concept of immunological surveillance comprises recognition and destruction of potentially malignant cells in a way comparable to recognition of pathogen infected cells by the immune system (41). This theory had been discussed controversially until it was discovered that many cancerous tissues express TAA. These TAA are not at all or only negligibly weak expressed in healthy tissue and can be recognized by the immune system (42, 43). Today the crucial role of innate and adaptive immunity in tumour control is widely accepted and utilized in clinical practice.

Although different arms of the immune system, including components of the adaptive as well as innate immune system, are involved in cancer control, cytotoxic T cells represent the key players.

1.2.1 Re-direction of T cells towards Tumour Associated Antigens

T cells can mediate tumour-specific immune responses via recognition of peptides derived from tumour antigens. Two classes of tumour antigens are distinguished, namely tumour-specific antigens (TSA) and TAA. TSA are strictly tumour-specific and can arise from point mutations or viral oncogenes. However, peptide processing and major histocompatibility complex (MHC) binding is thought to be impaired for TSA and thus T-cell activation is not efficient to stimulate an effective response (44).

TAA are only expressed in certain cell types or are highly overexpressed in cancerous tissue compared to healthy tissue, such as HER-2/neu for instance. TAA can also comprise differentiation or germ cell antigens, like tyrosinase or MAGE, respectively (45).

Although anti-tumour immune responses against TSA and TAA may be induced in patients spontaneously, such incidences are exceptional. The goal of anti-tumour immunotherapy is therefore to provoke these responses and thereby specifically eliminate tumour cells, what can effectively be achieved by 'adoptive T-cell therapy'.

One way of adoptive T-cell therapy against cancer is to isolate TAA-specific tumour infiltrating lymphocytes (TIL) directly from the patient, which are expanded *ex vivo* and then re-infused back into the patient. Another approach is the transfer of TAA-specific TCR genes into the patient's lymphocytes utilizing retroviral vectors, hence re-directing the patient's T cells towards TAA. T cells that have been equipped with a TAA-specific TCR are *in vitro* expanded followed by transfusion into the patient.

It has been demonstrated in several studies that virus- or tumour-specific T cells can be stimulated and expanded *in vitro*, rendering them into effective target-specific killer cells that are capable of destroying infected or tumourigenic cells. Patients with EBV (46, 47) and CMV (48, 49) have been treated successfully with adoptive T cell transfer. Autologous TILs that were isolated from melanoma lesions were successfully used to treat melanoma patients (50, 51). Moreover, the therapeutic benefit of TCR gene-modified T cell transfer has been shown in melanoma patients by Morgan et al. (52). TILs from HCC patients have been isolated by

Kawata et al., proving anti-tumour cytotoxicity *in vitro* (53). A potential clinical benefit of HCC-derived TILs has not been investigated so far.

1.2.2 Adoptive T-cell Therapy Using Allogeneic Tumour-specific T cells

Although prolonged survival in melanoma patients treated with autologous TILs has been shown by Dudley and Rosenberg as described above, a broad application of this therapeutic approach is hardly feasible (50, 51). Isolation of sufficient numbers of TILs from tumour specimens is not always possible. Even with sufficient quantity of cells available, tumour reactive high avidity autologous T cells are often exceedingly rare and cannot be obtained from many patients (54). Finally, TIL isolation and *ex vivo* expansion is time consuming and disproportional expensive.

An alternative to the isolation of TILs from tumour tissue is to stimulate tumour reactive T cells *in vitro* and transfer their antigen-specific TCR genes into the patient's T cells. Many TAA are self-proteins and therefore TAA-specific T cells with high functional avidity are deleted from the natural T cell repertoire during negative selection in the thymus as described in more detail in 1.3.3. In order to circumvent this effect that is called central tolerance, T cells can be isolated after allorestricted stimulation using a foreign MHC class I (MHC I) molecule for antigen presentation (Figure 3).

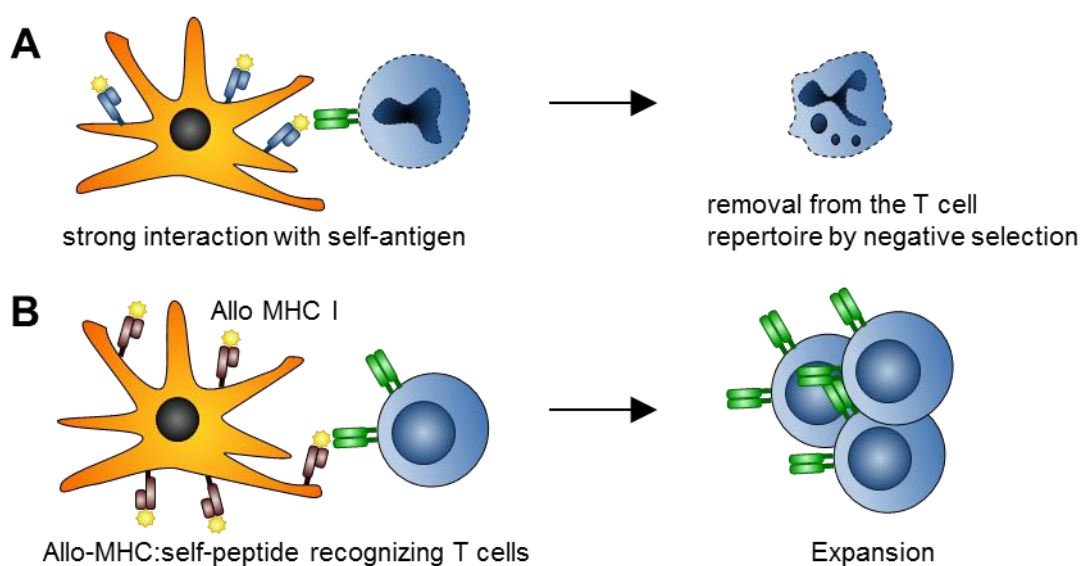


Figure 3 Circumvention of central tolerance by allorestricted T-cell stimulation. (A) Self-peptide:self-MHC restricted T cells are removed from the natural T cell repertoire during T cell development in the thymus by negative selection. (B) When T cells are stimulated against self-peptides in context of allo MHC I, activation and expansion of T cells with high avidity for self-peptides can be achieved.

T cells cannot only recognize self but also other MHC I, more precisely T cells can recognize allelic polymorphism in allogeneic MHC I molecules, a circumstance that is described as alloreactivity. For instance, alloreactivity is utilized by hematopoietic stem cell transplantation (HSCT) in leukaemia patients, where the graft versus leukaemia or tumour effect (GvL or GvT) of allogeneic donor T cells reduces the risk of cancer relapse by effective eradication of tumour cells (55-57). Approximately 1-10% of the natural T cell repertoire are thought to be alloreactive (58) and show similar TCR binding to peptide:foreign-MHC I complexes compared to conventional TCR recognition of peptide:self-MHC I complexes (59).

Stimulation of alloreactive tumour-specific T cells can be achieved utilizing different antigen presenting cells (APC), such as peptide pulsed T2 cells or dendritic cells (DC). A method recently described by Wilde et al. (60) utilizes monocyte-derived mature dendritic cells (moDC), which co-express the desired TAA and MHC I after transfection with *in vitro* transcribed RNA (*ivt*-RNA) (Figure 4). MoDC and CD8⁺ T cells are derived from a donor who is negative for the targeted MHC I, which in the present study is HLA-A2. In context of the TAA peptide:foreign-MHC I complex the T cells are therefore naïve, which allows isolation and expansion of high avidity allorestricted TAA-specific T cells and characterisation of their corresponding TCR gene sequences (60).

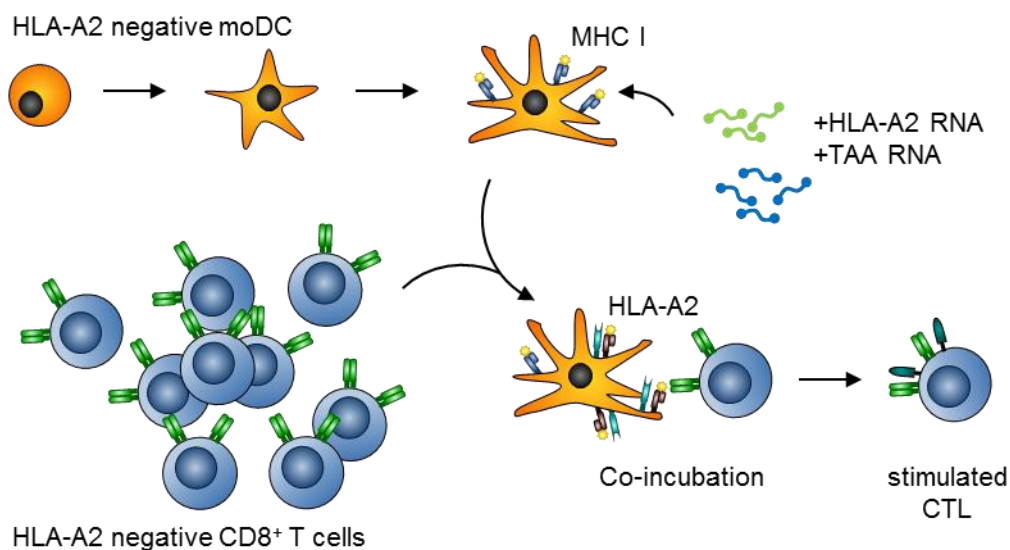


Figure 4 Allorestricted T-cell stimulation. T cells from the HLA-A2 negative repertoire are stimulated with *ivt*-RNA pulsed monocyte-derived mature DC from the same HLA-A2 negative donor.

Another approach to obtain high avidity TAA-specific T cells while circumventing central tolerance is the usage of transgenic mice with human MHC and TCR genes. T cell responses towards TAA can be stimulated in these mice by TAA protein vaccination (61).

With the TCR gene sequence of TAA-specific T cells on hand, the specificity of any donor lymphocytes with appropriate MHC type can be re-directed towards the TAA using TCR gene transfer. This technique allows production of large populations of high avidity TAA-specific T cells that can be used in adoptive T cell therapy.

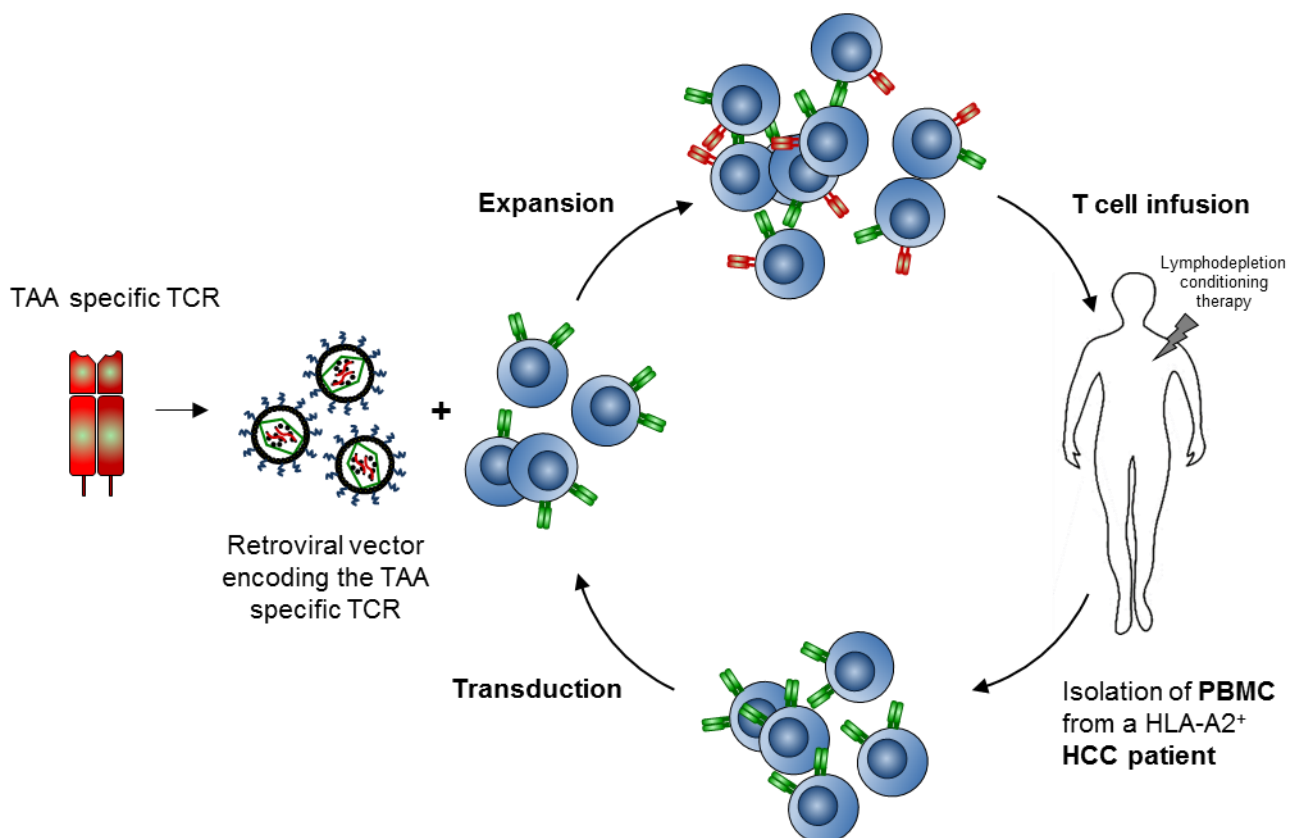


Figure 5 Adoptive T cell transfer. For adoptive T-cell therapy the patient's T cells are isolated, retrovirally transduced with a TAA-specific TCR and *ex vivo* expanded. The TAA re-targeted T cells are then re-infused back into the patient.

For adoptive T cell transfer of allorestricted TAA-specific TCR equipped T cells, fresh peripheral blood mononuclear cells (PBMC) are isolated from the patient and *ex vivo* re-directed towards TAA by retroviral TCR gene transfer. TAA-specific T cells are expanded and their antigen specificity is confirmed *in vitro* before they are transfused back into the patient (Figure 5). In order to improve the therapeutic outcome, patients receive lymphodepletion

conditioning therapy before T cell transfusion, which eliminates regulatory T cells (T_{reg}) and decreases competition of transferred T cells with other T cells for homeostatic cytokines (62). Clinical trials using TCR gene transfer for T cell re-direction towards MART-1 (52, 63), gp100 (63), and NY-ESO-1 (64) report notable success in patients with melanoma. Nevertheless on-target cytotoxicity towards normal tissue has been observed using MART-1- and gp100-specific TCR, underlining the importance of choosing an antigen that is solely expressed in tumour and not in healthy tissue (52, 63).

1.3 Cytotoxic T cells

The adaptive immune response is divided into humoral immune responses mediated by B lymphocytes, and cellular immune responses mediated by T lymphocytes. T cells originate from pluripotent hematopoietic stem cells in the bone marrow and mature in the thymus, for which reason they are called thymus-dependent (T) lymphocytes or simply T cells. T cells are characterised by the ability to express highly variable TCRs that can specifically recognize pathogen infected or malignant cells. They are divided into $CD8^+$ and $CD4^+$ T cells, according to the expression of the co-receptors CD8 or CD4. Among these cell-types, $CD8^+$ T cells have the unique ability to directly recognize malignant or infected cells and subsequently exert appropriate effector functions. Such effector functions include production of cytokines and induction of target cell apoptosis by release of the cytotoxins granzyme and perforin. Induction of apoptosis can additionally be mediated by Fas-Fas ligand interaction. $CD8^+$ T cells recognize peptides only in the context of MHC I molecules that are ubiquitously expressed by all nucleated cells and play a critical role in recognition and control of tumourigenic or infected cells (45).

1.3.1 The T-cell Receptor Complex

A schematic illustration of the TCR complex with all of its components is shown in Figure 6. TCRs belong to the immunoglobulin superfamily and consist of a highly variable $\alpha\beta$ -heterodimer. α - and β -chain each consist of a variable (V) and a constant (C) domain, a hinge region, a transmembrane region and a short intracellular domain. The TCR α - and β -chains

are linked by a disulfide bond. A minority of T cells (1-10%) carries a TCR composed of the alternative $\gamma\delta$ -heterodimer (65). Antigen-recognition properties and functions of these $\gamma\delta$ T cells are not yet fully understood, but a connective function between innate and adaptive immunity has been suggested (66).

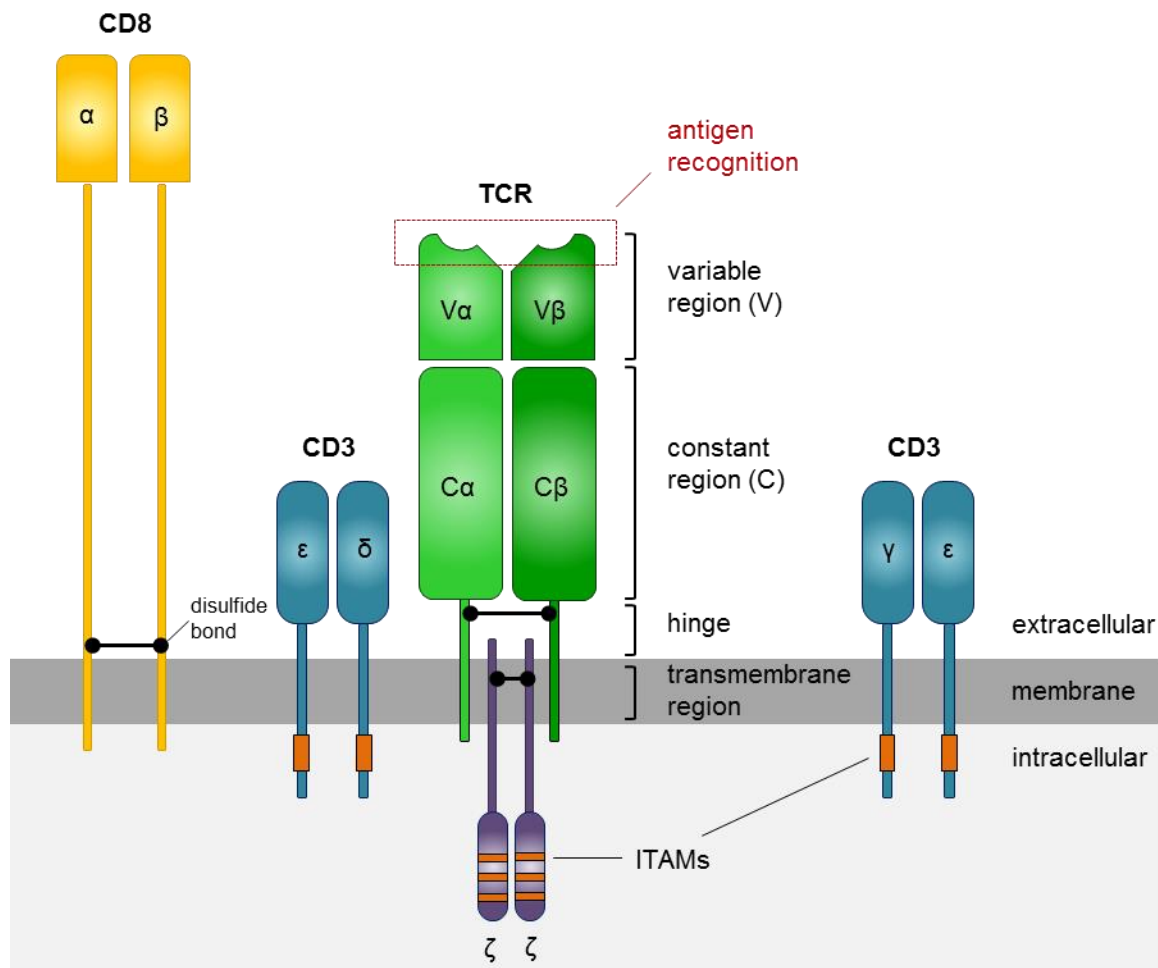


Figure 6 The T-cell receptor complex. The TCR consists of a highly variable $\alpha\beta$ -heterodimer, wherein both chains have a V, C, hinge, transmembrane and short intracellular domain. Antigen-MHC I complex recognition is mediated by the highly variable part of the TCR that is highlighted with a red box. Stability and signal transduction are mediated by the CD3 complex that is formed by a $\epsilon\delta$ - and a $\epsilon\gamma$ -heterodimer. The ζ -chain homodimer plays an important role in signal transduction. Signalling of the complex is mediated via phosphorylation of ITAMs. The CD8 co-receptor is assembled by an $\alpha\beta$ -heterodimer or alternatively an $\alpha\alpha$ -homodimer. Location of ITAMs and disulfide bonds are indicated.

The $\alpha\beta$ -heterodimer is responsible for recognition and binding of peptide-MHC I complexes; however, the dimer itself is not able to signal to the cell that antigen has been recognized. For expression of a functional TCR on the cell surface other molecules are required in addition. One of those is the CD3 complex, assembled of a $\epsilon\delta$ - and a $\epsilon\gamma$ -heterodimer. The CD3 complex stabilizes the $\alpha\beta$ -heterodimer during its transport to the cell membrane and ensures that all

TCRs expressed on the cell surface are properly assembled. The second molecule required for a functional TCR complex is the ζ -chain that exists as a disulfide-linked homodimer (45).

Signalling by the TCR complex is mediated via immunoreceptor tyrosine-based activation motifs (ITAM) within the CD3 complex and the ζ -chain. CD3 ϵ , CD3 δ and CD3 γ each have a single ITAM, the two ζ -chains contain three ITAMs each, which together add up to 10 ITAMs within the TCR complex. Phosphorylation of ITAMs leads to induction of the signalling cascade after antigen recognition (67). Simplified, signal transduction is further mediated by phosphorylated phospholipase C- γ (PLC- γ), which catalyses production of the second messenger inositol 1,4,5-triphosphate (IP₃) and diacylglycerol (DAG). Finally the transcription factors NF κ B, NFAT and AP-1 get activated and induce expression of genes responsible for cell proliferation and differentiation (45).

The CD8 co-receptor is composed of a disulfide-linked $\alpha\beta$ -heterodimer or rarely an α -homodimer. Within the TCR complex, CD8 is responsible for recognition of MHC I. During antigen recognition, CD8 binds to sites of the MHC I molecule that are not involved in peptide-binding.

Each single T cell bears numerous copies of a TCR with unique specificity. The great variety of antigens that can be recognized is owed to billions of lymphocytes that are produced in every individual. The wide range of antigen specificities is due to variations in the amino acid sequence of the antigen binding site of the TCR, which in turn is then highly specific for its antigen. Variety and specificity of TCRs arise from somatic recombination of the TCR gene loci, which takes place during T cell development in the thymus. The TCR α locus consists of 70-80 V, 61 joining (J) and one C gene segments. The TCR β locus contains 2 diversity (D) gene segments in addition to 52 V, 13 J and 2 C gene segments. TCR α and β loci organisation is schematically depicted in Figure 7.

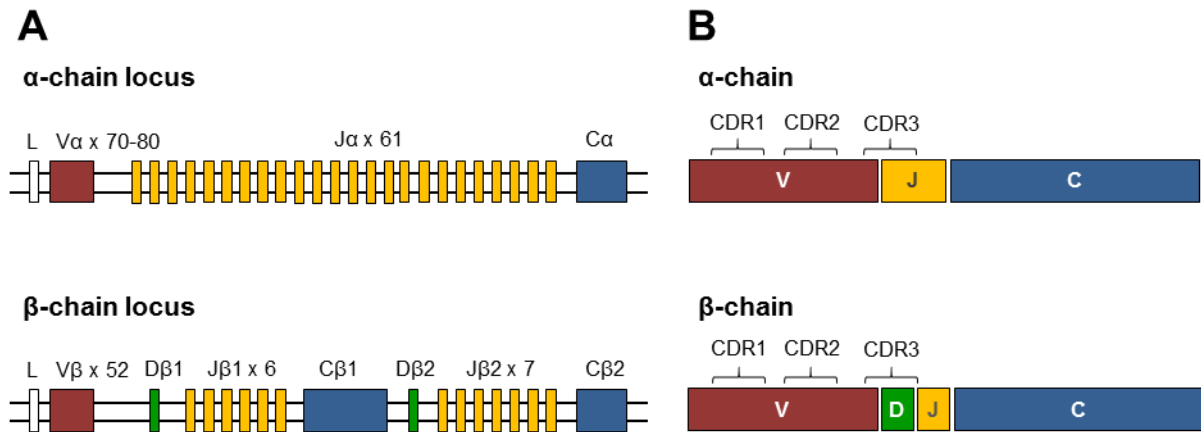


Figure 7 Schematic illustration of TCR α and β gene organisation. (A) Germline organisation of TCR α and β locus. The TCR α locus contains 70-80 V, 61 J and one C gene segments. The TCR β locus consists of 2 D gene segments in addition to 52 V, 13 J and 2 C gene segments. Both precede with an exon encoding the leader sequence (L). (B) Rearranged TCR α and β gene segments. After somatic recombination, α - and β -chains consist of one domain of V, J and C each. The β -chain contains a D domain in addition. CDR1 and CDR2 are incorporated within the variable domain. CDR3 is located at the intersection between V, D and J. The constant domains encode for hinge, transmembrane and intracellular regions. Adapted from Janeway's Immunobiology (45).

The TCR V(D)J gene segments encode the variable TCR domains. The C gene segment translates into hinge, transmembrane and intracellular region. The broad diversity of TCRs is further enhanced by addition of a series of palindromic 'P'- and random N-nucleotides in the junctions between V, D and J gene segments of the rearranged chains (45).

The centre of the MHC I antigen binding site of a TCR is formed by the highly variable complementary-determining region (CDR) 3 that is located at the V(D)J gene junction. The less variable CDR1 and CDR2 regions are located within the V segment and form loops in the periphery of the antigen-binding site, where they interact with the less variable MHC components (45).

1.3.2 Antigen Presentation by MHC I Molecules

Antigen presentation to CD8⁺ T cells is mediated via MHC class I molecules, which are expressed in different levels on all body cells except for red blood cells. MHC I molecules consist of two polypeptide chains, the α -chain and the smaller β_2 -microglobulin chain, which are non-covalently associated with each other. The complete MHC I molecule is composed of four domains. Three of them are formed by the α -chain (α_1 , α_2 , α_3), which also harbours a transmembrane domain. The β_2 -microglobulin chain represents the fourth domain of the MHC I

molecule. The peptide-binding groove of MHC I is formed by α_1 and α_2 and is responsible for the high polymorphism of MHC I molecules that determines their peptide specificity. MHC I molecules bind peptides with 8 to 10 AA in length (68). In Figure 8 TCR binding to a peptide-MHC I complex is shown.

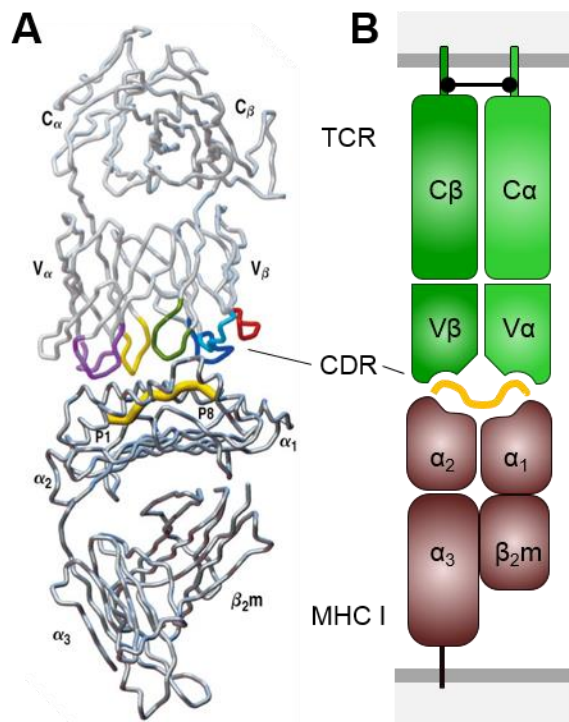


Figure 8 TCR binding to a peptide-MHC I complex. (A) Secondary structure and (B) schematic illustration of the TCR, consisting of variable and constant α - and β -domains that bind to the peptide-MHC I complex. MHC I is composed of three α -chains and one β_2 -microglobulin (β_{2m}). CDR domains of the TCR are indicated in colour. α -chain: CDR1 and 2 in purple; CDR3 in yellow. β -chain: CDR1 and 2 in blue; CDR3 in green. The bound peptide is indicated in yellow. Part (A) adapted from Janeway's Immunobiology (45).

Cytosolic proteins are processed by the proteasome and delivered to the endoplasmic reticulum by transporters associated with antigen processing (TAP), where short fragments of these polypeptides are loaded onto MHC I. Once the peptide is bound to MHC I the complex gets transported to the surface of the cell (45).

On the genetic level, human MHC class I molecules are classified into three human leukocyte antigen (HLA) genes: HLA-A, HLA-B and HLA-C that are encoded by a variety of 414, 728 and 210 different alleles, respectively (45).

1.3.3 CD8⁺ T cells Undergo Positive and Negative Selection in the Thymus

The broad diversity of the TCR repertoire offers the possibility of recognizing millions of infected or tumourigenic cells on the one hand, but also implies the risk of self-peptides being recognized on the other hand. Strong recognition of self-peptides and thereby autoimmunity is prevented by positive and negative T cell selection, which takes place during T cell

development in the thymus. This process by which T cells are rendered non-reactive to self-proteins is called 'central tolerance' (69).

CD4-CD8 double positive T cells are positively selected if they carry receptors that interact with self-peptide:self-MHC complexes and proceed to become mature CD4 or CD8 cells. Only 10-30% of T cells recognize self-peptide:self-MHC complexes with the appropriate affinity and are selected for survival. T cells that interact with self-peptide:self-MHC complexes too strongly undergo apoptosis, a process called 'negative selection'. Both, positive and negative selection, ensure that only T cells that are self-MHC restricted but self-tolerant are released into the periphery, a fraction that accounts for only 5% of the original T cell population (70).

1.3.4 CD8⁺ T cell Activation

The initial activation of naïve CD8⁺ T cells upon first encounter with an antigen is termed priming and requires three signals that are delivered by professional antigen presenting cells (pAPC). The first signal is the antigen-specific TCR-dependent stimulus derived from the interaction of the TCR with its specific peptide-MHC I complex. The second signal required for T cell activation is provided by co-stimulatory molecules, mainly members of the B7 family. B7 is upregulated on pAPC during inflammation or infection. The co-stimulatory receptor for the B7 molecule on the T cell surface is CD28. Signal 2 is required for induction of optimal activation, maintaining viability and preventing anergy of naïve cells. Alternatively to B7, CD70 can provide potent co-stimulatory signals via interaction with members of the TNF family expressed on the T cell surface, such as CD27. On previously activated and effector T cells signal 2 is usually derived from inducible T cell co-stimulator (ICOS) signalling. As a third signal soluble mediators, such as IL12, IL6 or TGF β , are required for sufficient T cell differentiation and activation. After T cells have been activated, proliferation and differentiation is further driven by IL2 that is mainly produced by the T cells themselves (45).

The absence of co-stimulation results in T cell anergy and induction of apoptosis, making it an important factor in avoiding autoimmunity. An anergic T cell is refractory to activation even in presence of the specific antigen, a mechanism termed 'peripheral tolerance' (71).

pAPCs can also deliver inhibitory signalling, for example by binding to PD-1 and CTLA-4, which are upregulated on T cells during their activation. This inhibitory signalling is crucial for maintaining overall T cell homeostasis and tolerance to self-antigens by silencing the specific response (72).

1.3.5 CD8⁺ T cell Differentiation

According to the linear differentiation model naïve T cells are thought to initially differentiate into an effector cell population and subsequently develop into effector memory cells with poor proliferation, but potent functional capacity (73). During their maturation, CD8⁺ T cells undergo four phases. (I) Naïve T cells are primed by mature pAPCs such as dendritic cells (DC), macrophages or B cells, which induce a massive expansion and differentiation of CD8⁺ T cells to effector T cells as described in 1.3.4. (II) Successfully activated T cells expand and differentiate into a population of cells with poor proliferation capacity but strong functionality and high migration capacity. (III) 90-95% of the expanded cells undergo apoptosis in the contraction phase. (IV) 5-10% of CD8⁺ T cells survive the contraction phase to form the memory pool, which can remain stable in number for lifetime and are able to respond faster and stronger upon second antigen re-encounter (45, 73).

1.3.6 CD8⁺ T cell Mediated Cytotoxicity

CD8⁺ T cells are major players in exerting anti-tumourigenic and antiviral activity through cytotoxic as well as non-cytotoxic mechanisms. If effector CD8⁺ T cells encounter their antigen presented on a MHC class I molecule, they bind tightly to the respective target cell and focus the release of effector molecules to the site of target cell binding by rearrangement of the cytoskeleton. They can either directly kill target cells by induction of apoptosis or release of cytokines (45).

The main principle of action of CD8⁺ T cells is the calcium-dependent release of cytotoxic granules that contain perforin, granzyme and granulysin. Perforin delivers the contents of granules into the cytoplasm of the target cell, where granzyme activates apoptosis via BID and pro-caspase-3 cleavage. Granulysin induces apoptosis as well but has antimicrobial function

in addition. Furthermore CD8⁺ T cells act by producing the effector cytokines interferon gamma (IFN γ), tumour necrosis factor alpha (TNF α) and lymphotoxin alpha (LT α). IFN γ can directly inhibit viral replication and induces upregulation of MHC I on target cells. Together, IFN γ , TNF α and LT α can recruit and activate macrophages or directly kill target cells through induction of apoptosis by interaction with TNFR-1 (45). An important anti-tumourigenic role of IFN γ has been suggested in several studies (74-76). Fas-mediated apoptosis is induced via interaction with Fas ligand and is mainly used to regulate lymphocyte numbers. Lymphocytes express both Fas and Fas ligand and can therefore kill one another through activation of caspases, in order to balance proliferation (45).

1.4 Aim of the Study

The aim of this project was to isolate GPC3-specific HLA-A2 restricted T cells for adoptive T-cell therapy of HCC. GPC3 was selected as targeted TAA, because it is expressed in approximately 75% of HCC patients but not in healthy tissues. Additionally, a beneficial outcome in GPC3 targeting immunotherapies has been shown in phase I clinical trials, as described above. HLA-A2 was selected as MHC class I, since HLA-A2 is most frequently (40-50%) expressed in the Caucasian population and described best (77).

In this study, immunodominant epitopes within the GPC3 protein were identified. GPC3-specific T cells were stimulated in an allorestricted fashion, using peptide pulsed T2 cells or peptide / RNA pulsed moDC as described by Wilde et al. (60). T cells that are specific for GPC3 were isolated by A2-GPC3 multimer sorting. GPC3 specificity of expanded monoclonal T-cell clones was investigated by cytokine production and killing of GPC3 expressing target cells. After successful isolation and characterisation of functional T-cell clones, the TCR sequence was analysed and subsequently cloned into a retroviral expression construct. The cloned TCR was then transferred into fresh T cells to evaluate the functionality of transduced T cells *in vitro* and *in vivo*. Using such TCR constructs in order to re-direct T cells towards tumour cells might constitute a promising tool for future therapeutic applications in HCC patients.

2 Materials

2.1 Reagents and Chemicals

Product	Manufacturer
1-Bromo-3-chloropropane	Sigma
Acetic acid	Roth
Acrylamide, linear	Ambion
Acrylamide/ Bisacrylamide (40%)	Roth
Agarose	PeqLab
Aminocaproic acid	Sigma
Ammonium persulfate (APS) (30%)	Sigma
Ampicillin (50 mg/ml)	Roth
Biotin	Sigma
Blasticidine	Gibco
Bovine serum albumin (BSA)	Sigma
Bradford reagent	Sigma
Brefeldin A (1 mg/ml)	Sigma
Bromophenol blue	Roth
Chloroform	Roth
Coelenterazine	PJK
Collagen R	Serva
Complete Protease Inhibitor cocktail (25x)	Roche
Diethylpyrocarbonat (DEPC)	Roth
Dimethyl sulfoxide (DMSO)	Sigma
DNA Smart ladder (1kb)	Eurogentec
dNTP's (25 mM)	Thermo Scientific
Ethanol	Roth
Ethidium monoazide (EMA)	Life Technologies
Ethylenediaminetetraacetic acid (EDTA)	Roth
Fetal calf serum (FCS)	Gibco
Ficoll LSM 1077	PAA
Geneticin	Gibco
Gentamicin (40 mg/ml)	Life Technologies
Glucose	Roth
Glycerol	Roth
Glycin	Roth
Glyoxal Sample Load Dye	Ambion
Heparin sodium 25000	Ratiopharm
HEPES (4-(2-hydroxyethyl)-1-piperazineethanesulfonic acid)	Roth
Histosec® mit DMSO, Paraffinpastillen	Merck Millipore

Materials

Human serum	AG Protzer
Hydrochlorid acid (HCl)	Roth
Isofurane	Abbott Laboratories
Isopropanol	Merck
LB Broth	Sigma
LB Broth with agar	Sigma
L-Glutamin (200 mM)	Gibco
Lipofectamine 2000	Life Technologies
Methanol	Roth
MgCl ₂ (25 mM)	Thermo Scientific
Milk powder	Roth
Non-essential amino acids (NEAA) (100x)	Gibco
Page ruler™ Prestained Protein ladder	Thermo Scientific
Paraformaldehyde (PFA) 4%	Medite
Passive lysis buffer	Promega
PBS VLE	Biochrom
Penicillin / Streptomycin (P/S) (5000 U/ml)	Gibco
Phenol	Roth
Phosphate buffered saline (PBS) 10x	Gibco
Poly-L-lysine	Sigma
Propidiumiodide	Roth
Retronectin (1 µg/µl)	Takara
RNA ladder (0.5 kb- 10 kb)	Invitrogen
Roti®-Safe GelStain	Roth
Sodium chloride (NaCl)	Roth
Sodium dihydrogen phosphate dihydrate	Roth
Sodium dodecyl sulfate (SDS)	Roth
Sodium hydroxide (NaOH)	Roth
Sodium pyruvate (100 nM)	Gibco
Tetramethylethylenediamine (TEMED)	Roth
Tris hydrochloride (Tris HCl)	Roth
Tris-(hydroxymethyl)-aminomethane	Roth
Triton X 100	Roth
Trizol	Life Technologies
Trypan blue	Gibco
Tryptone	Roth
Tween 20	Roth
Versene EDTA	Gibco
VLE PBS	Biochrome
Yeast extract	Roth
β-Mercaptoethanol (50 nM)	Gibco

2.2 Buffers and Solutions

Buffer	Composition
10x Running buffer (WB)	250 mM Tris HCl 2 M Glycin 1% SDS in H ₂ O
4% PFA	4% PFA in 1x PBS
4x SDS loading buffer (WB)	10 ml Glycerol 0,5 M Tris HCl pH 6.8 10% SDS 0.1 g Bromphenol blue 100 µl/ml β-Mercaptoethanol
50x TAE buffer	2 M Tris HCl pH 8.0 50 mM EDTA 2 M Acetic acid in H ₂ O
Anode buffer A1 (WB)	0,3 M Tris HCl 200 ml MetOH in 1 l H ₂ O
Anode buffer A2 (WB)	25 mM Tris 200 ml MetOH in 1 l H ₂ O
Blocking buffer (WB)	5% milk powder in TBS-T
Cathode buffer C (WB)	25 mM Tris HCl 40 mM Aminocapron acid 200 ml MetOH in 1 l H ₂ O
Cell lysis buffer	15 mM Tris HCL 1x complete protease inhibitor cocktail 2.5% glycerol 10% SDS in 1x PBS
DEPC-H ₂ O	0.1% DEPC in H ₂ O
FACS buffer	0.05% BSA in 1x PBS
LB-Agar	15 g Agar 10 g Tryptone 5 g Yeast extract 10 g NaCl in 1 l H ₂ O
Protein lysis buffer	10 mM Tris HCl pH 7.5 150 mM NaCl 2 mM EDTA 0.5% Triton X 100 1x Complete Protease Inhibitor cocktail in 1X PBS
RNA gel electrophoresis buffer	1 mM Sodium dihydrogen phosphate dihydrate

Materials

	in DEPC- H ₂ O
LB medium pH 7.0	10 g Tryptone 5 g Yeast extract 10 g NaCl in 1 l H ₂ O
10x TBS-T buffer pH7.4 (WB)	200 mM Tris 1,4 M NaCl 1% Tween 20 in H ₂ O
0.5 M Tris pH6.8/ SDS (WB)	0.5 M Tris HCl 0.4% SDS in H ₂ O
1.5 M Tris pH8.8/ SDS (WB)	1.5 M Tris HCl 0.4% SDS in H ₂ O

Unless stated otherwise, buffers were prepared in ultrapure H₂O milliQ. The pH was adjusted with HCl or NaOH.

2.3 Kits

Product	Manufacturer
CellTiter-Blue® Cell Viability Assay	Promega
Cytofix/Cytoperm™	Becton Dickinson
Dynabeads® untouched™ human CD8	Invitrogen
ECL Western Blotting Detection	Pierce
ELISA MAX™ Standard Set Human IFN γ	BioLegend
First Strand cDNA Synthesis Kit for RT-PCR (AMV)	Roche
GeneJET Gel Extraction Kit	Thermo Scientific
GeneJET Plasmid Miniprep Kit	Thermo Scientific
IOTest Beta Mark TCR Vbeta Repertoire Kit	Beckman Coulter
mMESSAGE mMACHINE™ T7	Ambion
NucleoBond® Xtra Maxi Kit	Macherey & Nagel
peqGOLD total RNA Kit	peqlab
Phusion® Hot Start Flex Kit	New England Biolabs
Poly(A) Tailing Kit	Ambion
PuReTaq™ Ready-To-Go™ PCR beads	GE Healthcare
QIAquick® Agarose gel extraction Kit	Qiagen
QIAquick® PCR Purification Kit	Qiagen
Rapid Dephosphorylation and Ligation Kit	Roche
RNeasy® Mini Kit	Qiagen
SuperScript® III Kit	Life Technologies

2.4 Enzymes

Product	Manufacturer
AMV Reverse Transcriptase	Roche
<i>BamH I</i>	Life Technologies
<i>Bgl II</i>	Life Technologies
Dnase I	Roche
<i>EcoR I</i>	Life Technologies
<i>Hind III</i>	Life Technologies
<i>Nhe I</i>	Life Technologies
<i>Not I</i>	Life Technologies
Phusion® Hot start II DNA Polymerase	Finnzymes
Proteinase K	Roth
Rnase H	Macherey-Nagel
RNase inhibitor	AMV
T4 DNA Ligase	Life Technologies
Trypsin-EDTA (0.5%)	Gibco

All enzymes were used in combination with the buffers recommended and provided by the manufacturer.

2.5 Synthetic Oligonucleotides (Primers)

All oligonucleotides were synthesized at Life Technologies.

Table 1 Amplification primers used for plasmid construction. Primer concentrations were 10 pmol/μl.

Name	Sequence 5' - 3'
hGlyp3 fw	CATGGCGAACAACAATTTCA
hGlyp3 rev	ACAGCACGATTGAACATGGA

Table 2 Primers used for TCR identification. Primer concentrations were 2.5 pmol/μl.

Name	Sequence 5' - 3'
3'T-Cα	GGTGAATAGGCAGACAGACTTGTCCTGGA
CA2	GTGACACATTTGTTTGAGAATC
CP1	GCACCTCCTTCCCATTAC
P-3'αST	CTTGCCTCTGCCGTGAATGT
P-5'αST	CTGTGCTAGACATGAGGTCT
PANVα1	AGAGCCCAGTCTGTGASCCAG, S = C/G
PANVα1.1	AGAGCCCAGTCRGTGACCCAG, R = A/G
VP1	GCIITKIYTGGTAYMGACA, I = inosine, W = A/T, M = A/C, Y = C/T, K = G/T
VP2	CTITKTWTTGGTAYCIKCAG, I = inosine, W = A/T, M = A/C, Y = C/T, K = G/T

Materials

VPANHUM	TGAGTGTCCCPGAPGG2P, P = A or G; 2 = A, G or T
V α 2	GTTTGGAGCCAACRGAAGGAG
V α 3	GGTGAACAGTCAACAGGGAGA
V α 4	TGATGCTAAGACCACMCAGC
V α 5	GGCCCTGAACATTCAGGA
V α 6	GGTCACAGCTTCACTGTGGCT A
V α 7	ATGTTTCCATGAAGATGGGAG
V α 8	TGTGGCTGCAGGTGGACT
V α 9	ATCTCAGTGCTTGTGATAATA
V α 10	ACCCAGCTGCTGGAGCAGAGCCCT
V α 11	AGAAAGCAAGGACCAAGTGTT
V α 12	CAGAAGGTA ACTCAAGCGCAGACT
V α 13	GAGCCAATTCCACGCTGCG
V α 14.1	CAGTCCCAGCCAGAGATGTC
V α 14	CAGTCTCAACCAGAGATGTC
V α 15	GATGTGGAGCAGAGTCTTTTC
V α 16	TCAGCGGAAGATCAGGTCAAC
V α 17	GCTTATGAGA AACTGCGT
V α 18	GCAGCTTCCCTTCCAGCAAT
V α 19	AGAACCTGACTGCCCAGGAA
V α 20	CATCTCCATGGACTCATATGA
V α 21	GTGACTATACTAACAGCATGT
V α 22	TACACAGCCACAGGATACCCTTCC
V α 23	TGACACAGATTCTGCAGCTC
V α 24	GAAGTGCCTCTTCAATGC
V α 25	ATCAGAGTCCTCAATCTATGTTTA
V α 26	AGAGGGAAAGAATCTCACCATAA
V α 27	ACCCTCTGTTCCCTGAGCATG
V α 28	CAAAGCCCTCTATCTCTGGTT
V α 29	AGGGGAAGATGCTGTCACCA
V α 30	GAGGGAGAGAGTAGCAGT

Table 3 Primers used for TCR amplification and cloning. Primer concentrations were 10 pmol/ μ l.

Name	Restriction cutting site	Sequence 5' - 3'
5' TRAV8-3*01-NotI-Kozak	<i>NotI</i>	CAGGCGGCCGCCACCATGCTCCTGGAGCTTATC
3' TRAC-EcoRI	<i>EcoRI</i>	TGGAATTCTCAGCTGGACCACAGCCGCAGC
5' TRBV30*0.1-NotI-Kozak	<i>NotI</i>	CAGGCGGCCGCCACCATGCTCTGCTCTCTC
3' TRBC_2-EcoRI	<i>EcoRI</i>	TGGAATTCCTAGCCTCTGGAATCCTTTCTC
5'-TRBV9-0.1-NotI-Kozak	<i>NotI</i>	CAGGCGGCCGCCACCATGGGCTTCAGGCTCCTC
5' TCR β NotI Kozak	<i>NotI</i>	TCCCTCTCTCCAAGCTCACT

TCR β rev	-	GCTCGAACAGGGACACCTT
TCR β fw	-	GAAGATCTGAGGAACGTGACC
P2A rev	-	CCGGGGTTCTCTCCACGTC
5'TCR α P2A	-	AAGCAGGCCGGCGACG
TCR α rev	-	TCTGGGGTCTTCAGCTGGT
TCR α fw	-	CCGCCGTGTACCAGCTGAA
EcoRI rev	<i>EcoRI</i>	TGGAATTCTCAGCTGGACCACAGCC

Table 4 Primers used for sequence analysis.

Name	Sequence 5' - 3'
GATC-PrimMP71 fw	GCAGCATCGTTCTGTGTTGT
GATC-PrimMP71 rev	CAGGAAACAGCTATGAC
GATC-T7	TAATACGACTCACTATAGGG
GATC-CMV-F	CGCAAATGGGCGGTAGGCGTG

2.6 Peptides

Name	AA Sequence	Manufacturer
S ₁₇₂	WLSLLVPFV	JPT Peptide Technologies
AFP ₁₅₈	FMNKFIYEI	IBA
10	LVVAMLLSL	P&E
44	RLQPGLKWV	P&E
92	LLQSASMEL	P&E
144	FVGEFFTDV	P&E
155	YILGSDINV	P&E
162	NVDDMVNEL	P&E
169	ELFDSLFPV	P&E
173	SLFPVIYTQ	P&E
186	GLPDSALDI	P&E
206	KVFGNFPKL	P&E
222	SLQVTRIFL	P&E
281	VMQGCMAGV	P&E
295	YWREYILSL	P&E
312	RIYDMENVL	P&E
315	DMENVLLGL	P&E
319	VLLGLFSTI	P&E
326	TIHDSIQYV	IBA
326	TIHDSIQYV	P&E
340	KLTTTIGKL	P&E
367	FIDKKVLKV	IBA
367	FIDKKVLKV	P&E

Materials

383	TLSSRRREL	P&E
404	ALPGYICSH	P&E
451	KMKGPEPVV	P&E
468	HINQLLRMT	P&E
512	GMIKVKNQL	P&E
518	NQLRFLAEL	P&E
550	STFHNLGNV	P&E
554	NLGNVHSPL	P&E
564	LLTSMAISV	P&E
565	LTSMASVV	P&E
571	SVVCFFLV	P&E

2.7 Antibodies

Specificity	Clone	Purpose	Source	Working dilution
A2-AFP ₁₅₈	-	FACS	AG Busch	0.4 µg
A2-GPC3 ₃₂₆	-	FACS	AG Busch	0.4 µg
A2-GPC3 ₃₆₇	-	FACS	AG Busch	0.4 µg
A2-GPC3 ₅₂₂	-	FACS	AG Busch	0.4 µg
CD14-PE	-	FACS	Becton Dickinson	1:100
CD28	-	T cell stimulation	eBiosciences	-
CD3	OKT3	T cell stimulation	AG Kremmer	-
CD3-V500	SP34-2	FACS	Becton Dickinson	1:200
CD4-APC	OKT4	FACS	Becton Dickinson	1:200
CD4-PE/Cy7	OKT4	FACS	ImmunoTools	1:100
CD8 –APC	MEM-31	FACS	Becton Dickinson	1:100
CD80-FITC	-	FACS	Becton Dickinson	1:25
CD83-APC	RPA-T8	FACS	Becton Dickinson	1:25
CD8-PB	DK25	FACS	Dako	1:50
CD8-PE	-	FACS	Becton Dickinson	1:25
GPC3-APC	307801	FACS	R&D	1:20
HLA-A2-FITC	-	FACS	Labgene	1:200
IFN γ -FITC	-	FACS	Becton Dickinson	1:17
IL-2-APC	-	FACS	Becton Dickinson	1:17
mouse- α -GPC3 IgG	8H5	WB	BioMosaics	1:1000
rabbit- α -mouse IgG-HRP	-	WB	Santa Cruz	1:20000
Strep-Tactin APC	-	FACS	IBA	1:50
Strep-Tactin PE	-	FACS	IBA	1:50
TNF α -PE	-	FACS	Becton Dickinson	1:25

2.8 Cytokines

Name	Manufacturer
GM-CSF	Granzyme
IL-15	Peprtech
IL-1 β	R&D
IL-2	Novatis
IL-4	CellGenix
IL-6	CellGenix
IL-7	Promokine
PGE ₂	Pfizer
TNF α	Milteni Biotec

2.9 Plasmids

Plasmid	Description	Antibiotic resistance	Source
pALF10A1 (78)	Murine leukemia virus (MLV) gene of the 10A1 viral envelope (env)	Ampicillin	Kindly provided by Wolfgang Uckert
pcDNA3.1(-)GPC3	Template for GPC3 RNA	Ampicillin	Produced in this work
pcDNA3.1(Hygro)-HLA-A2	Template for HLA-A2 RNA	Ampicillin	Kindly provided by Martin Sprinzl
pcDNA3.1(-)GFP	Template for GFP RNA	Ampicillin	Produced in this work
pcDNA3.1-MLV gag/pol	Gene for group specific antigens and polymerases under CMV promoter (gag-pol)	Ampicillin	Kindly provided by Wolfgang Uckert
pcDNA3-GFP	Template for GFP RNA	Ampicillin	Kindly provided by Richard Klar
pLenti6V5-DEST-Luc	Lentiviral expression vector for Gaussian luciferase	Ampicillin	Kindly provided by Yuchen Xia
pMP71 G _{PRE} (79)	Retroviral expression vector, MPSV-LTR controlled, complemented with mSS and PRE	Ampicillin	Kindly provided by Wolfgang Uckert
pMP71-TCR-S ₁₇₂	Template for murinized constant TCR domains; Mock TCR for T cell transductions	Ampicillin	Kindly provided by Karin Wisskirchen
pMP71-TCR-P1-1	Retroviral expression vector coding for a GPC3-specific TCR	Ampicillin	Produced in this work

2.10 Cell lines

Cell line	Description	ATCC number
HEK 293T	Derivative of human embryonic kidney 293 cells that contains the SV40 T-antigen	CRL-3216
HepG2	Human hepatoma derived cell line	HB-8065
Huh7	Hepatocarcinoma cell line	-
Jurkat	Human T lymphocyte cell line	TIB-152
K562	Human myelogenous leukemia cell line	CCL-243
LCL	Human lymphoblastoid cell line	-
T2 cells	Human T-B-cell hybridoma cell line that is TAP deficient (80)	CRL-1992

2.11 Bacteria Strains

Bacteria	Description	Source
<i>OneShot® STBL3™</i>	<i>E.coli</i> , chemical competent Genotyp: F-mcrB mrrhsdS20(rB-, mB-) recA13 supE44 ara-14 galK2 lacY1 proA2 rpsL20(StrR) xyl-5 λ-leumtl-1 Used for amplification of retroviral plasmids.	Invitrogen
<i>XL-1 blue</i>	<i>E.coli</i> , chemical competent Genotype: recA1 endA1 gyrA96 thi-1 hsdR17 supE44 relA1 lac [F' proAB lacIqZΔM15 Tn10 (Tetr)]. Used for amplification of all other plasmids.	AG Protzer

2.12 Cell Culture Media

Medium	Manufacturer	Composition
DC medium	Biochrom	1.5% HS 50 U/ml P/S in RPMI 1640 VLE
DMEM	Gibco	10% FCS 50 U/ml P/S 2 mM L-Glutamine 1x NEAA 1 mM Sodium pyruvate in DMEM
Freezing medium	-	DMSO 10% in FCS
Human T cell medium (hTCM)	Gibco	10% HS 50 U/ml P/S 2 mM L-Glutamine 1x NEAA 1 mM Sodium pyruvate 0.15% Gentamicin in RPMI Dutch modified
LB-Ampicillin	Sigma	50 µg/ml Ampicillin in LB medium
Opti-MEM	Gibco	-

RPMI	Gibco	10% FCS 50 U/ml P/S 2 mM L-Glutamine 1x NEAA 1 mM Sodium pyruvate in RPMI 1640
Wash medium	Gibco	50 U/ml P/S in RPMI 1640

2.13 Mouse Strains

Mouse strain	Description	Source
SCID/Beige	CB17.Cg-Prkdc ^{scid} Lyst ^{tg-J} /CrI	Charles River

2.14 Consumables

Product	Manufacturer
Nunc™ Cell Culture Treated T75 Flasks with Filter Caps	NUNC
Cell culture flasks, dishes, plates	TPP
Cell strainer 100 µM	BD Falcon
CellStar 12 ml cell culture tubes	Greiner
Cyro vials	Greiner Bio One
Electroporation cuvette	Bio-Rad
ELISA 96 well plates Nunc MaxiSorb	Thermo Scientific
E-plate 96 well culture plate	Roche
FACS 96 well V-bottom plates	Roth
FACS tubes Titertube Micro Test	Bio-Rad
Falcon tubes (15, 50 ml)	BD Falcon
Filter 0.45 µm	StarLab
Freezing device	Nalgene
LUMA plate-96	Perkin Elmer
MACS separation columns	Miltenyi Biotech
Non-tissue culture treated plates (24 well)	Greiner Bio One
Nunc™ 96 well plate, flat-bottom	NUNC
PCR tubes	Thermo Scientific
Pipette tips	TipOne, Greiner Bio One
Pipettes (2, 5, 10, 25, 50 ml)	Greiner Bio One
PVDF membrane	GE Healthcare
Reaction vials (1.5, 2 ml)	Eppendorf, Greiner Bio One
Reagent reservoirs	Corning
Serological pipettes	Greiner
Syringes	Braun
Whatman Filter paper	GE Healthcare

2.15 Technical Devices

Product	Manufacturer
FACS Aria™	Becton Dickinson
Flow Cytometer FACS Cantoll™	Becton Dickinson
Fluorescence microscope Axio Z1	Zeiss
Freezing container	Nalgene
Fusion FX7™	Peqlab
Gelelectrophoresis	Bio-Rad
Gene Pulser Xcell™ Electroporation System	Bio-Rad
Heating block	Eppendorf
High capacity centrifuge 4K15	Sigma
Incubator Cell 150	Heraeus
Irradiation device	Buchler
IVIS Series Pre-clinical In Vivo Imaging System	Perkin Elmer
MACS separator	Miltenyi Biotech
Microcentrifuge 5417R	Eppendorf
MoFlo	Beckman Coulter
NanoVue Plus Spectrophotometer	GE Life Sciences
Counting chamber BLAUBRAND® Neubauer improved	BRAND
SevenEasy™ pH meter	Mettler Toledo
Semi-Dry Blotting Chamber	Bio-Rad
Shaker and incubator for bacteria	Heraeus
Table-top centrifugar 54173	Eppendorf
TECAN Infinite F200 reader	Tecan
Thermocycler T300	Biometra
xCELLigence	ACEA Biosciences

2.16 Software

Product	Manufacturer
FACS Diva™	Becton Dickinson
FlowJo	TreeStar Corp
FUSION-CAPT	Vilber
GeneArt® Gene Synthesis	Life Technologies
GraphPad Prism 5.0	GraphPad Software
i-control™ software	Tecan
Living Image® software	Perkin Elmer
MS Office	Microsoft
RTCA Software 1.2	ACEA Biosciences
Serial cloner	Serialbasics

3 Methods

3.1 Molecular Biological Techniques

3.1.1 Analytical Gel Electrophoresis

3.1.1.1 DNA Gel Electrophoresis

To verify the sizes of PCR products or fragments resulting from restriction digestion, electrophoresis in 1% agarose gels was performed. Gels were prepared using 1x TAE buffer and the fluorescent, DNA-intercalating dye Roti[®]-Safe (3 µl / 100 ml gel) was added for visualization of DNA. The DNA-solution was mixed with loading buffer. 2.5 µl of a 1 kb DNA ladder were used as a mass standard. Electrophoresis was conducted at 100 V for 30 min. After electrophoresis, the gel was analysed and photographed under UV-excitation (312 nm).

3.1.1.2 RNA Gel Electrophoresis

To verify the sizes and quality of isolated or *in vitro* synthesized RNA, electrophoresis in 1% agarose gels prepared with DEPC-H₂O supplemented with 1 mM sodiumphosphat was performed. Agarose gel electrophoresis of RNA requires addition of denaturing agents in order to avoid formation of compact secondary structures, which alter the relation between molecular weight and mobility. For visualization of RNA 3 µl of the nucleic acid intercalating Roti[®]-Safe were added per 100 ml gel. The RNA samples were mixed with glyxacol loading buffer in a 1:1 ratio. In general 1 µl RNA was applied. The RNA-mix was heated up to 50 °C for 30 min and then kept on ice until it was applied to the gel. As a mass standard 3 µl of a 0.5- 10 kb RNA ladder mixed with 3 µl glyxacol loading buffer heated to 50 °C were used. Electrophoresis was conducted at 80 V for 20-30 min. After electrophoresis the gel was analysed and photographed under UV-excitation (312 nm).

3.1.2 DNA Purification from Agarose Gels

Gel electrophoresis was also used to isolate DNA fragments or to clean DNA from other reaction components, such as enzymes, prior to further use. The fragment of interest was excised from agarose gels after electrophoresis with a scalpel and DNA was extracted using

the GeneJET Gel Extraction Kit according to the manufacturer's instructions. DNA was eluted in 30 μl H_2O .

3.1.3 Restriction Enzyme Digestion

Restriction digestions of DNA were performed at 37 °C for 1 h. All enzymes were used with the buffer recommended by the manufacturer. In general, 1 unit enzyme was used to digest 1 μg of DNA. Digestion reactions were always carried out in 20 μl reaction volume. Gel electrophoresis was used for analytical purpose in order to confirm digestion success.

3.1.4 Ligation

For ligations, DNA fragments were combined at a vector to insert ratio of 1:3 under consideration of the different molecular sizes of vector and insert. Concentrations were estimated from agarose gels. 25 μl ligation reactions containing vector (50 ng) and insert (150 ng) DNA, 2 μl T4 DNA ligase (1 U/ μl) and 2.5 μl 10x T4 ligase buffer were incubated at room temperature for 1 h. 10 μl of the ligation reaction mix were used for transformation of 50 μl competent bacteria cells.

3.1.5 Transformation

To generate bacterial clones containing the plasmid of interest, chemical-competent *E.coli* bacteria cells were transformed by heat-shocking. 50 μl chemical-competent bacteria (stored at -80 °C) were thawed on ice and mixed with 10 μl of the ligation mix or 0.05 ng plasmid DNA for re-transformations. After an incubation time of 45 min on ice, bacteria were heat shocked for 2 min at 42 °C and immediately incubated in 1 ml LB-medium without antibiotics for 30 min at 37 °C. The bacteria were then carefully pelleted using a centrifuge (14,000 g, 30 s) and resuspended in a small amount (100 μl) of LB-medium. The bacteria were plated on LB-agar plates containing ampicillin and incubated overnight at 37 °C. All vectors used in this study contained an ampicillin resistance gene that allows for selection of positive clones on agar plates with ampicillin.

3.1.6 Culture of *E.coli*

E. coli (XL-1 blue or STBL3) bacteria were cultured on agar plates or in liquid culture under shaking at 37 °C. Table 5 lists the different culture strategies employed.

Table 5 Culture characteristics used for growth of *E. coli* bacteria.

Culture	Medium	Antibiotic	Volume
After transformation (30 min pre-culture)	LB-Medium	-	1 ml
After transformation (overnight)	LB-Agar-Plates	50 µg/ml ampicillin	-
Analytical plasmid preparation	LB-Medium	50 µg/ml ampicillin	4 ml
High yield plasmid preparation	LB-Medium	50µg/ml ampicillin	50 ml

3.1.7 Isolation of Plasmid DNA for Analytical Purpose (Mini-Prep)

After successful transformation colonies were picked and further cultured in LB-medium containing ampicillin. 4 ml of antibiotic-containing LB-medium were inoculated with bacteria derived from one colony grown on LB-agar plates. Bacteria were cultured overnight in a shaker at 37 °C and 300 g. The next day, 3 ml of the bacteria suspension were pelleted by centrifugation (14,000 g, 1.5 min). Plasmid isolation was conducted using the GeneJET Plasmid Miniprep Kit according to the manufacturer's instructions. Isolated DNA was resolved in 50 µl H₂O and DNA concentration was measured subsequently. A fraction (1 µl) was used for restriction enzyme digestion. If required one positive clone was selected for a larger culture to isolate plasmid DNA for future use.

3.1.8 High Yield Isolation of Plasmid DNA (Midi-Prep)

For high yield plasmid isolation, 50 ml ampicillin-containing LB-medium were inoculated with 5 µl of a bacteria overnight culture. The culture was shaken (300 g) at 37 °C overnight. The next day, bacteria were pelleted by centrifugation (4000 g, 4 °C, and 15 min). Plasmid isolation was conducted using the NucleoBond®Xtra plasmid purification Kit according to the manufacturer's instructions. Isolated DNA was taken up into 100 µl of H₂O. Subsequently DNA concentration was measured.

3.1.9 Determination of DNA or RNA Concentration

DNA or RNA concentrations were photometrically measured and calculated by their adsorption of light at a wavelength of 260 nm against an appropriate reference using the NanoVue spectrophotometer. Concentration was calculated using the following formula:

$$\text{DNA: } c \text{ (mg/ml)} = 50 \text{ mg/ml} \times \text{Measured } A_{260}; \text{ RNA: } c \text{ (mg/ml)} = 40 \text{ mg/ml} \times \text{Measured } A_{260}$$

3.1.10 Sequencing

In order to determine the identity of PCR products or to verify insertion of the correct gene sequence into plasmids, DNA was analysed by commercial sequencing. All DNA sequencing of purified PCR products or plasmid DNA samples was performed by GATC Biotech AG.

3.1.11 *In vitro* RNA Transcription

Capped messenger RNA was *in vitro* synthesized in order to express proteins in mammalian cells after electroporation with *ivt-RNA*. 1 µg linearized plasmid was used as a template. Plasmid DNA linearization with a restriction enzyme downstream of the gene of interest is essential for successful *in vitro* transcription. The T7 polymerase stops transcribing at the end of a template, hence circular plasmid templates would generate extremely long, heterogeneous RNA transcripts. Linearization of pcDNA3.1(-)GPC3 with *EcoRI* and pcDNA3.1(Hygro)-HLA-A2 with *NotI* was confirmed by agarose gel electrophoresis. *In vitro* RNA transcription was performed using the mMACHINE[®] T7 Transcription Kit according to the manufacturer's instruction. A 7-methyl guanosine cap structure was added at the 5' end during the procedure. To further increase RNA stability the *ivt-RNA* was later on polyadenylated employing the poly(A) Tailing Kit according to the manufacturer's instructions. Finally *ivt-RNA* was purified using the RNeasy Mini Kit from Qiagen according to the manufacturer's instructions. RNA was diluted in 33 µl DEPC-H₂O. RNA concentration was determined and RNA was stored at -80 °C.

All reactions were performed on ice and in DEPC-H₂O. DEPC serves as RNase inhibitor by modification of histidine residues in proteins.

3.2 Cell Culturing Techniques

Mammalian cells were cultured under sterile conditions and only handled under a clean hood with laminar air flow. Cell cultures were grown at 37 °C in an incubator with 5% CO₂ atmosphere and 95% humidity.

3.2.1 Culture of Adherent Cell Lines

Adherent cell lines were grown in monolayers in T75 flasks and maintained in 10 ml Dulbecco's modified Eagle's medium (DMEM) supplemented with 10% FCS, 50 U/ml streptomycin / penicillin, 1x non-essential amino acids, 1 mM sodium pyruvate and 2 mM L-glutamine. Once cells reached approximately 90% confluence, they were split at a ratio of 1:10. Medium was removed and cells were washed with PBS. After washing, the monolayer was trypsinised with 0.5 ml trypsin-EDTA solution and incubated at 37 °C for approximately 3 min to detach the cells. 5 ml fresh medium was added to the trypsin-solution and cells were singularized by resuspension. The required amount of cells was transferred into a fresh T75 flask with fresh medium or plated onto cell culture plates.

3.2.2 Culture of Suspension Cell Lines

Suspension cell lines were grown in T75 flasks and were maintained in 10-20 ml RPMI 1640 medium supplemented with 10% FCS, 50 U/ml streptomycin / penicillin, 1x non-essential amino acids, 1 mM sodium pyruvate and 2 mM L-glutamine. Every 3-4 days the cells were split at a ratio of 1:10. The required volume of the cell suspension was removed and replaced with the same volume of fresh medium.

3.2.3 Freezing / Thawing of Cells

For Freezing, cells were pelleted (1600 g, 10 min), resuspended at the desired cell concentration per ml in 1 ml freezing medium (90% fetal calf serum and 10% DMSO) and rapidly aliquoted into 1.5 ml cryovials. The cells were stored at -80 °C in freezing container (Nalgene®) for 24 h to provide the critical 1 °C/min cooling rate required for successful cryopreservation of cells. Cells were then transferred to a nitrogen tank for long-term storage.

Working quickly, cells were thawed in a 37 °C water bath and dispensed into 20 ml of wash media to buffer the toxic effects of DMSO before they were spun down for 10 min at 1600 g in order to wash cells. Subsequently the media was decanted and cells were resuspended in cell culture media. Cells were then ready for counting.

3.2.4 Cell Counting

Cells were counted using trypan blue staining. Trypan blue is a live-dead staining dye used to selectively colour dead cells blue. Trypan blue can only traverse the membrane of dead cells, but not viable cells with intact cell membranes. A 10 µl aliquot of cells was diluted in 10 µl of trypan blue and the viable not coloured cells were counted on a Neubauer improved haemocytometer under a light microscope. Two squares were counted and the cell number was calculated using the following formula:

$$N \text{ (cells/ml)} = \text{mean of two squares} \times \text{dilution factor} \times 10^4$$

3.2.5 Separation of Peripheral Blood Mononuclear Cells from Whole Blood

Venous blood was collected in tubes containing 200 µl of heparin (5000 IU/ml) to avoid coagulation. The blood was diluted with RPMI 1640 medium at a ratio of 1:1, carefully layered onto 15 ml ficoll at a ratio of 2:1 (blood:ficoll) in a 50 ml falcon and centrifuged for 20 min at 1800 g and room temperature without break. The visible PBMC layer was collected with a pipette and transferred into a fresh 50 ml falcon containing 10 ml of RPMI for washing. After two wash cycles, cells were resuspended in human T cell medium for counting.

3.2.6 Generation and Culture of Dendritic Cells

PBMC were isolated by ficoll density gradient centrifugation. Isolated PBMC were resuspended in DC medium at a concentration of 7.5×10^6 cells/ml. 10 ml cell suspension was incubated in a T75 culture flask (NUNC) at 37 °C. After incubation of 1 h, non-adherent cells were carefully removed by washing with VLE PBS. Remaining adherent monocytes were cultured in medium containing 100 ng/ml GM-CSF and 20 ng/ml IL4 for 48 h. On day 3 of

culture, the immature cells were differentiated into moDC by addition of medium containing 10 ng/ml IL-1 β , 15 ng/ml IL-6, 10 ng/ml TNF α and 1 mg/ml PGE₂ for 24 h.

3.2.7 Magnetic Separation of CD8⁺ T cells

CD8⁺ T cells were isolated from whole blood PBMC by negative selection using the Dynabeads® Untouched™ Human CD8 T cell isolation kit from Invitrogen. To isolate untouched CD8⁺ T cells a mixture of biotinylated monoclonal antibodies against the non-CD8⁺ cells was incubated with whole blood PBMC. To deplete the antibody labelled non-CD8⁺ cell fraction MyOne™ SA Dynabeads were added. The bead-bound cells were separated on a magnet and the flow through contained the untouched human CD8⁺ T cells. All steps were carried out under sterile conditions according to the manufacturer's instructions.

3.2.8 Peptide Loading of T2 cells

For exogenous peptide loading 1 x 10⁶ T2 cells were incubated with HLA-A2 restricted peptides in 200 μ l RPMI medium. The incubation was performed in CellStar 12 ml tubes to allow efficient cell-peptide contact. Peptide concentrations ranged from 10⁻⁵ M to 10⁻¹⁰ M. After 2 h of incubation at 37 °C, the cells were washed once with 10 ml RPMI wash medium to remove unbound peptides.

3.2.9 Transfection of Mammalian Cells

3.2.9.1 Lipofectamine Transfection

One to two days prior to transfection, 1 x 10⁶ cells/ well were plated into a 6 well culture dish achieving 70-80% confluency at the time of transfection. Transfection was performed with 10 μ l lipofectamine 2000 according to the standard lipofectamine transfection protocol. In brief, mix A and B were prepared in separate tubes as listed in Table 6, incubated for 5 min at room temperature, mixed and subsequently incubated for 30 min at room temperature. The transfection mix was added drop-wise to the cells and medium was changed 4-6 h post transfection. After 6 h, the medium was replaced with 2 ml fresh culture medium.

Table 6 Solutions used for transfection of mammalian cells with plasmid DNA.

Mix A	Mix B
4 µg DNA in 250 µl serum-free Opti-MEM®	10 µl Lipofectamin™2000 in 250 µl serum-free Opti-MEM®

3.2.9.2 Transfection via Electroporation

K562 cells and DC were transfected by electroporation with *in vitro* transcribed RNA. 3×10^6 cells were resuspended in 200 µl cold Opti-MEM® I Reduced Serum Medium, mixed with 25-50 µg *ivt*-RNA and incubated on ice for 5 min. Electroporation was performed in 4 mm electroporation cuvette at 300 V and 300 µF using the exponential protocol of the Gene Pulser Xcell™ Electroporation System. After pulsing the cells were taken up in 2 ml warm cell culture medium and incubated in a 6 well plate until further use.

3.3 Western blot for Protein Analysis

3.3.1 Preparation of Cell Lysates

For Western blotting (WB), total cell lysates were prepared by addition of 200 µl of protein lysis buffer to 1×10^6 cells and incubation for 20 min on ice. By centrifugation (14,000 g, 5 min) cell debris and nucleic acid were removed. To standardize protein concentrations a Bradford assay has been performed. Each sample was adjusted to contain 30 µg proteins by addition of H₂O. 4x SDS loading buffer was added in 1:4 ratio before the sample was heated at 96 °C for 5 min to denature proteins.

3.3.2 Bradford Assay

The Bradford assay is a colorimetric assay used to measure the concentration of protein in a solution. Cell lysates were diluted 1:5 with PBS and 5 µl of that dilution were mixed with 200 µl of the Bradford reagent. A serial dilution of albumin was used as a standard with final concentrations of 0 (blank), 16, 32, 64, 125, 250, 500, 1000 and 2000 ng/µl to determine the protein concentration. 5 µl of each standard dilution was mixed with 200 µl Bradford reagent. After 5 min of incubation at room temperature absorbance was measured at 595 nm on the Tecan Infinite F200 reader.

3.3.3 SDS-PAGE and Semi-Dry-Transfer of Proteins

For Sodium dodecyl sulphate polyacrylamide gel electrophoresis (SDS-PAGE) samples were applied to the pockets of the stacking gel and proteins were separated at 15 mA (stacking gel) and 30 mA (resolving gel) per gel. Composition of stacking gels and resolving gels are listed in Table 7.

Table 7 Composition of stacking gels and resolving gels for SDS-PAGE

Composition of stacking gel		Composition of resolving gel	
H ₂ O	5 ml	H ₂ O	10.1 ml
0.5 M Tris pH 6.8	2.1 ml	1.5 M Tris pH 8.8	7.7 ml
Acrylamide (40%)	1.5 ml	Acrylamide (40%)	12.9 ml
APS (30%)	84 µl	APS (30%)	96 µl
TEMED	15 µl	TEMED	45 µl

After electrophoresis a PVDF membrane was activated in methanol and equilibrated for 10 min in transfer buffer A1. Two Whatman papers each were incubated for 10 min in transfer buffer A1, A2 and C. Gel and membrane were placed between 4 layers of Whatman paper and into a semi-dry-blotting apparatus. Blotting was performed at 20 V for 60 min.

3.3.4 Detection of Proteins on the Membrane

After blotting, the nitrocellulose membrane was incubated in blocking buffer for 1 h at room temperature. After blocking, the membrane was washed 3 times for 10 min in TBS containing 0.1% Tween (TBS-T). For detection of the acquired protein, the membrane was incubated with primary antibody diluted in blocking buffer for 1 h at room temperature. The membrane was washed three times for 10 min with TBS-T to remove unbound antibody before adding the HRP-conjugated secondary antibody, diluted in blocking buffer for 1 h at room temperature. After repeating the washing steps, the membrane was developed with ECL substrate reagents according to the manufacturer's instructions. Depending on the size of the membrane, 1-2 ml substrate solution was used to cover the membrane. Protein-specific signals were detected using the Fusion FX7™ system. Proteins were analysed for correct molecular weight by comparison with the marker proteins. Applied antibody dilutions are listed in Table 8.

Table 8 Corresponding blocking buffers, primary and secondary antibodies and washing agents.

Blocking solution	Primary antibody (dilution)	Secondary antibody (dilution)	Washing agent
5% Milk in TBS-T	Mouse- α -GPC3 IgG (1:1000)	Rabbit- α -mouse IgG-HRP (1:20000)	TBS-T

3.4 Flow Cytometry

Fluorescent activated cell sorting (FACS) allows for analysis and sorting of cells on a single cell level. By aspiration through a fine needle and hydrodynamic focusing cells successively enter a detection channel, where they pass through a set of laser beams. Analysis of cell size, granularity and protein expression is based on the forward light scatter (FSC), the sideward light scatter (SSC) and the emission of light by laser-activated fluorochromes. The usage of several lasers and different fluorochromes with distinct emission spectra allows for simultaneous analysis of a variety of different markers. Analysis is possible for proteins expressed at the cell surface, as well as intracellular proteins after fixation and permeabilization of the cells. The optical readout from analysed cells is converted to digital information in a detector system and can be visualized and analysed using specific software such as FACS-Diva or FlowJo. Since emission spectra of some fluorochromes show partial overlaps each experiment contained single colour samples for each used fluorochrom. Using single colour samples cells that are truly positive can be defined and instrument settings can be adjusted in order to subtract signal overlaps for each detection channel.

Flow cytometry was conducted on FACS Canto II. Following staining, cells were fixed with PBS + 1% PFA. Samples were acquired on the same day. Lymphocytes were gated from total acquired cells based on the forward and side scatter profile that represents size and granularity respectively (Figure 9).

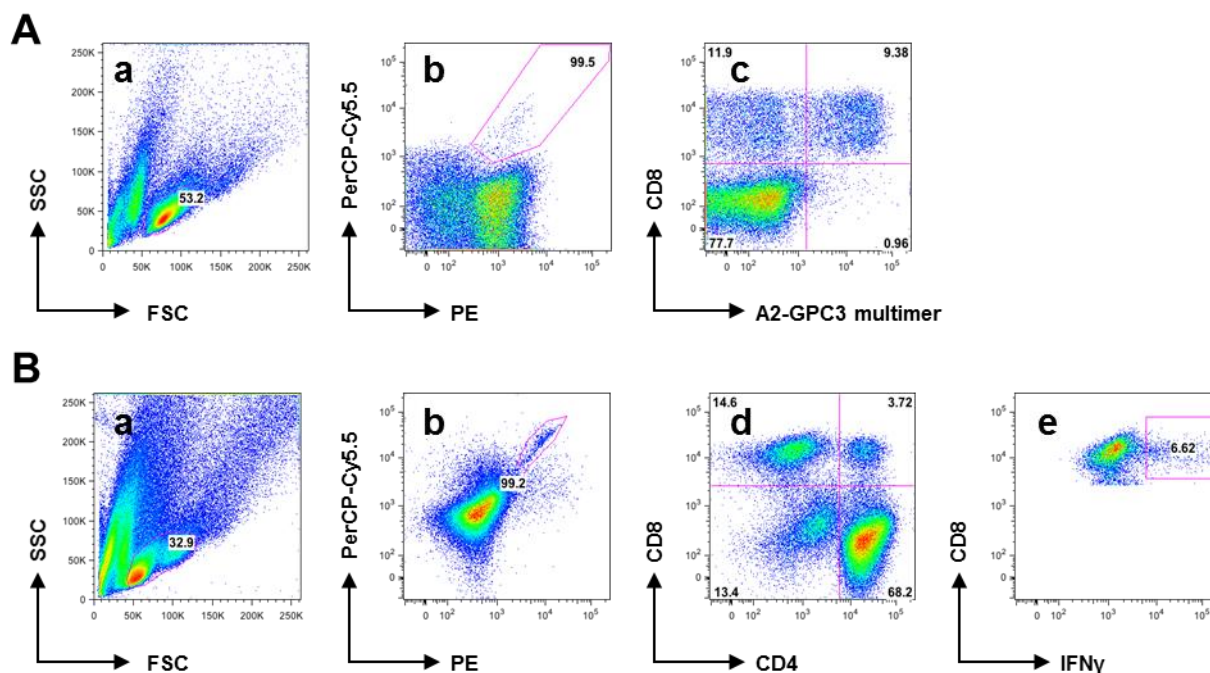


Figure 9 Schematic: FACS-Analysis. Representative gating strategies for MHC I multimer staining of CD8⁺ T cells (A) and ICS (B) are depicted. Lymphocytes were identified by typical FSC/SSC parameters (a), discriminated from dead cells (b: Live Dead-) and then analysed for surface markers (c: CD8, A2-GPC3 multimer; d: CD8, CD4). After ICS cytokine secreting CD8⁺ (e) or CD4⁺ T cells were identified.

3.4.1 Surface Staining

Detection of surface marker expression was performed by using fluorescent labelled antibodies. At most 1×10^6 cells were stained per sample. The cells were washed twice with FACS buffer and subsequently stained with specific fluorescently labelled antibodies for 30 min of ice in the dark. After washing the samples were resuspended in 200 μ l FACS buffer for flow cytometry. To exclude dead cells from the analysis 0.5 μ g/ml propidium iodide (PI) was added immediately before the sample was analysed. Results were analysed using FlowJo.

3.4.2 Multimer Staining and Sorting of Cells

In this study we used MHC streptamers, later on referred to as A2-GPC3 multimers, to stain for specific TCRs. Streptamers are a subgroup of multimers, consisting of MHC I-peptide complexes attached non-covalently to fluorescently labelled Strep-Tactin (Figure 10). The fluorescent complex consists of PE labelled Strep-Tactin and Strep-tag, which is a short peptide sequence with high affinity for the biotin-binding site of its complex partner. After cell sorting the MHC/Strep-Tactin multimer disassembles rapidly in the presence of low

concentrations of biotin, which has a much higher affinity to Strep-Tactin than Strep-tag. The remaining MHC molecules dissociate spontaneously from the T cell surface. Thereby the streptamer approach allows for stable and reversible staining of TCRs with certain specificities and consecutive detection by the fluorescent PE signal.

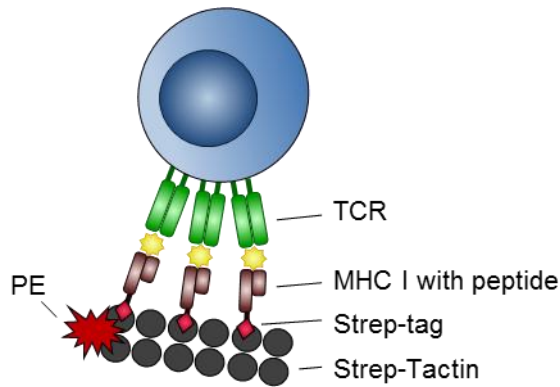


Figure 10 MHC I Streptamer for staining of TCRs with defined epitope specificity. The MHC I-Streptamer consists of MHC I peptide complexes that are linked via Strep-tag to a backbone made of multiple fluorochrom labelled Strep-Tactin molecules.

For multimer staining, at most 1×10^6 cells were stained with $0.4 \mu\text{g}$ PE labelled MHC streptamer for 10 min on ice and in the dark. All streptamer used in this study and the corresponded concentrations are listed in Table 9. Surface antibodies were added directly to the multimer mix and incubated for additional 20 min on ice in the dark. After washing, the samples were resuspended in $200 \mu\text{l}$ FACS buffer for flow cytometry. To exclude dead cells from the analysis $0.5 \mu\text{g/ml}$ PI was added immediately before acquisition on a FACS machine.

Table 9 MHC I streptamer labelling.

A2-multimer	A2-AFP₁₅₈	A2-GPC3₅₂₂	A2-GPC3₃₆₇	A2-GPC3₃₂₆
Concentration	1 $\mu\text{g}/\mu\text{l}$	0.8 $\mu\text{g}/\mu\text{l}$	0.825 $\mu\text{g}/\mu\text{l}$	0.95 $\mu\text{g}/\mu\text{l}$
0.4 μg	0.4 μl	0.5 μl	0.48 μl	0.42 μl
1 μl Strep-Tactin PE				
ad 50 μl FACS Buffer				

For sorting of MHC streptamer positive cells, $5-10 \times 10^6$ cells were stained with multimer and surface antibodies as described above and subsequently sorted on a FACS Aria high-performance instrument. Cells were sorted into human serum supplemented with 1 mM biotin. After a short incubation time to allow disassembling of the Strep-Tactin-Strep-tag complex the cells were centrifuged and resuspended in T cell medium. Sorting of cells on the FACS Aria

was kindly performed by Lynette Henkel (Institut für Medizinische Mikrobiologie, Immunologie und Hygiene, TUM).

3.4.3 Intracellular Cytokine Staining (ICS)

For ICS at least 0.2×10^5 cells were co-incubated with target cells for 5 h. Brefeldin A ($0.2 \mu\text{g/ml}$) was added 1 h after co-incubation was initiated to block secretion of cytokines. Following incubation, cells were stained with $0.5 \mu\text{g/ml}$ EMA for 15 min and upon exposure to light. EMA diffuses into dead cells where it intercalates and covalently binds to DNA. Since EMA does not diffuse into living cells EMA staining allows for exclusion of dead cells. After washing, the cells were stained with surface markers for 20 min on ice and in the dark. Fixation and permeabilization was performed for 20 min at 4°C . Subsequently cells were stained for intracellular cytokines in 1x cytofix/cytoperm buffer for 20 min on ice in the dark. After washing samples were resuspended in PBS + 1% PFA for flow cytometry.

3.5 Allorestricted Stimulation of GPC3-specific T cells

3.5.1 *De novo* Priming of T cells with T2 cells

HLA-A2⁺ T2 cells were loaded with HLA-A2 restricted GPC3 peptides as described above (see 3.2.8). CD8⁺ T cells from an HLA-A2 negative donor were isolated by negative separation with micro beads as described above (see 3.2.7). 1×10^5 peptide loaded, irradiated (35 Gy) T2 cells were used to stimulate 1×10^6 CD8⁺ T cells yielding in an effector to stimulator ratio of 10:1. Stimulation was performed in 24 well cell culture dishes and the cells were kept in T cell medium supplemented with 10 ng/ml IL-7 and 10 ng/ml IL-15 on day 0 and 50 IU/ml IL-2 on day 1 and day 3. Stimulation of CD8⁺ T cells as described above was performed twice (day 0 and day 5) and the cells were ready for sorting and analysis on day 12.

3.5.2 *De novo* Priming of T cells with moDC

Dendritic cells from an HLA-A2 negative healthy donor were prepared as described above (see 3.2.6). MoDC were co-transfected with 25 μg RNA coding for HLA-A2 and 50 μg RNA coding for GPC3 by electroporation (see 3.2.9.2). Autologous CD8⁺ T cells from the same HLA-A2

negative donor were isolated by negative separation with micro beads as described in 3.2.7 on the same day. Immediately after electroporation moDC were co-cultured with CD8⁺ T cells. 1x10⁶ CD8⁺ T cells were incubated with 1x10⁵ *ivt*-RNA loaded moDC per well of a 24 well cell culture dish in T cell medium supplemented with 5 ng/ml IL-7. The effector stimulator ratio was 10:1. Starting 2 days after co-culture, 50 IU/ml IL-2 were added every 2 days. CD8⁺ T cells were restimulated with freshly prepared and transfected moDC after 7 days as described above.

3.5.3 Culturing and Cloning of Peptide-specific Effector CD8⁺ T cells

After 2 weeks of stimulation with *ivt*-RNA loaded moDC, HLA-A2 restricted GPC3-specific CD8⁺ T cells were stained with a PE-conjugated A2-GPC3 multimer and were sorted as described in 3.4.2. CD8⁺ A2-GPC3 multimer positive T cells were either expanded as T-cell lines or cultured after limiting dilution in 96 well plates. For T-cell lines at least 500 cells were cultured per well of a 96 well plate. To establish monoclonal T cell populations by limiting dilution 0.3 cells were seeded per well of a 96 well plate containing feeder cells (Figure 11). The feeder cell and cytokine composition is described in Table 10. Proliferating T-cell clones were not touched during the first 14 days of incubation and were then transferred into 24 well plates for expansion.

Table 10 Feeder cell and cytokine composition for unspecific restimulation of peptide-specific CD8⁺ T cells.

	PBMC		LCL-B27		OKT3	IL-2	IL-7	IL-15	Volume
	No.	Gy	No.	Gy					
96 well	1x10 ⁵	35	1x10 ⁴	50	30 ng/ml	50 IU/ml	5 ng/ml	10 ng/ml	200 µl
24 well	1x10 ⁶	35	1x10 ⁵	50	30 ng/ml	50 IU/ml	5 ng/ml	10 ng/ml	1000 µl

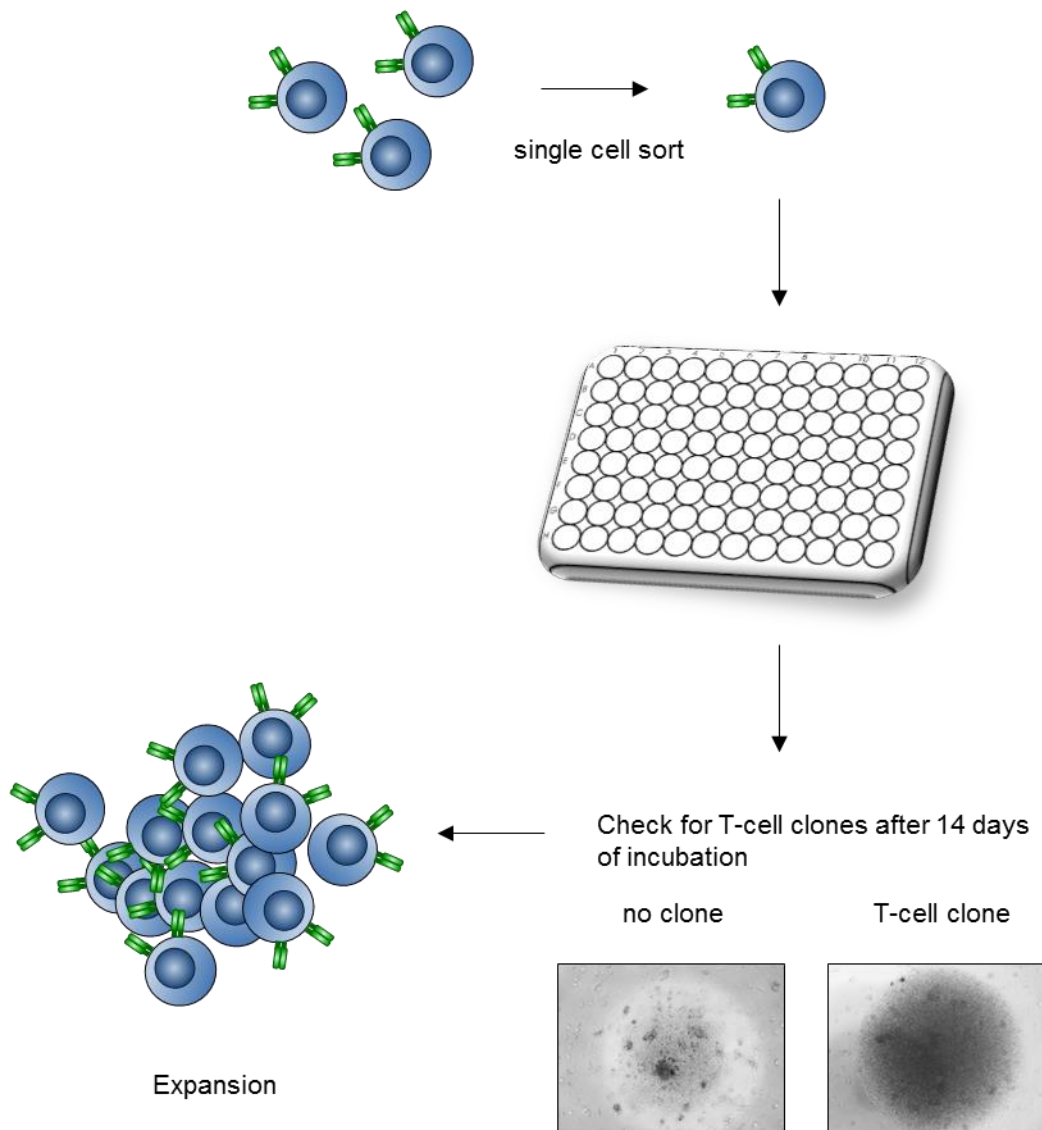


Figure 11 Limiting dilution cloning for generation of monoclonal T-cell clones. Stimulated T cells were sorted by anti-CD8 and A2-GPC3 multimer staining. 0.3 cells were seeded per well of a 96 well plate containing feeder cells. After 14 days of incubation the plates were screened for expanded T-cell clones that can clearly be distinguished from dead feeder cells by eye. T-cell clones were then transferred to a 24 well plate for further expansion.

3.5.4 Unspecific Restimulation of Peptide-specific CD8⁺ T cells

Every 14 days T-cell lines and T-cell clones were non-specifically restimulated using feeder cells, consisting of pooled allogeneic irradiated PBMC from 5 donors and irradiated allogeneic LCL-B27 cells. OKT3, IL-2, IL-7, and IL-15 were supplemented to the medium. For feeder cell and cytokine concentrations see Table 10. IL-2 was added every 3-4 days; IL-7 and IL-15 were added every 7 days.

3.6 Functional Analysis of Peptide-specific T cells

3.6.1 Co-incubation of T cells with Different Target Cells

For the assessment of their functional activity T cells were co-incubated with different target cells. T-cell lines or T-cell clones were used 12 to 14 days after the last restimulation and were deprived from cytokines for at least 3 days. Transduced T cells were used at day 4 post-transduction or later and were deprived from IL-2 for at least 3 days. For co-incubation T cells were added to target cells at different effector to target (E:T) ratios in a 96 well plate. Co-culture with suspension cell lines or adherent cell lines was conducted in a final volume of 200 μ l in round-bottom plates or flat-bottom plates, respectively. Effector and target cells were additionally cultured alone as internal controls. In order to assess IFN γ secretion by T cells or killing of target cells supernatants were harvested 24 to 72 h post co-incubation and frozen at -20 °C and / or viability assays were performed on target cells. For ICS co-incubation was aborted after 5 h, the cells were kept at 4 °C until staining and analysis was performed on the next day as described in 3.4.3.

3.6.2 IFN γ Enzyme-linked Immunosorbent Assay (ELISA)

Secreted levels of human IFN γ were measured from cell culture supernatants using BioLegend's ELISA MAX™ Standard Set according to the manufacturer's instructions. In brief, capture antibody was coated to a 96 well flat-bottom plate at 4 °C overnight. The plate was washed 4 times before samples were added for 2 h at room temperature. Detection was carried out by incubation with a detection antibody for 1 h, followed by incubation with Avidin-HRP for 30 min and subsequently substrate for 10-30 min. The plate was vigorously washed 4 times between each incubation step. Absorbance was measured at 450 nm and 570 nm using the Tecan Infinite F200 reader.

3.6.3 Cytotoxicity Assay

10⁴ target cells (HepG2 or Huh7 cells) were seeded in 96 well flat-bottom plates 3 days prior to co-incubation with T cells to achieve approximately 90% confluence of target cells. Effector

cells were added and co-incubated with target cells for 24 to 72 h. Viability was assayed using Promegase CellTiter-Blue® Cell Viability Assay according to the manufacturer's instructions.

Killing of target cells over time was analysed using the xCELLigence system. Adherent target cells were seeded on specially designed microtiter plates (E-plate 96 culture plates), which contain interdigitated gold microelectrodes to noninvasively monitor cell viability. After addition of effector cells, target cell viability was measured via electrode impedance and is later on displayed as cell index values.

3.7 Analysis and Cloning of TCRs from GPC3-specific T-cell Clones

3.7.1 RNA Isolation

For isolation of total cellular RNA 200 µl Trizol were added to approximately 10^5 cells. After 5 min of cell lysis, 40 µl 1-bromo-3-chloro-propan and 20 µl linear acrylamide were added to extract RNA. The samples were vortexed for 15 s, incubated for 5 min at room temperature and subsequently centrifuged at 12,000 g for 15 min at 4 °C. The aqueous upper phase contained the RNA and was transferred into a fresh tube. The lower and inter phase contained DNA and protein, respectively.

For RNA isolation, 100 µl of 100% isopropanol were added to the aqueous phase to precipitate RNA. After an incubation time of 10 min at room temperature the sample was centrifuged at 12,000 g for 12 min at 4 °C. The pellet was then washed with 1 ml of 75% ethanol and centrifuged at 12,000 g for 8 min at 4 °C. The RNA pellet was dried and then diluted in 20 µl of RNase free DEPC H₂O. RNA concentration was measured using the NanoVue spectrophotometer and RNA was stored at -80 °C.

3.7.2 Reverse Transcription PCR (RT-PCR)

Complementary DNA (cDNA) was prepared via reverse transcription of total RNA using SuperScript® III Reverse Transcriptase according to the manufacturer's instructions. In brief, 1 µg RNA, 1 µl Oligo(dT)-primers (50 µM) and 1 µl dNTPs (10 mM) in a total volume of 12 µl were denatured at 65 °C for 5 min and subsequently placed on ice. Reverse transcription was

performed by adding 1 μ l SuperScript[®] III Reverse Transcriptase, 1 μ l RNaseOut (40 U/ μ l) and 4 μ l 5x first strand buffer to the RNA mix. The reaction was carried out in a final volume of 20 μ l and was incubated for 1 h at 42 °C. The reaction was terminated at 70 °C for 15 min. cDNA-1 was then stored at -20 °C until further use.

Additionally cDNA was transcribed using the reaction mix listed in Table 11 with primer CA1 (5' AGACCTCATGTCTAGCACAG 3') that binds specifically to the constant domain of the TCR α -chain.

Table 11 Reaction conditions for synthesis of cDNA-2.

Reaction mix	
Reaction buffer (10x)	2 μ l
MgCl ₂ (25 mM)	4 μ l
dNTPs (25 mM)	2 μ l
Primer CA1 (10 pmol/ μ l)	2 μ l
RNase inhibitor	1 μ l
AMV reverse transcriptase	0.8 μ l
RNA (1 μ g)	x μ l
DEPC H ₂ O	ad 20 μ l

The reaction mix was incubated for 10 min at 25 °C followed by 1 h at 42 °C. The reaction was terminated at 99 °C for 5 min. cDNA-2 was then stored at -20 °C until further use.

3.7.3 TCR-V α β Repertoire Analysis

For TCR analysis variable parts of TCR α - and β -chains were amplified by PCR from previously generated cDNA with degenerated primer that cover the complete TCR variable α -domain (TRAV) (81) and 96% of the TCR variable β -domain (TRBV) (82) gene segment families followed by agarose gel purification and DNA sequencing. The primer VPANHUM covers the complete V α -gene segments. VP1 and VP2 cover 76% and 20% of the 55 V β -gene segments, respectively. The gene segments V β 10.1 and V β 16.1 cannot be identified using these primers. PCR reactions were performed using PuReTaq[™] Ready-To-Go[™] PCR beads that contain BSA, dNTPs, 2.5 U PuReTaq DNA polymerase and reaction buffer. cDNA was diluted 1:4 before used as a template.

The TRAV repertoire was additionally examined using 32 different 5'V α -primers that specifically bind one TRAV allele each. The corresponding 3' primer (3'T-C α) bound within the constant domain of the TCR gene segment. Furthermore an internal control with a primer pair (P5'- α ST and P3'- α ST) that binds within the constant domain has been added to every reaction.

All primers used for the TCR analysis are listed in 2.5 and a schematic illustration of the primer binding sites is depicted in Figure 12. Reaction conditions and temperature settings are listed in Table 12 to Table 15.

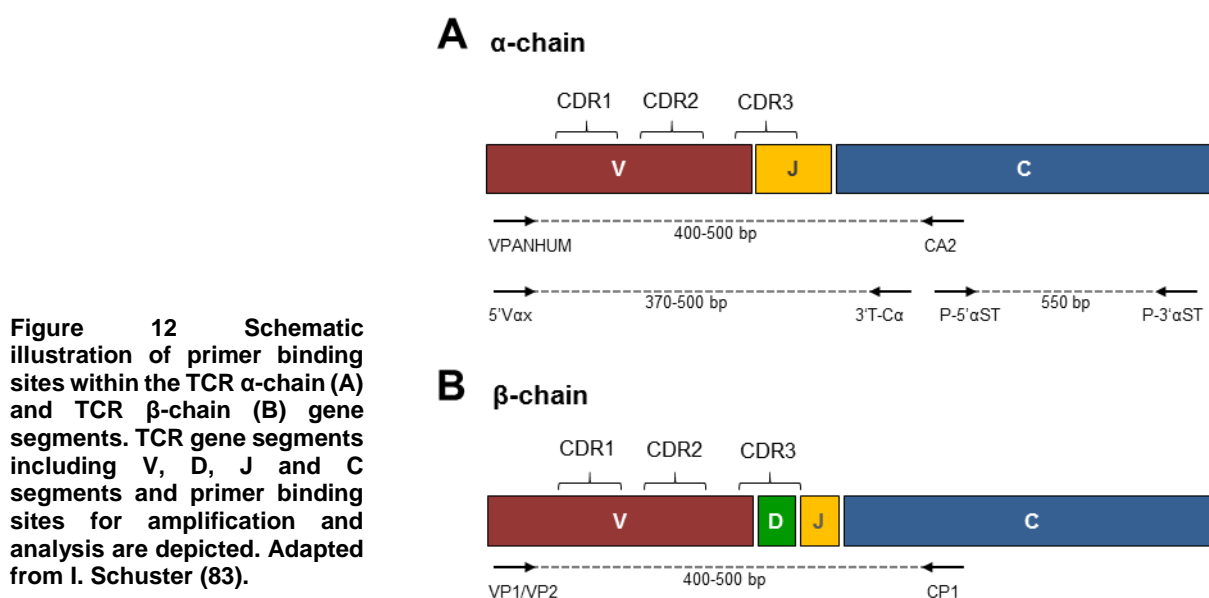


Table 12 Reaction conditions for TCR α - and β -chain PCR with degenerated primers.

PCR reaction mix			
TCR α -chain		TCR β -chain	
cDNA-2 derived from T-cell clones	1.5 μ l	cDNA-1 derived from T-cell clones	1.5 μ l
VPANHUM (5 pmol/ μ l)	8 μ l	VP1 or VP2 (5 pmol/ μ l)	8 μ l
CA2 (5 pmol/ μ l)	0.8 μ l	CP1 (5 pmol/ μ l)	0.8 μ l
PuReTaq™ PCR beads	1x	PuReTaq™ PCR beads	1x
H ₂ O	15 μ l	H ₂ O	15 μ l

Table 13 Temperature setting for TCR α - and β -chain PCR with degenerated primers.

PCR reaction conditions			
TCR α -chain		TCR β -chain	
95 °C	2 min	95 °C	2 min
95 °C	30 s	95 °C	30 s
50 °C	30 s	50 °C	30 s
72 °C	1 min	72 °C	1 min
72 °C	10 min	72 °C	10 min
4 °C	∞	4 °C	∞

Table 14 Reaction conditions for TCR α -chain PCR with specific primers.

PCR reaction mix	
TCR α -chain	
cDNA derived from T-cell clones	1 μ l
5'Vax (2.5 or 5 pmol/ μ l)	6 μ l
3'T-C α (5 pmol/ μ l)	4 μ l
P5' α ST (5 pmol/ μ l)	2.8 μ l
P3' α ST (5 pmol/ μ l)	2.8 μ l
PuReTaq TM PCR beads	1x
H ₂ O	8.5 μ l

Table 15 Temperature setting for TCR α -chain PCR with specific primers.

PCR reaction conditions	
TCR α -chain	
95 °C	2 min
95 °C	30 s
50 °C	30 s
72 °C	1 min
72 °C	10 min
4 °C	∞

3.7.4 Cloning of a TCR into the Retroviral Expression Vector pMP71

TCR α - and β -chain sequences were cloned into pMP71 (79) for expression in human T cells or Jurkat cells. The TCR α - and β -chain sequences were first amplified using primers specific for the identified sequence with a 5' primer binding in front of the start codon and a 3' primer that binds in the end of the constant domain. Restriction sites for cloning into pMP71 were added at both ends and a Kozak consensus sequence (CCRCCATGG, R = A or G) was added

to the 5' end. All primers applied are listed in 2.5. The PCR reaction was performed using Phusion® Hot Start II DNA Polymerase (Thermo Scientific) as described in Table 16 and Table 17. The optimal annealing temperature for each primer pair was calculated using the T_m calculator offered by New England Biolabs (84).

Table 16 Reaction conditions for TCR α - and β -chain PCR for cloning into pMP71.

PCR reaction mix	
cDNA derived from T-cell clones	2 μ l
5'-primer (5 pmol/ μ l)	2.5 μ l
3'-primer (5 pmol/ μ l)	2.5 μ l
Phusion® 2x mix	25 μ l
H ₂ O	18 μ l

Table 17 Temperature setting for TCR α - and β -chain PCR for cloning into pMP71

PCR reaction conditions	
98 °C	30 s
98 °C	10 s
50-70 °C	20 s
72 °C	20 s
72 °C	10 min
4 °C	∞

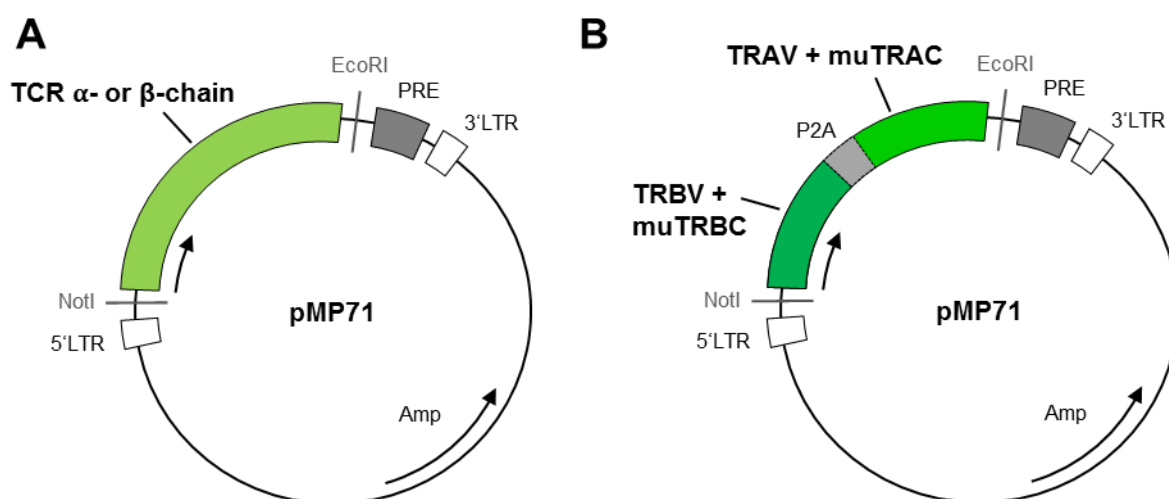


Figure 13 Schematic illustration of the retroviral vector pMP71. (A) Insertion of TCR α - or β -chain into pMP71. (B) Insertion of the complete TCR sequence, with codon optimized TRAV and TRBV sequences, murinized (μ) constant domains and the linker P2A between α - and β -chain. Restriction sites used for cloning are shown in grey. LTR: long terminal repeat, Amp: ampicillin resistance gene, PRE: Post-transcriptional regulatory element.

After digestion and agarose gel purification the PCR fragments were ligated into pMP71 and STBL3 *E.coli* were transformed with the ligation mix for plasmid amplification. The originated construct is depicted in Figure 13 A.

3.7.5 Cloning of the Optimized TCR P1-1 into pMP71

For optimal expression of the GPC3-specific TCR P1-1 in human cells, the sequences coding for the variable domains were codon optimized by GeneArt® (Life Technologies). Furthermore the constant domains were exchanged with murine constant domains to improve pairing of the transferred TCR in recipient T cells and avoid miss-pairing of transferred chains with endogenously expressed TCR chains (85). To achieve equimolar expression of both, α - and β -chain, in transduced cells, the TCR chains were cloned into one construct linked by a 'self-cleaving' 2A peptide sequence (P2A) derived from picornaviruses. The P2A linker allows expression of both chains as distinct proteins under control of the same promoter. Through ribosomal cleavage during the translation process α - and β -chain are expressed as separate proteins (86). The final construct is schematically shown in Figure 13 B.

For cloning of this construct a PCR in 3 steps was performed. First variable and constant domains of α - and β -chain were amplified using primers with overlapping sequences, as illustrated in Figure 14. Secondly, the variable and constant domain of α - and β -chain were annealed and amplified in one PCR step. Finally α - and β -chain PCR products were annealed via the P2A element. *EcoRI* and *NotI* restriction sites for later cloning into pMP71 were added in front and end of the sequence and a Kozak sequence was added in front of the start codon of the TRBV P1-1 sequence for optimal expression. All applied PCR settings are listed in Table 18 to Table 23.

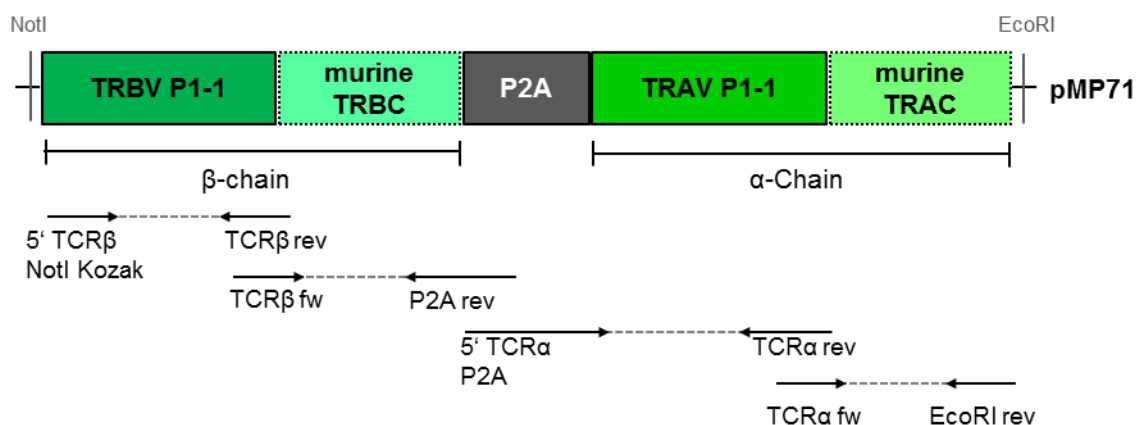


Figure 14 Schematic representation of primer binding sites for cloning of the optimized TCR P1-1 into pMP71. TRAV and TRBV sequences were codon optimized. TRBC and TRAC were murinized. α - and β -chain were linked via a P2A element. The construct was assembled by 4 PCR reactions followed by 2 annealing PCR reactions and cloning into pMP71 via *NotI* and *EcoRI* restriction sites.

Table 18 Reaction conditions and temperature settings for amplification of variable and constant domains of TCR P1-1.

PCR I			
PCR reaction mix		PCR reaction conditions	
template	5 μ l	98 $^{\circ}$ C	30 s
5'-primer (5 pmol/ μ l)	2.5 μ l	98 $^{\circ}$ C	10 s
3'-primer (5 pmol/ μ l)	2.5 μ l	50-70 $^{\circ}$ C	20 s
Phusion [®] 2x mix	25 μ l	72 $^{\circ}$ C	20 s
H ₂ O	18 μ l	72 $^{\circ}$ C	10 min
		4 $^{\circ}$ C	∞

Table 19 Primers and templates used for amplification of variable and constant domains of TCR P1-1.

Primers / templates used for PCR I				
	TRBV	Murine TRBC	TRAV	Murine TRAC
5'-primer	5' TCR β NotI Kozak	TCR β fw	5' TCR α P2A	TCR α fw
3'-primer	TCR β rev	P2A rev	TCR α rev	EcoRI rev
template	Codon optimized sequence form GeneArt	S ₁₇₂ -specific TCR (Karin Wisskirchen)	Codon optimized sequence form GeneArt	S ₁₇₂ -specific TCR (Karin Wisskirchen)

Table 20 Reaction conditions and temperature settings for annealing and amplification of α - and β -chain of TCR P1-1.

PCR II			
PCR reaction mix		PCR reaction conditions	
template	5 μ l	98 °C	30 s
5'-primer (5 pmol/ μ l)	2.5 μ l	98 °C	10 s
3'-primer (5 pmol/ μ l)	2.5 μ l	50-70 °C	20 s
Phusion® 2x mix	25 μ l	72 °C	20 s
H ₂ O	18 μ l	72 °C	10 min
		4 °C	∞

} 40x

Table 21 Primers and templates used for annealing and amplification of α - and β -chain of TCR P1-1.

Primers / templates used for PCR II		
	TRBV + murine TRBC	TRAV + murine TRAC
5'-primer	5' TCR β NotI Kozak	5' TCR α P2A
3'-primer	P2A rev	EcoRI rev
template	TRBV and murine TRBC PCR I products	TRAV and murine TRAC PCR I products

Table 22 Reaction conditions and temperature settings for annealing and amplification of TCR P1-1.

PCR III			
PCR reaction mix		PCR reaction conditions	
template	5 μ l	98 °C	30 s
5'-primer (5 pmol/ μ l)	2.5 μ l	98 °C	10 s
3'-primer (5 pmol/ μ l)	2.5 μ l	50-70 °C	20 s
Phusion® 2x mix	25 μ l	72 °C	20 s
H ₂ O	18 μ l	72 °C	10 min
		4 °C	∞

} 40x

Table 23 Primers and templates used for annealing and amplification of TCR P1-1.

Primers / templates used for PCR III	
TRBV + Murine TRBC + TRAV + Murine TRAC	
5'-primer	5' TCR β NotI Kozak
3'-primer	EcoRI rev
template	PCR products from PCR II

PCR products of all steps were purified by agarose gel electrophoresis before they were used as templates for the next step. The product from PCR III, assembling the complete optimized TCR P1-1 was digested with *NotI* and *EcoRI* and subsequently ligated into pMP71. The vector

was amplified in STBL3 *E.coli*. After plasmid preparation sequence identity was verified by sequencing.

3.8 Retroviral TCR Transfer into Human T cells or Jurkat cells

3.8.1 Virus Production in 293T cells

In order to assemble the TCR coding retrovirus, the helper cell line 293T was used. One to two days prior to transfection, 1×10^6 cells / well were plated into a 6 well culture dish so that the cells become 70-80% confluent at the time of transfection. 293T cells were then co-transfected with 2 μ g retroviral plasmid pMP71-TCR, 1 μ g pcDNA3.1-Mo-MLV and 1 μ g pALF-10A1, whereby the latter two represent plasmids that carry the retroviral genes for gag/pol and env, respectively. Transfection was performed with 10 μ l lipofectamine 2000 according to the standard lipofectamine transfection protocol described in 3.2.9.1. After 6 h, the medium was replaced with 2 ml fresh T cell medium. After 24 h and 48 h, the retrovirus containing supernatant was collected and purified from cell debris through a 0.45 μ m filter.

3.8.2 Activation of PBMC

Freshly isolated human PBMC were activated on anti-CD28 (0.05 μ g/ml) and OKT3 (5 μ g/ml) coated non-tissue treated 24 well plates at a concentration of 1×10^6 cells/well. The cells were cultured in hTCM supplemented with 300 IU/ml IL-2 for two days.

3.8.3 Transduction of T cells or Jurkat cells

Transduction was performed on RetroNectin-coated culture dishes to increase transfection efficacy. Non-tissue treated 24 well plates were coated with 200 μ l RetroNectin (20 μ g/ml) for 2 h at room temperature. The plates were subsequently blocked with 200 μ l of 2% BSA in PBS before they were washed with 2 ml PBS twice. Virus containing supernatant of transfected 293T cells was harvested two days after transfection and added to RetroNectin-coated 24 well culture plates. The virus was spinoculated for 2 h at 32 °C and 2000 g. After centrifugation media was replaced with 1×10^6 activated PBMC/well in hTCM supplemented with 100 IU/ml IL-2. T cells were spinoculated with 1000 g for 10 min at 32 °C. The transduction was repeated

in the same manner with freshly harvested virus supernatant on the following day. After 24 h of incubation medium was replaced with fresh hTCM containing 50 IU/ml IL-2 and T cells were incubated for additional 48 h. Transduced T cells were analysed by A2-GPC3 multimer staining and in functional assay at multiple time points. PBMC treated in the exactly same manner but without addition of a TCR containing pMP71 were used as mock control. Transduction of Jurkat cells was performed as described for T cells but without addition of IL-2.

3.9 Adoptive Transfer of TCR P1-1⁺ T cells *In Vivo*

3.9.1 Generation of Luciferase Expressing HepG2 cells

HepG2 cells were transfected with pLenti-Luc coding for Gaussian luciferase and a blasticidine resistance gene by standard lipofectamine transfection. 2 days after transfection the cells were selected for antibiotic resistance by addition of 5 µg/ml blasticidine to the culture medium. Blasticidine resistant cells were expanded and subsequently luciferase activity was measured from cell lysates and living cells. Total cell lysates were prepared from 1×10^6 cells. The cells were washed twice with PBS, 200 µl passive lysis buffer was added and the lysate was incubated for 2 h at -20 °C. Cell lysates were stored at -20 °C until further use. 35 µl cell lysate was combined with 35 µl of 4.4 µM coelenterazine ($C_{end} = 2.2 \mu\text{M}$), the substrate for G-Luc, in a 96 well white microtiter plates. Immediately after addition of the substrate, bioluminescence was measured on the Tecan Infinite F200 reader. The background was normalized by measuring wells containing only buffer with substrate. Luciferase activity in living cells was assayed immediately after addition of 2.2 µM coelenterazine in 100 µl cell culture medium using Perkin Elmer's In Vivo Imaging System (IVIS).

3.9.2 Adoptive Transfer of P1-1⁺ T cells in Tumour Bearing SCID/Beige Mice

5×10^5 HepG2-luc cells were injected into the splenic pulp of 8 week-old female severe combined immunodeficiency (SCID)/Beige mice on day -12/-13. On day 0 mice were treated with TCR P1-1 transduced human T cells or mock transduced T cells. TCR P1-1 was expressed in approximately 50% of CD8⁺ and CD4⁺ T cells that accounted for 20% and 50% of the total PBMC population, respectively. 1×10^7 transduced total PBMC (1×10^6 P1-1⁺ CD8⁺

T cells) were resuspended in 200 μ l PBS and injected intraperitoneally (i.p.). Tumour growth was monitored by bioluminescence imaging using the IVIS Imaging system on day -3, 0 and 3 before the mice were sacrificed.

3.9.3 Bioluminescence Imaging

Tumour growth was monitored every 3-4 days by bioluminescence imaging using the IVIS Imaging System. Mice were anesthetized using 2% isoflurane. Immediately before *in vivo* imaging 4 mg/kg coelenterazine was i.p. injected. For quantification, regions of interest (ROI) were selected and quantified as photons/second using Living Image[®] software.

3.10 Statistical Analysis

Data is reported as mean values \pm standard deviation (SD) where possible¹. To evaluate statistical differences between paired data sets the two-way-ANOVA with Bonferroni post-test was used. P values less than 0.05 were regarded as statistically significant. P values are indicated in the graphics as follows: P>0.05 (ns), P<0.05 (*), P<0.01 (**), P<0.001 (***). All analysis was performed with GraphPad Prism 5.0.

¹ Screening of GPC3 specific T cell clones has only been performed in duplicates, due to the low cell numbers available at this stage of the experiment. Therefore no SD is shown.

4 Results

4.1 Selection of GPC3 Epitopes for T cell Stimulation

Selecting the right epitope specificity is essential for the development of effective T-cell therapies. In this study we focused on HLA-A*0201 restricted epitopes because it is expressed by 40-50% of the Caucasian population (77). Thus, an HLA-A*0201 restricted TCR can most probably find the broadest clinical application. Immunodominant epitopes for GPC3 are not well described. O'Beirne et al. showed that T cells can be stimulated towards the HLA-A2 restricted epitope GPC3₅₂₂ (87). The HLA-A24 restricted epitope GPC3₂₉₈ and HLA-A2 restricted epitope GPC3₁₄₄ were proposed to be immunogenic by Komori et al. (21), but no further publications confirmed these results.

One possibility to identify potential HLA-A*0201 binding immunogenic epitopes of GPC3 is to use bioinformatical prediction models. Those prediction models utilize computerized algorithms by which the peptide binding affinity is predicted based on the AA sequence. In this study SYFPEITHI (88), BIMAS (89) and NetMHC (90, 91) were used for peptide prediction. SYFPEITHI predicts peptide binding with scores ranging from 0 to 36, with 36 representing the highest binding probability. Within the BIMAS model peptides are ranked based on predicted half-time of dissociation of the peptide MHC complex. The higher the score the stronger is the peptide-MHC binding. Using the NetMHC prediction model, peptide binding affinities are predicted in molar concentrations. Peptides with affinities below 50 nM are defined as strong binders, peptides with binding affinities below 500 nM as weak binders.

Using the bioinformatical prediction models SYFPEITHI, BIMAS and NetMHC, 24 GPC3 peptides were predicted to bind the HLA-A2 molecules with high affinity. The scores of the 24 GPC3 peptides, HBV S₁₇₂ and the peptide AFP₁₅₈ (20) that was used for mock peptide controls in this study are listed in Table 24. Based on current literature and Table 24, GPC3₅₂₂ was chosen for T cell stimulation. It has been published that stimulation with RNA pulsed moDC can stimulate HLA-A2 restricted GPC3₅₂₂-specific T cells (87). Furthermore GPC3₅₂₂ was

Results

predicted to bind HLA-A2 with high affinity by SYFPEITHI and NetMHC. By BIMAS GPC3₅₂₂ is ranked as a peptide with medium half-time of dissociation.

Table 24 Evaluation of different GPC3 peptides with regard to their HLA-A2 binding affinity. The thresholds for a peptide being a binder in each of the tools were set to SYFPEITHI score ≥ 22 , NetMHC predicted affinity ≤ 500 nM and BIMAS half time ≥ 20 min.

Peptide		HLA-A*0201 binding			Literature
Position ¹	AA	SYFPEITHI (88)	BIMAS ² (89)	NetMHC ³ (90, 91)	
10	LVVAM <u>LL</u> SL	23	7	234	
44	RLQPGL <u>KW</u> V	27	879	83	
92	LLQSAS <u>MEL</u>	24	36	27	
102	FLIIQ <u>NAA</u> V	26	319	13	
144	FVGEF <u>ETD</u> V	18	828	33	Komori et al.
153	SLYIL <u>GSD</u> I	22	33	1627	
155	YILGSD <u>IN</u> V	24	162	11	
162	NVDDM <u>VNEL</u>	22	7	984	
169	ELFDS <u>LFP</u> V	23	1055	3	O'Beirne et al.
173	SLFPV <u>IYT</u> Q	22	0.1	250	
197	CLRGAR <u>RDL</u>	22	0.3	25445	
222	SLQVTR <u>IFL</u>	22	117	432	O'Beirne et al.
232	ALNLG <u>IEVI</u>	27	4.8	706	
254	RMLTR <u>MWYC</u>	10	1259	157	
281	VMQGC <u>MAGV</u>	24	196	16	
299	YILSL <u>EELV</u>	23	79	12	O'Beirne et al.
302	SLEEL <u>VNGM</u>	24	2.9	520	
319	VLLGL <u>FSTI</u>	26	124	40	
326	TIHDS<u>IQYV</u>	23	496	50	
340	KLTTT <u>I</u> GKL	26	22	776	
367	FIDKK<u>V</u>LKV	27	40	28	
461	QIIDK <u>L</u> KHI	23	13	3448	
522	FLAEL<u>AYDL</u>	27	402	5	O'Beirne et al.
564	LLTSM <u>AISV</u>	23	118	17	
AFP ₁₅₈	FMNKF <u>IYEI</u>	26	302	2	Butterfield et al.
HBV S ₁₇₂	WLSLL <u>V</u> PFV	26	4047	7	

¹ AA position within the GPC3 or otherwise indicated protein

² Estimated half time of dissociation (min)

³ Affinity (nM)

In the AA sequence main anchors according to SYFPEITHI are in bold, secondary anchors are underlined.

Red: T cells with specificities against these peptides have been isolated successfully in this study.

Orange: T cells were stimulated against this peptide without success.

4.1.1 Identification of Novel HLA-A2 Restricted GPC3 Peptides Presented by Human Hepatoma Cells

In order to select the best epitope for successful T cell stimulation, it is of utmost importance to choose epitopes that are presented at sufficient levels on the targeted tumour tissue. Bioinformatical prediction models are merely based on computerized algorithms and do not allow conclusions on the actual protein processing and peptide presentation in tumour cells. To prioritize predicted peptides and identify which are presented after intracellular processing, we eluted peptides after immune-affinity purification of HLA-I complexes from HLA-A2⁺ GPC3⁺ HepG2 (21) cells.

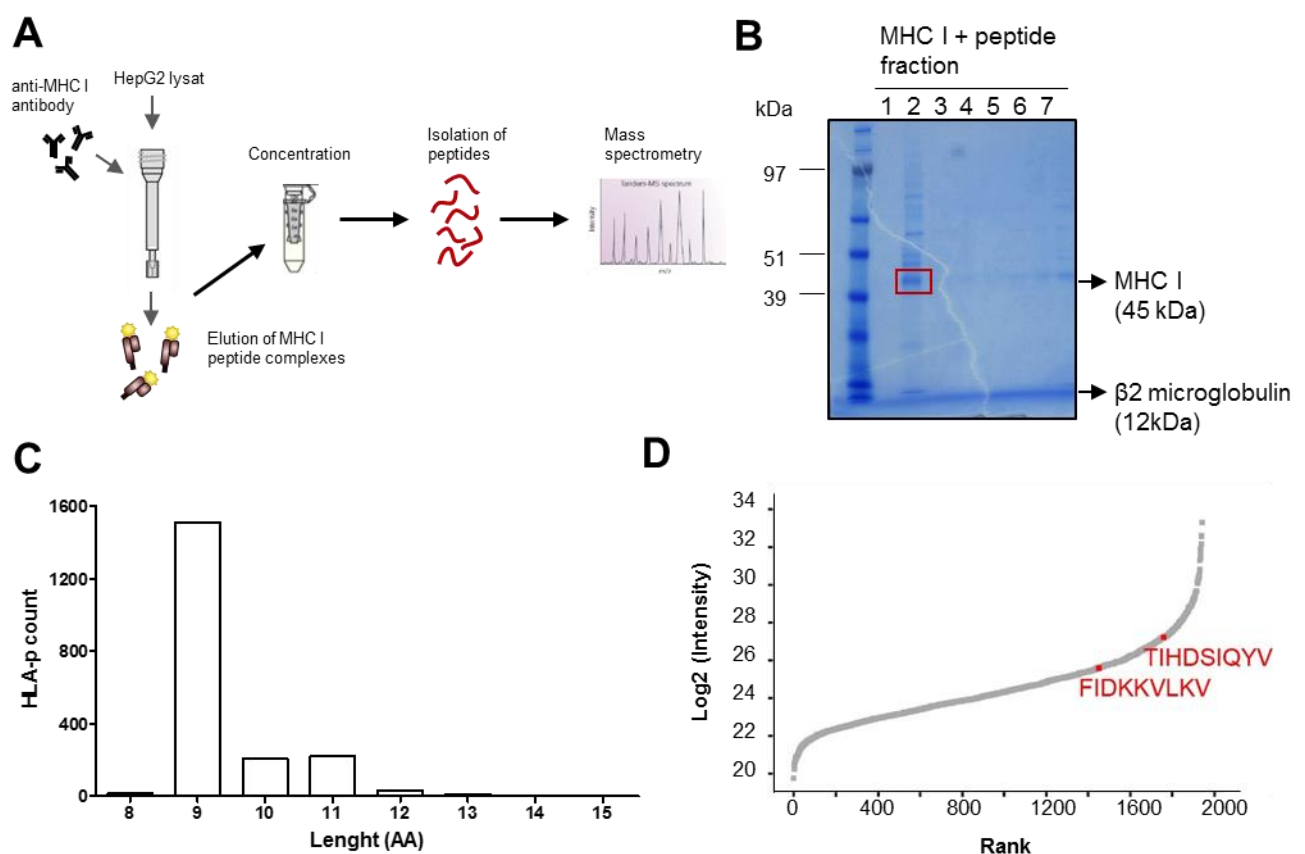


Figure 15 Identification of novel HLA-A2 restricted GPC3 peptides presented by human hepatoma cells. (A) Schematic overview of the experimental setup. MHC I complexes were immune-affinity purified from HepG2 cells lysates using anti-MHC I (W6-32) antibody cross linked to agarose beads. MHC I peptides were purified from the heavy chain based on their hydrophobicity. The enriched mixture of MHC I peptides was measured on a quadrupole Orbitrap mass spectrometer (Q Exactive). Peptides sequences were identified using MaxQuant software. (B) Peptide-MHC I complex containing fractions were identified by coomassie staining after gel electrophoresis. Peptide-MHC I complexes were found to be enriched in fraction 2. (C) Length distribution of 2004 MHC I peptides identified from HepG2 cells shows the typical length of MHC I peptides of mainly 9, 10 and 11 mer peptides. (D) Ranked measured intensity of the identified MHC I peptides. The two epitopes from GPC3 proteins are among the top 30% supporting their high presentation level on the surface of HepG2 cells.

A schematic overview of the experimental setup is shown in Figure 15 A. After enriching of MHC I peptide complexes (Figure 15 B) and specific elution of the peptides they were analysed by mass spectrometry. We identified in total 2004 unique MHC I peptides, most of which had a length of 9 AA (Figure 10 C), among them two GPC3 peptides. The peptides GPC3₃₆₇ (TIHDSIQYV) and GPC3₃₂₆ (FIDKKVLKV) were identified and synthetic peptides were used to validate the mass spectrometry data. Mass spectra of the two purified peptides and their synthetic counterparts are shown in the appendix (see 8.1). GPC3 epitopes are among the top 30% most abundant peptides (Figure 15 D), indicating a substantial presentation of these epitopes on the surface of HepG2 cells.

All mass spectrometric analysis have been performed by Michal Bassani-Sternberg (Max Plank Institute of Biochemistry, Munich). Details about the experimental procedure were kindly provided by her and can be found in the appendix (see 8.2).

4.1.2 Analysis of GPC3 Peptide Binding to HLA-A2

GPC3₅₂₂, GPC3₃₂₆ and GPC3₃₆₇ were predicted to be strong HLA-A2 binder; moreover GPC3₃₂₆ and GPC3₃₆₇ were detected to be presented by HLA-A2⁺ human hepatoma cells. In order to assess the peptide binding strength of GPC3₅₂₂, GPC3₃₂₆ and GPC3₃₆₇ to HLA-A2 experimentally, a peptide competition assay was performed. Therefore T2 cells were first loaded with a tenfold excess of GPC3 peptides for 30 min before HBV S₁₇₂ peptide was added for 1 h. Peptide loaded T2 cells were then co-incubated with HBV S₁₇₂-specific T cells and IFN γ secretion was measured. When GPC3 peptides have bound to HLA-A2, binding of HBV S₁₇₂ is inhibited and therefore IFN γ secretion by HBV S₁₇₂-specific T cells is decreased compared to IFN γ secretion after co-incubation with target cells loaded only with HBV S₁₇₂.

IFN γ secretion by HBV S₁₇₂-specific T cells was reduced to 70% when the target cells were loaded with GPC3₅₂₂ or GPC3₃₆₇ prior to HBV S₁₇₂, verifying HLA-A2 binding of GPC3₅₂₂ and GPC3₃₆₇ (Figure 16). HLA-A2 binding of GPC3₃₂₆ was not strong enough to inhibit HBV S₁₇₂ binding in a level sufficient to decrease IFN γ secretion by HBV S₁₇₂-specific T cells. T2 cells that were only loaded with GPC3 peptides were not recognized.

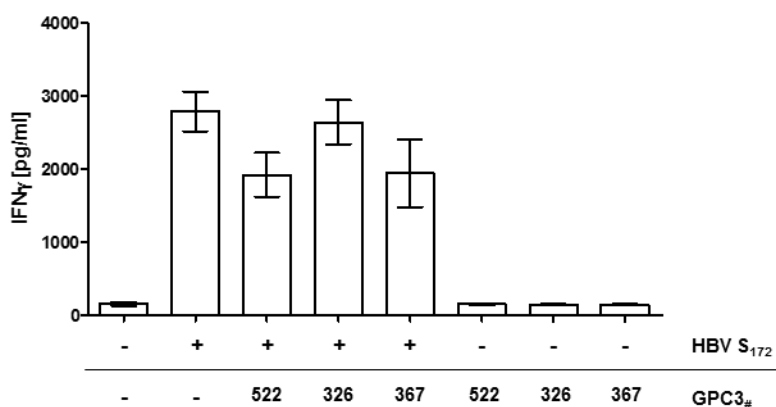


Figure 16 Peptide competition assay for investigation of HLA-A2 binding affinity of chosen GPC3 peptides. T2 cells were loaded with a tenfold excess of GPC3 peptide (100 μ M) for 30 min. After washing the cells were loaded with HBV S₁₇₂ (1 μ M) for 1 h. T2 cells that were only loaded with GPC3 / HBV peptides were used as controls. Peptide loaded target cells were co-incubated with HBV S₁₇₂-specific T cells for 24 h before IFN γ secretion was measured by standard ELISA. E:T ratios of 2.5:1 were used. SD of triplicates are shown.

These results are in conformity with bioinformatically predicted HLA-A2 binding affinity according to which GPC3₅₂₂ and GPC3₃₆₇ are slightly stronger binders than HBV S₁₇₂, while GPC3₃₂₆ is a weaker binder compared to HBV S₁₇₂.

4.2 Allorestricted Stimulation of GPC3-specific T cells

In this study we performed three attempts to stimulate GPC3-specific HLA-A2 restricted T cells. In Table 25 the accomplished stimulations, including peptide specificities, cells used as APCs and results obtained are summarized.

Table 25 Stimulations of GPC3-specific HLA-A2 restricted T cells performed in this study.

	Peptide specificity	APC	Results	Chapter
Stimulation 1	GPC3 ₅₂₂	moDC + peptide	No T-cell clones	4.3
Stimulation 2		T2 cells + peptide	Unspecific T-cell clones	4.4
Stimulation 3	GPC3 ₃₂₆ and GPC3 ₃₆₇	moDC + RNA	Specific T-cell clones	4.5
			TCR analysis	4.6
			<i>In vitro</i> and <i>in vivo</i> evaluation	4.7

Orange: T cells were stimulated against this peptide without success.

Red: T cells with specificities against these peptides have been isolated successfully in this study.

4.3 Stimulation of HLA-A2 Restricted GPC3₅₂₂-specific T cells with HLA-A2 *ivt*-RNA Pulsed and GPC3₅₂₂ Peptide Loaded moDC

In our first stimulation we aimed to stimulate GPC3₅₂₂-specific T-cell clones. GPC3₅₂₂ has been reported to effectively prime CD8⁺ T cell before (87). This stimulation was performed before the mass spectrometric analysis of the HLA-A2 peptidome of HepG2 cells had been performed, where GPC3₅₂₂ was not found to be presented by MHC I on the surface of HepG2 cells.

In order to stimulate HLA-A2 restricted GPC3₅₂₂-specific T cells, PBMC from a healthy HLA-A2 negative donor were stimulated with HLA-A2 *ivt*-RNA and GPC3₅₂₂ peptide pulsed moDC in two cycles over 7 days each as described in 3.5.2. No clear A2-GPC3₅₂₂ multimer⁺ CD8⁺ T cell population was detected after stimulation with HLA-A2⁺ GPC3₅₂₂ loaded moDC on day 14. Double positive cells were sorted and stained with A2-GPC3₅₂₂ multimer again after 7 days of incubation. Expansion of A2-GPC3₅₂₂ multimer⁺ CD8⁺ T cell was not possible as seen in Figure 17 A. In contrast detected frequencies of A2-GPC3₅₂₂ multimer⁺ CD8⁺ T cell decreased from 0.89% on day 14 to 0.06% on day 21 (Figure 17 A).

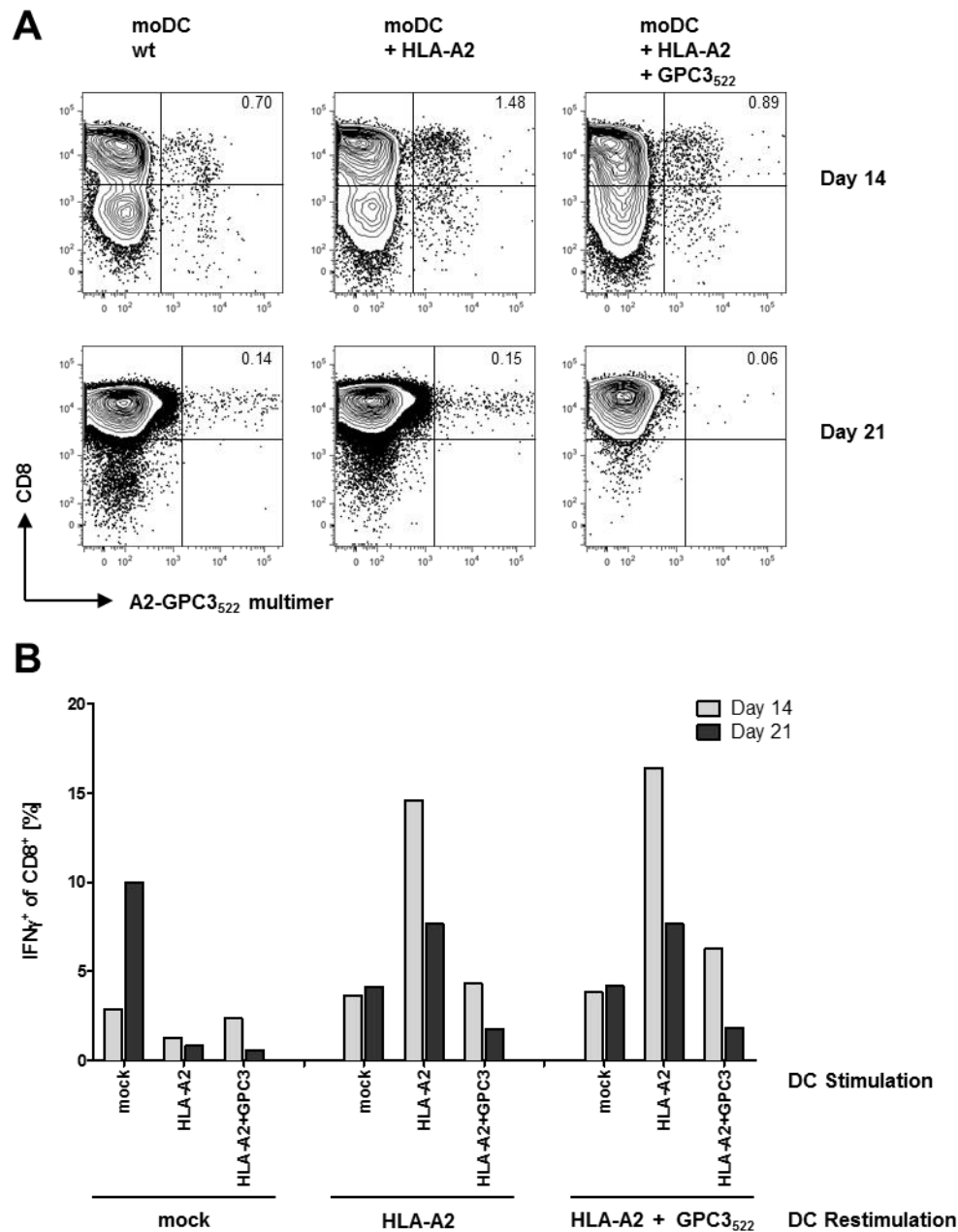


Figure 17 T cells stimulated with HLA-A2 *ivt*-RNA and GPC3₅₂₂ peptide pulsed moDC show no streptamer binding and target cell specificity. (A) Bulk T cell cultures after two cycles of stimulation (Day 14) and A2-GPC3₅₂₂ multimer enriched T-cell lines (Day 21) were stained with anti-CD8 antibody and A2-GPC3₅₂₂ multimer for flow cytometry. T cells stimulated with HLA-A2 *ivt*-RNA and GPC3₅₂₂ peptide pulsed moDC, HLA-A2 *ivt*-RNA only pulsed moDC and untreated moDC were compared. Percentage of A2-GPC3 multimer⁺ CD8⁺ cells is shown in the upper right corner of each plot. (B) T cells were restimulated with moDC as indicated and IFN γ secretion was detected by intracellular IFN γ staining after 5 h of incubation.

In addition to the multimer staining, IFN γ secretion after restimulation with moDC was measured in order to screen for HLA-A2 restricted GPC3₅₂₂-specific T cells. No specific IFN γ secretion profile was detected on day 14 or on day 21 (Figure 17 B). High secretion of IFN γ in the moDC+HLA-A2 stimulated group was observed, which probably resulted from allo-reactive T cells in the population.

Isolation and expansion of A2-GPC3₅₂₂ multimer⁺ CD8⁺ cells was not successful using the methods applied in this study. Either the immunogenic capacity of peptide GPC3₅₂₂ was not sufficient for effective T cell stimulation or the prepared moDC did not present the peptide in an adequate way for successful T cell stimulation. Thus, we decided to focus on the epitopes GPC3₃₂₆ and GPC3₃₆₇ that were newly identified in this study for stimulation of GPC3-specific T cells in all further experiments.

4.4 Stimulation of HLA-A2 Restricted GPC3₃₆₇- and GPC3₃₂₆-specific T cells with Peptide Loaded T2 cells

HLA-A2 restricted T cells can be stimulated utilizing peptide loaded T2 cells as APCs. T2 cells are HLA-A2⁺ and TAP deficient, resulting in highly impaired endogenous peptide processing (80). Peptide loaded T2 cells are therefore very suitable to stimulate HLA-A2 restricted T cells against the epitope of interest. Besides, T2 cells were used successfully for stimulation of TAA-specific HLA-A2 restricted T cells several times in the past (44, 92, 93).

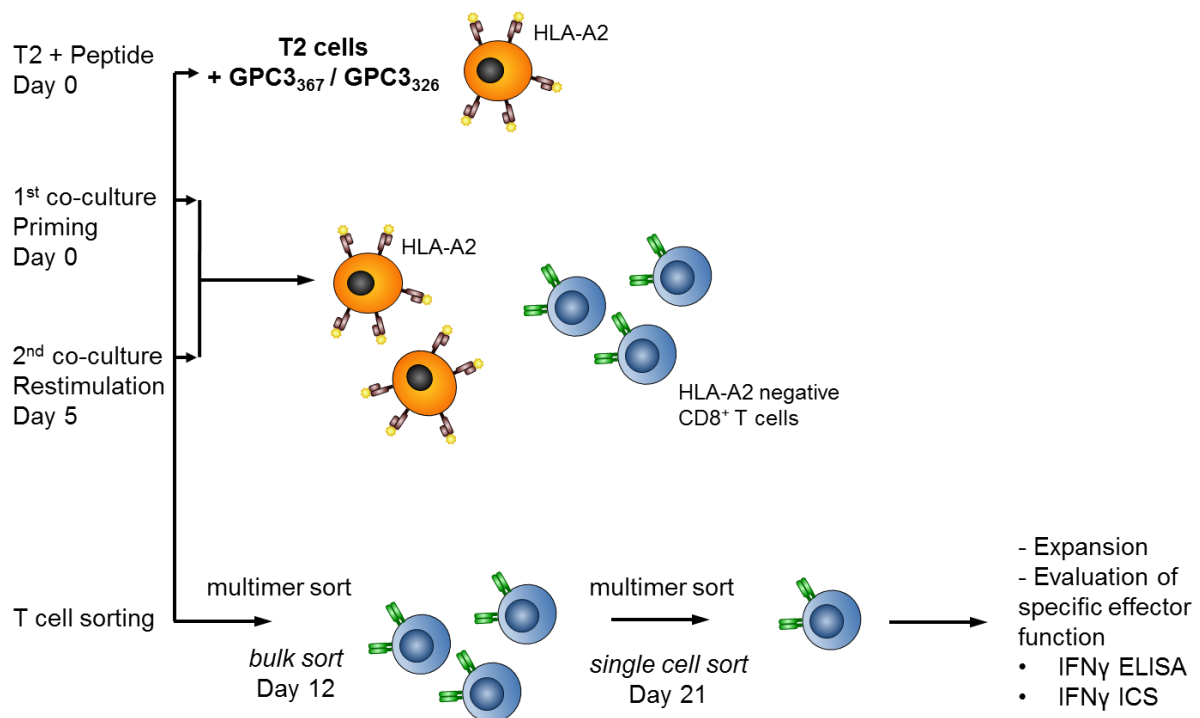


Figure 18 Schematic illustration of the allorestricted stimulation protocol of naïve T cells with peptide pulsed T2 cells. CD8⁺ enriched T cell from an HLA-A2⁻ donor were stimulated with peptide loaded HLA-A2⁺ T2 cells on day 0 and day 5. On day 12 GPC3 HLA-A2 restricted CD8⁺ T cells were stained with A2-GPC3 multimer and anti-CD8 antibody followed by cell sorting. Double positive populations were expanded, sorted again on day 21 and cloned by limiting dilution cultures to establish monoclonal T-cell clones.

GPC3₃₂₆ or GPC3₃₆₇ loaded T2 cells were used to stimulate freshly isolated CD8⁺ enriched T cells from an HLA-A2 negative donor in a ratio of 1:10 (T2:T cells). The stimulation was repeated with freshly prepared T2 cells after 5 days. Stimulated T cells were sorted with A2-GPC3 multimer and anti-CD8 antibody on day 12 for expansion of GPC3-specific CD8⁺ T cells in bulk cell lines. On day 21 GPC3-specific cell lines were sorted again and were immediately cloned in a limiting dilution to obtain monoclonal T-cell clones (Figure 18).

Specific multimer binding could neither be observed for multimer A2-GPC3₃₂₆ nor for A2-GPC3₃₆₇. Frequencies of detected multimer⁺ CD8⁺ T cells lay between 0.1 and 0.34% (Figure 19 A). Around 3% of A2-GPC3₃₆₇ multimer⁺ cells were detected after stimulation with GPC3₃₆₇ loaded T2 cells as well as mock peptide loaded T2 cells, indicating that the observed multimer binding was unspecific (data not shown). Nevertheless double positive cells were sorted and stained again with A2-GPC3 multimer after 7 days of expansion. Again no clear CD8⁺ A2-GPC3 multimer⁺ population was detected for neither of the peptide specificities.

T-cell clones originating from sorted CD8⁺ A2-GPC3 multimer⁺ cells showed no A2-GPC3 multimer binding (Figure 19 B, C). GPC3 specificity of T-cell clones was investigated by co-incubation with peptide loaded T2 cells for 24 h and subsequent measurement of IFN γ secretion. None of the T-cell clones showed specific IFN γ secretion towards T2 cells loaded with GPC3₃₂₆ (Figure 19 B) or GPC3₃₆₇ (Figure 19 C) in comparison to mock loaded T2 cells or T2 cells without peptide. Therefore no further investigations were done on this stimulation.

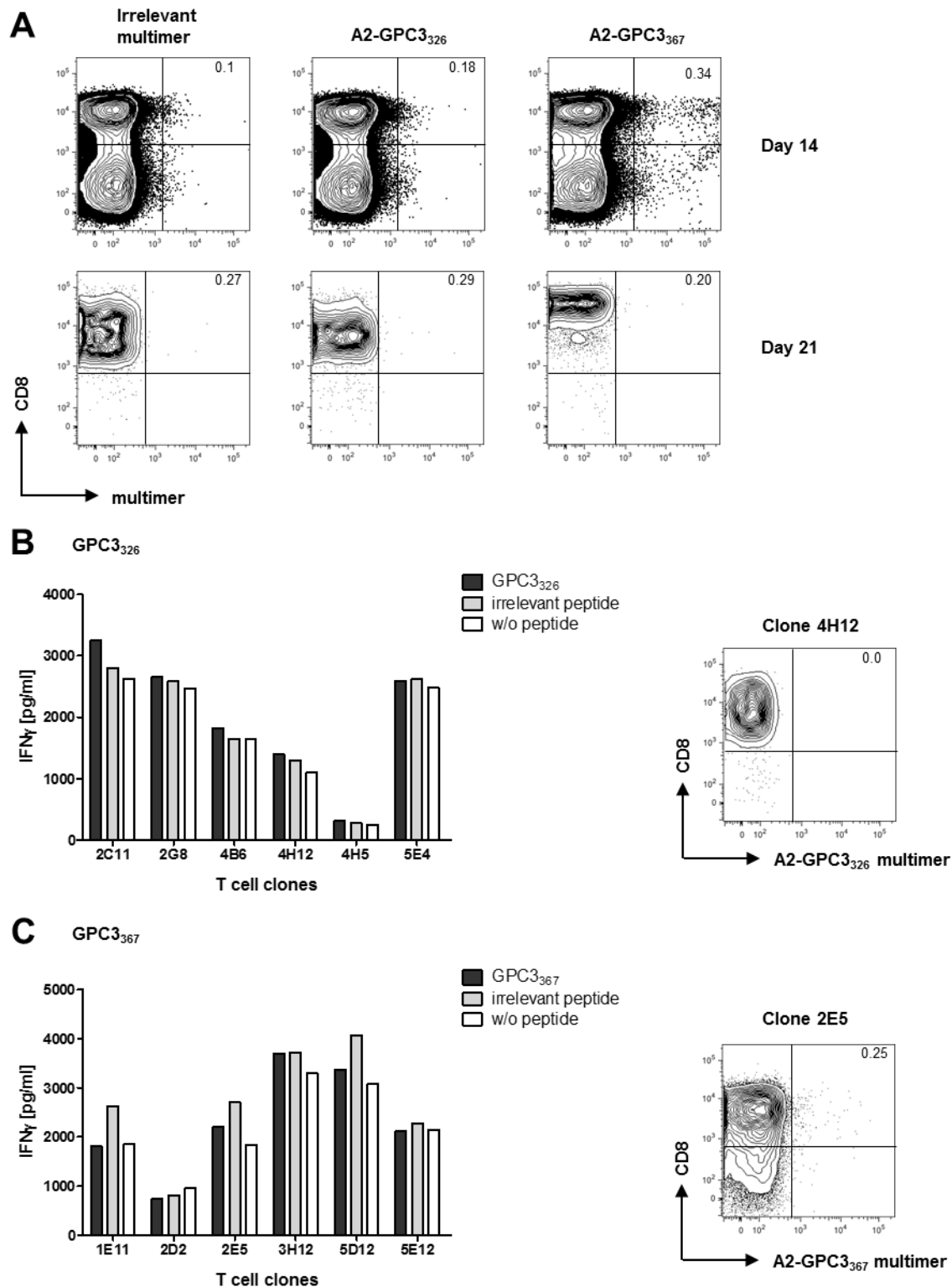


Figure 19 T cells stimulated with HLA-A2⁺ GPC3 peptide loaded T2 cells show no streptamer binding or target cell specificity. (A) Bulk T cell cultures after two cycles of stimulation (Day 14) and A2-GPC3 multimer enriched CD8⁺ T-cell lines (Day 21) were stained with anti-CD8 antibody and A2-GPC3 multimer for cell sorting. Staining with irrelevant multimer specificity (AFP₁₅₈) is shown as control. Percentage of A2-GPC3 multimer⁺ CD8⁺ cells is shown in the upper right corner of each plot. Peptide recognition of the A2-GPC3₃₂₆ (B) or A2-GPC3₃₆₇ (C) multimer sorted T-cell clones was investigated using T2 cells loaded with GPC3, irrelevant peptide or without peptide loading. Supernatants were harvested after 24 h of co-culture and IFN γ levels were analysed by IFN γ ELISA. E:T ratios of 0.2:1 were used. One representative T-cell clone stained with anti-CD8 antibody and A2-GPC3 multimer is shown for each peptide specificity.

4.5 Stimulation of HLA-A2 Restricted GPC3₃₆₇- and GPC3₃₂₆-specific T cells with *ivt*-RNA

Pulsed moDC

In the third stimulation performed in this study allorestricted GPC3₃₆₇- and GPC3₃₂₆-specific T cells were generated by stimulation with *ivt*-RNA pulsed moDC. All further results refer to this stimulation.

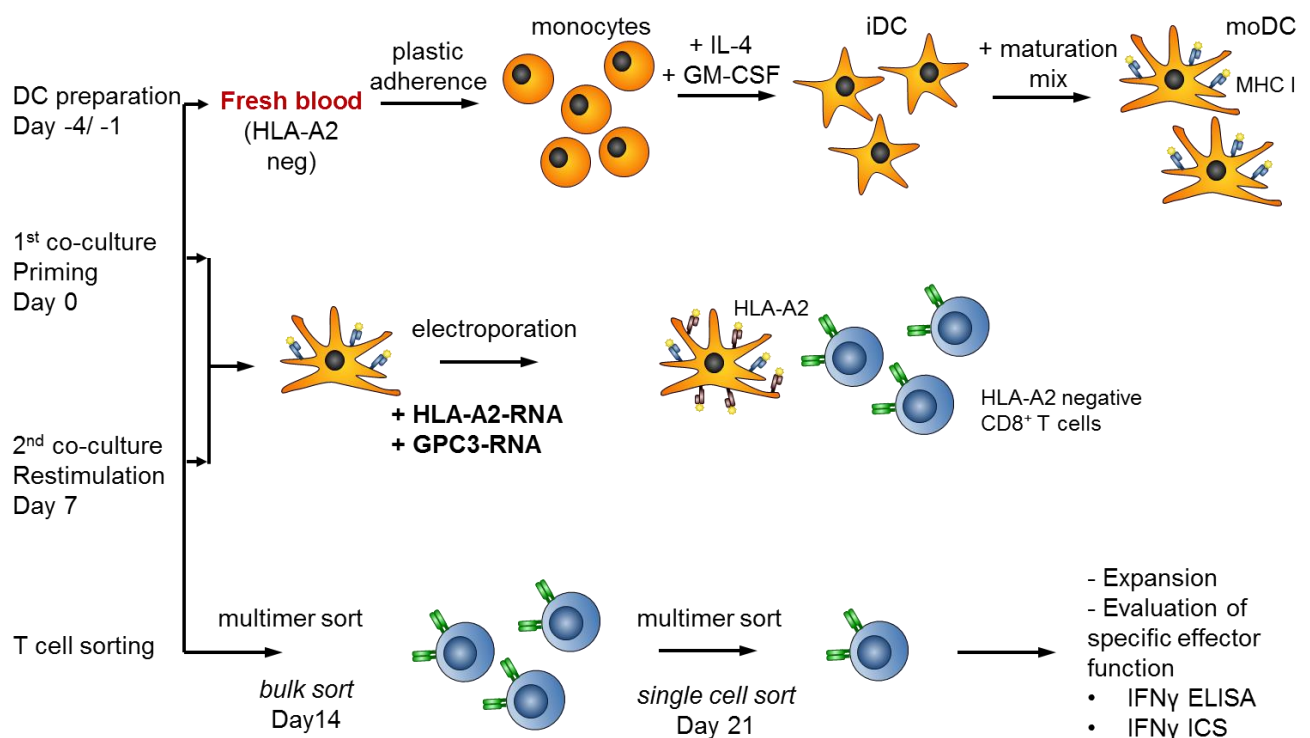


Figure 20 Schematic illustration of the allorestricted stimulation protocol of naïve T cells with RNA pulsed moDC. Monocytes were isolated from total PBMC from the HLA-A2 negative repertoire by plastic adherence and stimulated with IL-4 and GM-CSF for 48 h to produce immature DC on day -3. Maturation of moDC was completed after 24 h (day -1) of incubation with a maturation mix. MoDC were pulsed with 60 μ g HLA-A2 *ivt*-RNA and 35 μ g GPC3 *ivt*-RNA on day 0. Co-incubation with autologous CD8⁺ enriched T cells was initiated immediately after RNA pulsing. T cells were restimulated with freshly prepared moDC after 7 days. A2-GPC3 multimer⁺ CD8⁺ T cells were sorted expanded in T-cell lines over 7 days before they were sorted again and cloned by limiting dilution to obtain monoclonal T-cell clones on day 21. Adapted from Wilde et al. (60).

The experimental procedure can roughly be divided into three parts (Figure 20). The first phase involves the preparation of moDC that co-express HLA-A2 and GPC3. MoDC were generated by maturation of freshly isolated monocytes from a healthy HLA-A2 negative donor over three days as described before by Dauer et al. (94).

The second step of the stimulation procedure accomplished the actual stimulation. For that purpose freshly generated moDC were pulsed with HLA-A2 and GPC3 *ivt*-RNA and were

directly used to stimulate CD8⁺ enriched T cells from the same HLA-A2 negative donor. A ratio of 1:10 for moDC to T cells was used. The stimulation was repeated with freshly prepared moDC after 7 days.

In the third phase stimulated T cells were sorted with A2-GPC3 multimer and anti-CD8 antibody on day 14 for expansion of GPC3-specific CD8⁺ T cells in bulk cell lines. On day 21 GPC3-specific cell lines were sorted again and were immediately cloned by limiting dilution to obtain monoclonal T-cell clones. Details are described in the following sections.

4.5.1 Expression of GPC3 and HLA-A2 after *ivt*-RNA pulsing of moDC

For successful stimulation of TAA-specific cytotoxic T cells with *ivt*-RNA pulsed moDC, stable surface expression of MHC I and TAA expression levels that are sufficient for peptide processing and loading to MHC I are fundamental. We therefore established a protocol to co-express HLA-A2 and GPC3 in moDC.

4.5.1.1 Cloning of a GPC3 Expression Construct

In order to express GPC3 in moDC after RNA electroporation a GPC3 expression vector was constructed. RNA was isolated from the GPC3⁺ human hepatoma cell line Huh7, reverse transcribed into cDNA and used as a template to amplify the GPC3 gene sequence. The GPC3 sequence was then cloned into pcDNA3.1(-) under control of a CMV promoter (Figure 21 A) (see 8.3 for vector map). GPC3 sequence identity was confirmed by sequencing. Expression of GPC3 after cells had been transfected with pcDNA3.1(-)GPC3 was demonstrated in 293T cells. Western blot analysis using an antibody against GPC3 showed that GPC3 was expressed in 293T cells 24 h after transfection. A product of approximately 65 kDa, corresponding to the size expected for the GPC3 protein was detected (Figure 21 B). In addition products of 130 and 230 kDa were detected in 293T cells, which represent glycanated forms of GPC3. The human hepatoma cells Huh7 and HepG2 were used as positive controls. In both cell lines the 65 kDa GPC3 core protein as well as the 130 kDa glycanated form of GPC3 were detected.

The HLA-A2 expression vector pcDNA3.1(Hygro)-HLA-A2 (see 8.3 for vector map) already existed in the laboratory and could directly be used for the following experiments.

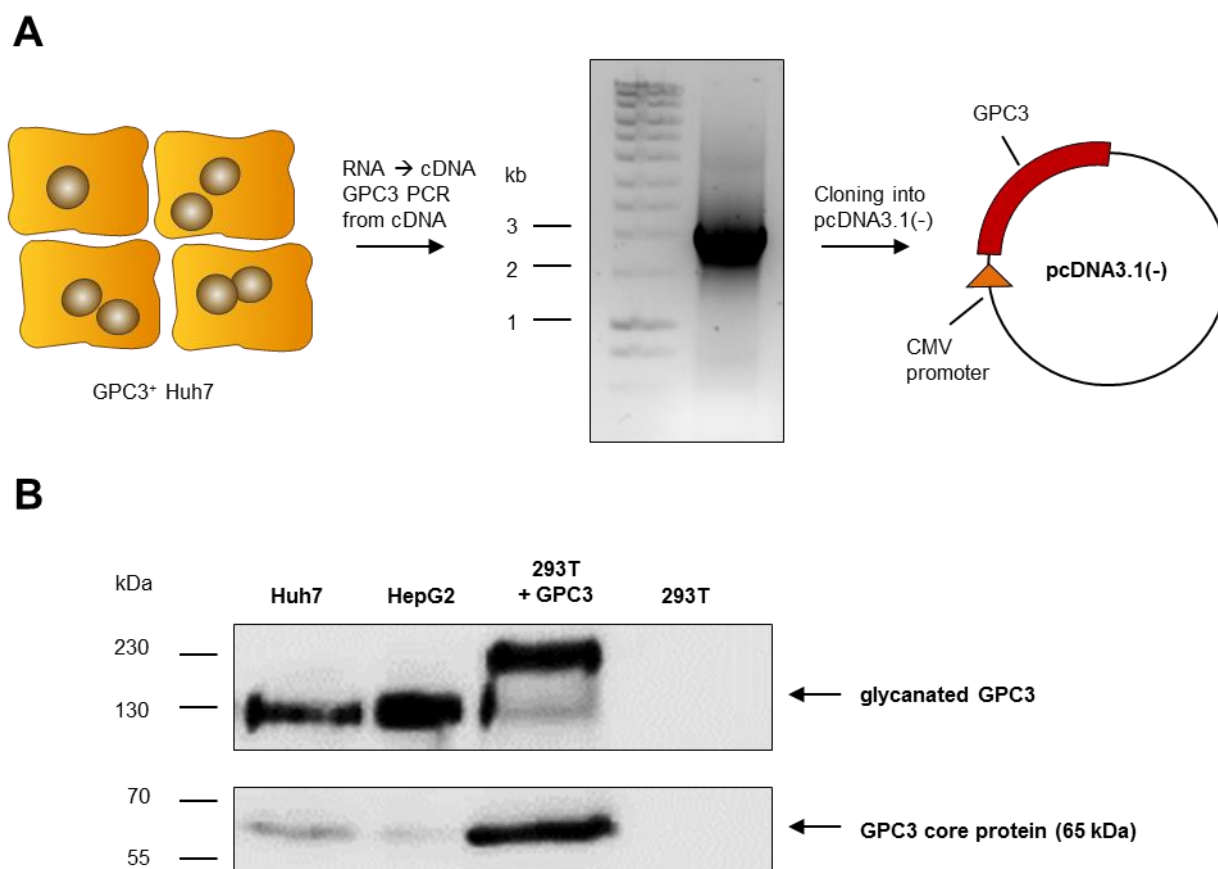


Figure 21 Construction and evaluation of a GPC3 expression vector. (A) The GPC3 gene was amplified from cDNA derived from Huh7 cells and cloned into pcDNA3.1(-). **(B)** Expression of GPC3 after transient transfection of 293T with pcDNA3.1(-)GPC3. HepG2 and Huh7 cells were used as positive controls. Cell lysates were taken after 24 h and separated on a SDS-PAGE gel before Western blotting was performed. GPC3 was detected by monoclonal antibody staining.

4.5.1.2 Expression of GPC3 and HLA-A2 after *ivt*-RNA Electroporation of K562 cells

GPC3 and HLA-A2 RNA were *in vitro* transcribed and polyadenylated using the mMACHINE mMESSAGE T7 kit and Poly(A) tailing kit. RNA quality and stability was confirmed by RNA agarose gel electrophoresis. As expected *ivt*-RNA transcription of GPC3 and HLA-A2 resulted in products of 1.7 kb and 1.2 kb, respectively, corresponding to the size of the two genes. After polyadenylation approximately 300-500 bp were added (Figure 22 A).

To establish the electroporation protocol, K562 cells were transfected with *in vitro* transcribed and polyadenylated RNA. 91.8% of the GFP transfected K562 cells showed a positive signal 24 h after electroporation, confirming a very good transfection efficacy (Figure 22 B). Surface

expression of HLA-A2 and GPC3 in *ivt*-RNA pulsed K562 cells was investigated 24 h post electroporation by flow cytometry. HLA-A2 expression was detected in 31.4% and GPC3 in 80% of K562 cells (Figure 22 B). The mean fluorescent intensity (MFI) in HLA-A2 *ivt*-RNA pulsed cells was 264 compared to 115 in untreated K562. In GPC3 *ivt*-RNA electroporated cells MFI was 1683 compared to 132 in untreated cells.

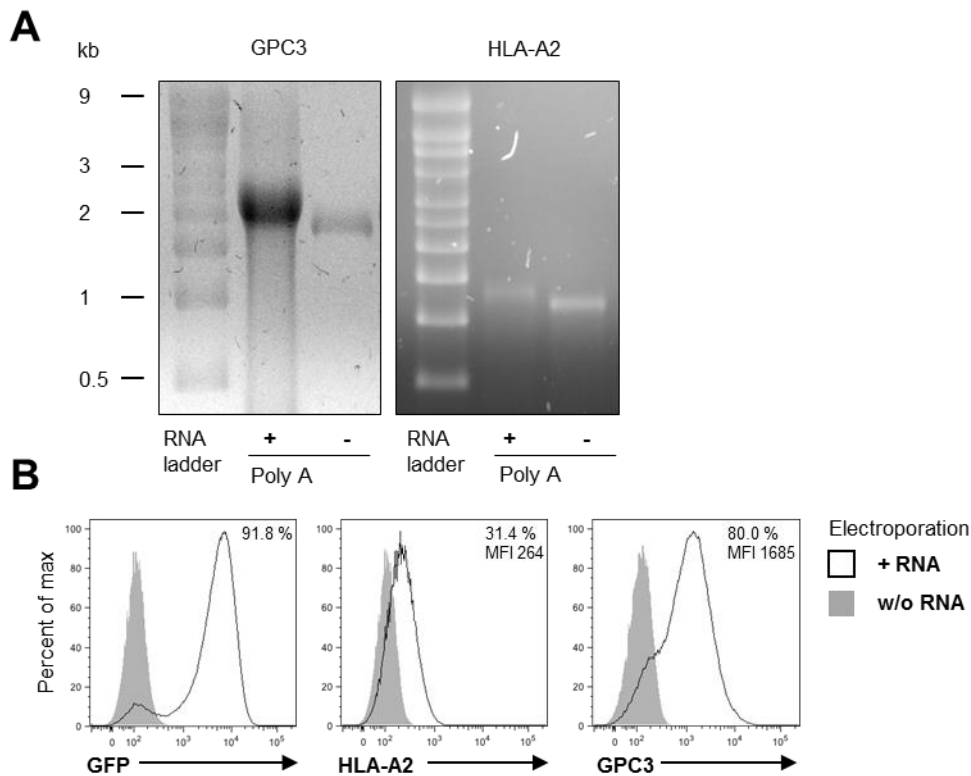


Figure 22 *In vitro* transcribed GPC3 and HLA-A2 RNA is expressed in K562 cells. (A) GPC3 and HLA-A2 RNA was *in vitro* transcribed and polyadenylated using a commercially available kit. RNA integrity and polyadenylation (PolyA +/-) was analysed by agarose gel electrophoresis. (B) K562 cells were electroporated with either 50 µg GFP, HLA-A2 or GPC3 *ivt*-RNA. Expression of GFP, HLA-A2 and GPC3 was analysed 24 h post electroporation by flow cytometry. Untreated K562 cells are represented by filled grey areas and *ivt*-RNA transfected K562 cells by black curves. Percentage of positive cells and MFI are shown in the upper right corner of each plot.

The suitability of *ivt*-RNA for expression of GPC3 and HLA-A2 in the performed experimental setup was thereby confirmed and GPC3 and HLA-A2 *ivt*-RNA could be used to express the proteins in moDC.

4.5.1.3 Maturation and GPC3 and HLA-A2 *ivt*-RNA Electroporation of DC

MoDC were generated by maturation of freshly isolated monocytes as described in Figure 20. Flow cytometry of moDC confirmed a mature phenotype with high CD80, CD83 and HLA-DR expression and low CD14 expression. Unspecific antibody binding was excluded by staining with an IsolG₁ antibody (Figure 23 A). MoDC were larger and showed clear formation of dendrites compared to their monocytic precursor cell (Figure 23 B).

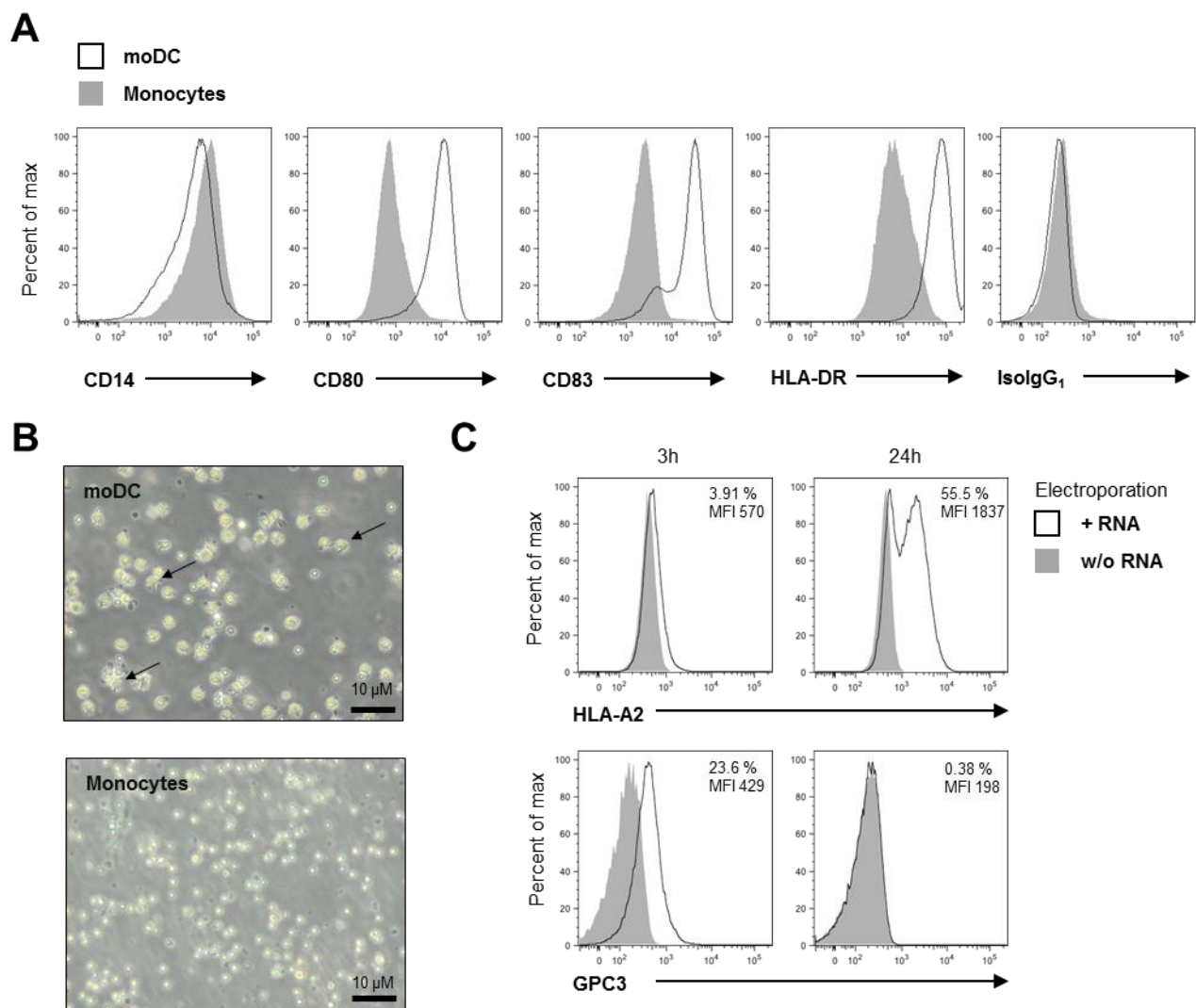


Figure 23 Generation of HLA-A2⁺ GPC3⁺ moDC for T cell stimulation. (A) Phenotype of monocytes and moDC. Expression of the cell surface molecules CD14, CD80, CD83 and HLA-DR on moDC was detected by flow cytometry. Staining with an IsolG₁ antibody is shown as a control. Monocytes are represented by filled grey areas and moDC by black curves. (B) The size and the morphology of monocytes and moDC was analysed by light microscopy. Arrows indicate dendrite formation. (C) MoDC were co-electroporated with HLA-A2 and GPC3 *ivt*-RNA. Expression of HLA-A2 and GPC3 was analysed 3 h and 24 h post electroporation by flow cytometry. Untreated moDC are represented by filled grey areas and *ivt*-RNA transfected moDC by black curves. Percent positive cells and MFI are shown in the upper right corner of each plot.

For T cell stimulation moDC must co-express GPC3 and HLA-A2, whereupon stable expression of HLA-A2 on the cell surface is crucial for efficient antigen presentation and T cell activation. Freshly prepared moDC were electroporated with *in vitro* transcribed and polyadenylated RNA. Surface expression of HLA-A2 and GPC3 in RNA pulsed moDC was investigated 3 h and 24 h post electroporation by flow cytometry. HLA-A2 expression was detected in 4% of moDC after 3 hours and increased to stable surface expression on 56% of moDC within 24 hours. In contrast GPC3 surface expression was detected in 24% of moDC after 3 h and not detectable anymore after 24 h (Figure 23 C). MFI in HLA-A2 *ivt*-RNA pulsed moDC increased from 570 after 3 h up to 1837 after 24 h compared to 480 in untreated moDC. The MFI of GPC3 was 592 and 198 after 3 h and 24 h, respectively. In untreated cells the MFI of GPC3 staining was 197. Untreated moDC were stained in the same manner and used as controls.

4.5.2 Stimulation of HLA-A2 Restricted GPC3-specific T cells with *ivt*-RNA Pulsed moDC

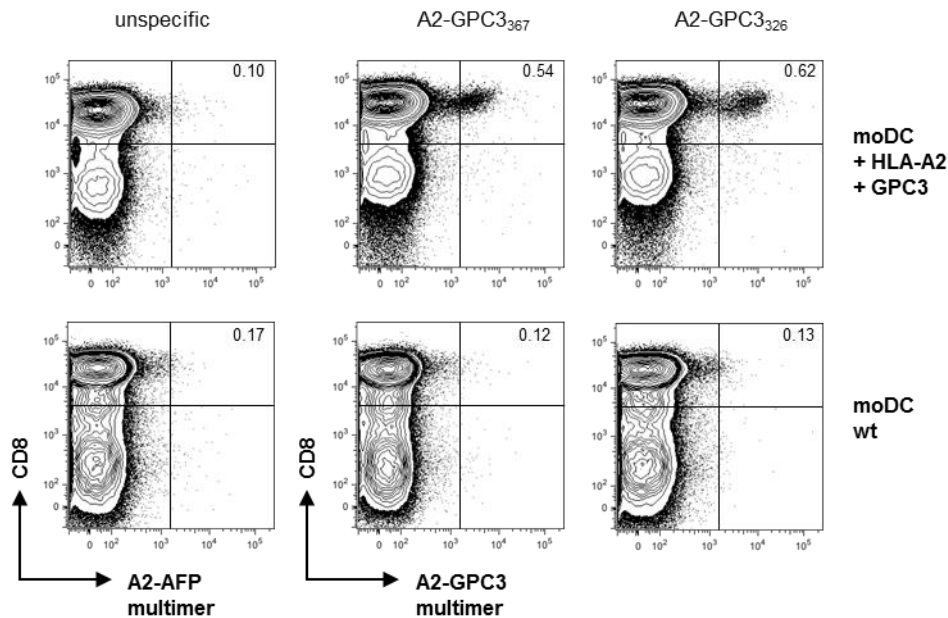
Freshly isolated autologous CD8⁺ enriched T cells were stimulated with freshly prepared GPC3⁺ HLA-A2⁺ moDC or untreated moDC on day 0 and day 7 as described in Figure 20. On day 14 T cells were stained with anti-CD8 and A2-GPC3 multimer or anti-CD137 for cell sorting.

4.5.2.1 Isolation of Multimer Sorted GPC3-specific T-cell Clones

Percentage of detected A2-GPC3 multimer positive CD8⁺ T cells differed clearly between T cell populations stimulated with HLA-A2⁺ GPC3⁺ and untreated moDC. 0.54% A2-GPC3₃₆₇ and 0.62% A2-GPC3₃₂₆ multimer⁺ CD8⁺ T cells were detected after stimulation with HLA-A2⁺ GPC3⁺ moDC (Figure 24 A). This double positive population was not visible (0.12% / 0.13%) after stimulation with untreated moDC and also not after staining with a multimer with irrelevant peptide (AFP₁₅₈) specificity (0.10%). After 7 days of *in vitro* expansion sorted A2-GPC3 multimer⁺ CD8⁺ T-cell lines were enriched to 61.2% and 20.5% double positive cells for multimer A2-GPC3₃₆₇ and A2-GPC3₃₂₆, respectively (Figure 24 B). Binding of multimers with

unrelated specificities was not observed. A2-GPC3 multimer⁺ CD8⁺ T cells were sorted and subsequently cloned by limiting dilution to obtain monoclonal T-cell clones that are specific for either GPC3₃₆₇ or GPC3₃₂₆.

A Day 14 – Bulk culture



B Day 21 – T-cell line

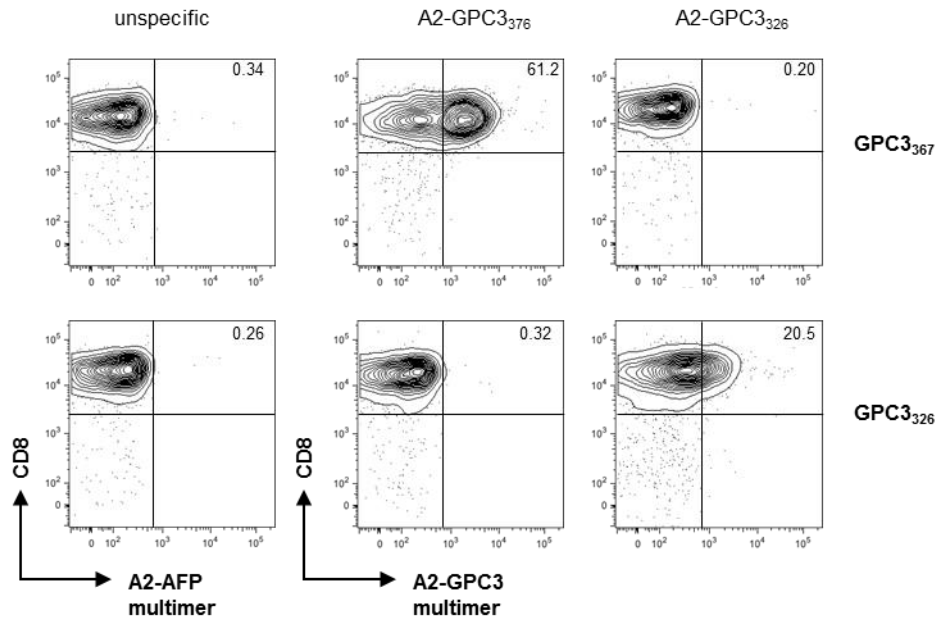


Figure 24 T cells stimulated with HLA-A2 and GPC3 *ivt*-RNA pulsed moDC show specific multimer binding. (A) Bulk T cell cultures after two cycles of stimulation and (B) A2-GPC3₃₆₇ or A2-GPC3₃₂₆ multimer enriched T-cell lines were stained with anti-CD8 antibody and A2-GPC3₃₆₇, A2-GPC3₃₂₆ or irrelevant multimer for cell sorting. T cells stimulated with GPC3 and HLA-A2 *ivt*-RNA pulsed moDC and untreated moDC were compared. Percentage of A2-GPC3 multimer⁺ CD8⁺ cells is shown in the upper right corner of each plot.

Binding of A2-GPC3₃₆₇ multimer (21-98%) was also confirmed in 16 established CD8⁺ T-cell clones (Figure 25 A). Multimer staining of 6 representative GPC3₃₆₇-specific T-cell clones and 1 inactive clone is shown. To investigate functional specificity of T-cell clones and the T-cell line we co-incubated them with peptide loaded T2 cells over 24 hours and measured IFN γ secretion from the supernatants. IFN γ was secreted by the T-cell line and 21 out of 107 screened T-cell clones after co-culture with GPC3₃₆₇ loaded T2 cells but not with T2 cells loaded with irrelevant peptide. 6 representative GPC3-specific T-cell clones, 1 allo-reactive and 1 inactive clone (neg) are shown as examples in Figure 25 B. Alloreactive T-cell clones showed high IFN γ secretion levels on target cells loaded with GPC3₃₆₇ as well as irrelevant peptide (Figure 25 B). Recognition of endogenously processed peptides by the T-cell line and by 17/21 selected T-cell clones was confirmed by co-incubation with HLA-A2⁺ GPC3⁺ HepG2 cells or HLA-A2⁻ GPC3⁺ Huh7 cells. IFN γ secretion was detected after co-incubation with HepG2 cells but not Huh7 cells, thus depended on GPC3 peptide presentation in context of HLA-A2 on the target cells (Figure 25 C).

Killing of peptide loaded T2 cells after 24 h of co-incubation with GPC3₃₆₇-specific T-cell clones was observed by light microscopy. T2 cells loaded with GPC3₃₆₇ were completely destroyed whereas T2 cells loaded with irrelevant peptide or without peptide showed no signs of cell death (Figure 25 D).

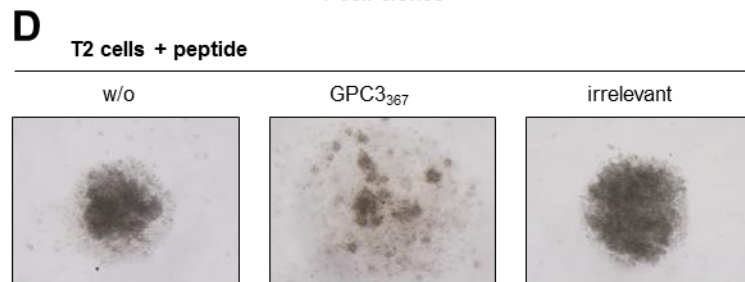
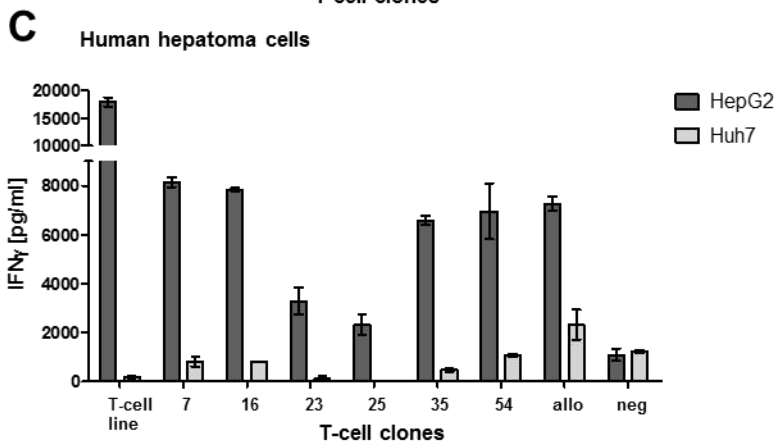
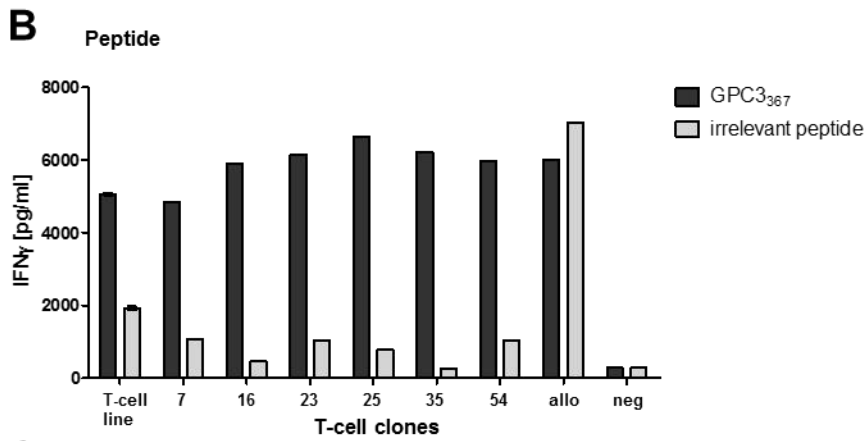
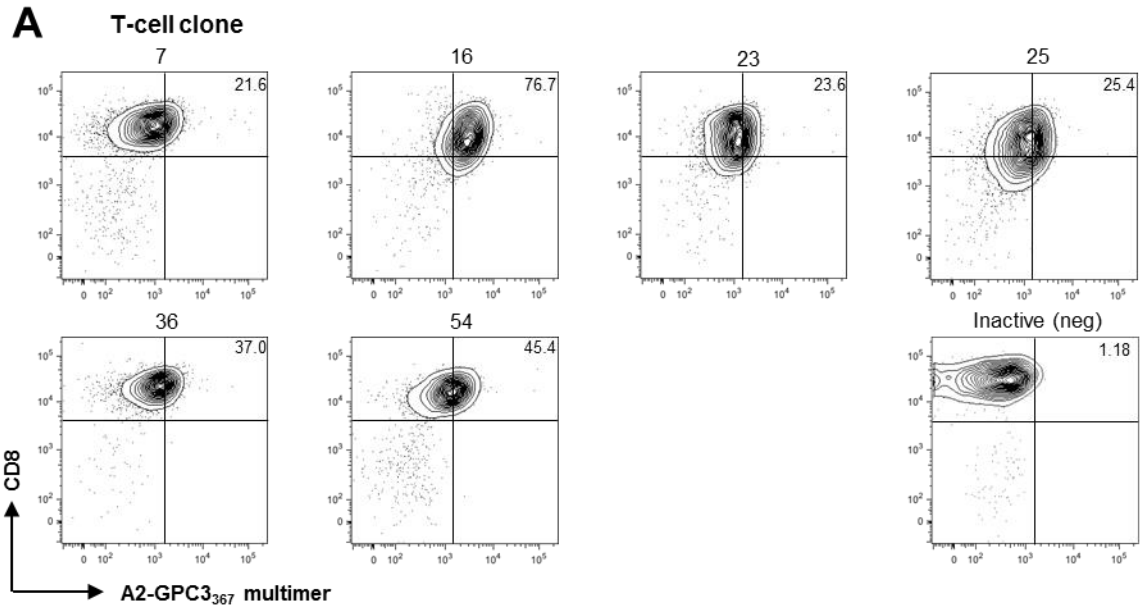


Figure 25 GPC3₃₆₇ sorted T-cell clones show streptamer binding and target cell specificity. (A) T-cell clones established by limiting dilution cloning were stained with anti-CD8 antibody and A2-GPC3₃₆₇ multimer for flow cytometry. Percentage of A2-GPC3 multimer⁺ CD8⁺ cells is shown in the upper right corner of each plot. **(B)** Peptide recognition of the A2-GPC3₃₆₇ multimer sorted T-cell line and derived T-cell clones was investigated using T2 cells loaded with GPC3₃₆₇ or irrelevant peptide. Supernatants were harvested after 24 h of co-culture and IFN γ levels were analysed by ELISA. E:T ratios of 0.2:1 were used. SD of triplicates are shown where possible. **(C)** Recognition of endogenously processed peptide was analysed by co-incubation of the A2-GPC3₃₆₇ multimer sorted T-cell line and derived T-cell clones with human hepatoma cells HepG2 (HLA-A2⁺ GPC3⁺) or Huh7 (HLA-A2⁻ GPC3⁺). IFN γ secretion was analysed after 24 h. E:T ratios of 0.2:1 were used. SD of triplicates are shown.

Results obtained for T-cell clones derived from CD8⁺ A2-GPC3₃₂₆ multimer sorted T cell populations were similar, although only two clones (Clone 5 and 7) showed high percentage of A2-GPC3₃₂₆ multimer binding in the CD8⁺ T cell population with 41% and 67%, respectively. Clone 8, 20 and 23 showed only low percentage of A2-GPC3₃₂₆ multimer⁺ CD8⁺ T cells (< 20%). Compared to clone 19 several clones were not purely CD8⁺ indicating an oligoclonal instead of a monoclonal phenotype (Figure 26 A). Multimer staining of 6 representative GPC3₃₂₆-specific T-cell clones and 1 inactive clone is shown, in total 15 T-cell clones showed at least low percentage of A2-GPC3₃₂₆ multimer⁺ CD8⁺ T cells, comparable to clone 8, 20 and 23.

As described above target cell specificity was investigated by measurement of IFN γ secretion after co-incubation with peptide loaded T2 cells or human hepatoma cells. 6 representative GPC3-specific T-cell clones, 1 allo-reactive and 1 inactive clone (neg) are shown. 25 out of 57 screened clones were identified to be GPC3₃₂₆-specific by detection of specific IFN γ secretion on GPC3₃₂₆ loaded T2 cells (Figure 26 B). 13 out of these 25 pre-selected clones furthermore secreted IFN γ when co-incubated with HLA-A2⁺ GPC3⁺ HepG2 cells (Figure 26 C). No IFN γ secretion was observed from those clones after co-incubation with T2 cells loaded with irrelevant peptide or without peptide or Huh7 cells. For the parental T-cell line specific IFN γ secretion was observed on peptide loaded T2 cells as well. The T-cell line could not be used in the IFN γ secretion assay on HepG2 cells, because available cell numbers were too low.

Killing of GPC3₃₂₆ peptide loaded T2 cells after 24 h of co-incubation with GPC3₃₂₆-specific T-cell clones was observed by light microscopy (data not shown) comparable to the GPC3₃₆₇-specific T-cell clone shown in Figure 25 D.

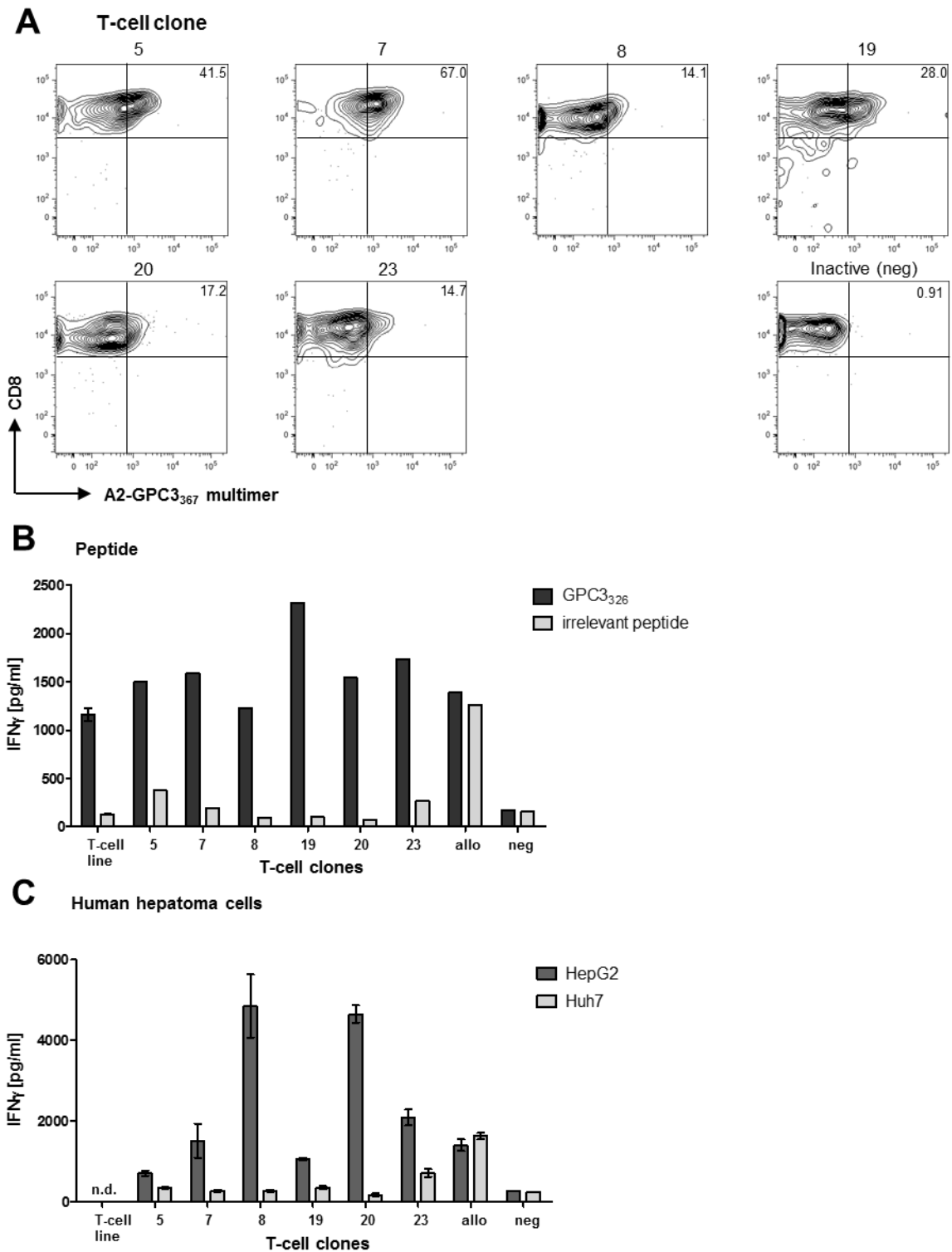


Figure 26 GPC3₃₂₆ sorted T-cell clones show streptamer binding and target cell specificity. (A) T-cell clones established by limiting dilution cloning were stained with anti-CD8 antibody and A2-GPC3₃₆₇ multimer for cell sorting. Percentage of A2-GPC3₃₆₇⁺ CD8⁺ cells is shown in the upper right corner of each plot. (B) Peptide recognition of the A2-GPC3₃₂₆ multimer sorted T-cell line and derived T-cell clones was investigated using T2 cells loaded with GPC3₃₂₆ or irrelevant peptide. Supernatants were harvested after 24 h of co-culture and IFN γ levels were analysed by ELISA. E:T ratios of 0.2:1 were used. SD of triplicates are shown where possible. (C) Recognition of endogenously processed peptide was analysed by co-incubation of the A2-GPC3₃₆₇ multimer sorted T-cell line and derived T-cell clones with human hepatoma cells HepG2 (HLA-A2⁺ GPC3⁺) or Huh7 (HLA-A2⁻ GPC3⁺). IFN γ secretion was analysed after 24 h. E:T ratios of 0.2:1 were used. SD of triplicates are shown.

4.5.2.2 Isolation of CD137 Sorted GPC3-specific T-cell Clones

An alternative attempt to sort activated T cells has been performed utilizing CD137 expression. CD137 is a co-stimulatory and anti-apoptotic molecule that promotes proliferation and survival of T cells. By sorting with A2-GPC3₃₂₆ and A2-GPC3₃₆₇ multimer only two defined specificities can be detected. However the T cells were stimulated with moDC that expressed the whole GPC3 protein therefore all possible epitopes can be presented and T cells with specificities against the complete range of GPC3 epitopes can be stimulated. 24 h after T cell stimulation CD137 is up-regulated, allowing for isolation of antigen-specific CD8⁺ T cells independent of prior knowledge of the specific epitopes recognized (95).

After stimulation with HLA-A2⁺ GPC3⁺ moDC, 5.72% of CD8⁺ T cells expressed CD137 compared to 2.07% and 0.4% after stimulation with wt moDC and without moDC stimulation, respectively (Figure 27A). In Figure 27 B a quantification of CD137 expression levels and IFN γ secretion levels 24 h post restimulation with moDC are shown. Both CD137 and IFN γ secretion were highest in T cells that have been stimulated with HLA-A2⁺ GPC3⁺ moDC.

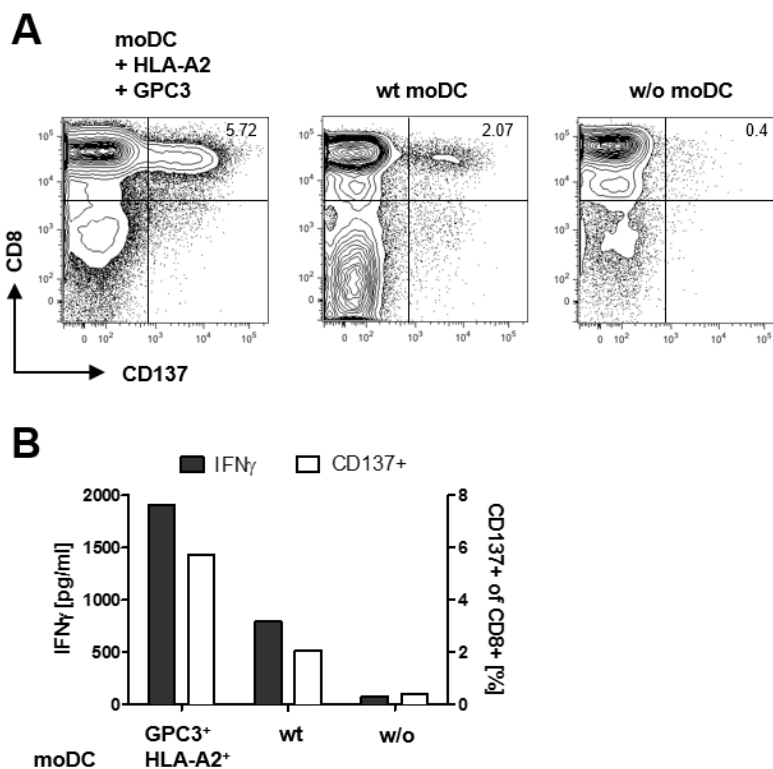
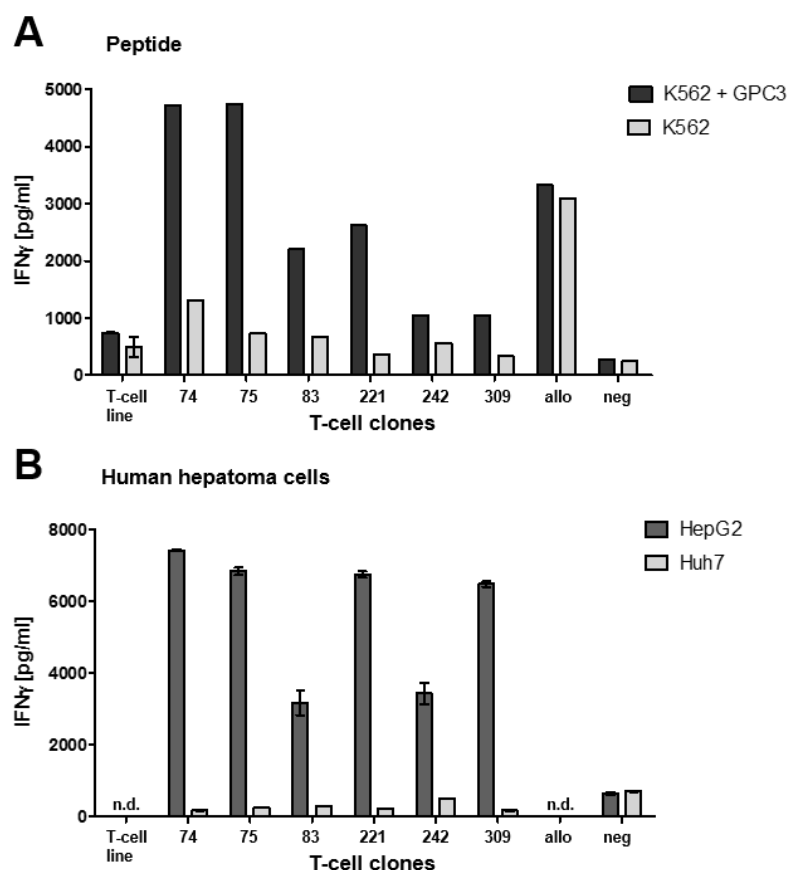


Figure 27 T cells stimulated with HLA-A2 and GPC3 *ivt*-RNA pulsed moDC upregulate CD137. (A) Bulk T cell cultures after two cycles of stimulation were restimulated with freshly prepared moDC, incubated for 24 h and stained with anti-CD8 and anti-CD137 antibody for cell sorting. T cells stimulated with GPC3 and HLA-A2 *ivt*-RNA pulsed moDC and untreated moDC were compared. Percentage of CD137⁺ CD8⁺ cells is shown in the upper right corner of each plot. (B) Quantification of CD137 expression and IFN γ secretion 24 h after restimulation with moDC.

CD137⁺ CD8⁺ T cells were sorted and cloned by limiting dilution to obtain monoclonal T-cell clones. To investigate their functional specificity, T-cell clones and the T-cell line were co-incubated with GPC3 *ivt*-RNA pulsed HLA-A2⁺ K562 cells or wt HLA-A2⁺ K562 cells for 24 h and IFN γ secretion was measured from the supernatants. 19 out of 318 screened T-cell clones secreted IFN γ on GPC3 expressing K562 cells but not wt K562 cells (Figure 28 A). The T-cell line, 6 representative GPC3-specific T-cell clones, 1 allo-reactive and 1 inactive clone (neg) are shown. Furthermore we confirmed recognition of endogenously processed peptides by 10 out of 19 pre-selected T-cell clones by co-incubation with HLA-A2⁺ GPC3⁺ HepG2 cells or HLA-A2⁻ GPC3⁺ Huh7 cells. IFN γ secretion was detected after co-incubation with HepG2 cells but not Huh7 cells (Figure 28 B). T-cell clones derived from CD137 sorted T cell populations showed no binding of A2-GPC3₃₂₆ or A2-GPC3₃₆₇ multimer (data not shown).

Figure 28 CD137 sorted T-cell clones show target cell specificity. (A) GPC3 peptide recognition of the CD137 sorted T-cell line and derived T-cell clones was investigated using K562 cells pulsed with GPC3 RNA or wt K562 cells. Supernatants were harvested after 24 h of co-culture and IFN γ levels were analysed by ELISA. E:T ratios of 0.2:1 were used. SD of triplicates are shown where possible. (B) Recognition of endogenously processed peptide was analysed by co-incubation of the CD137 sorted T-cell line and derived T-cell clones with human hepatoma cells HepG2 (HLA-A2⁺ GPC3⁺) or Huh7 (HLA-A2⁻ GPC3⁺). IFN γ secretion was analysed after 24 h. E:T ratios of 0.2:1 were used. SD of triplicates are shown.

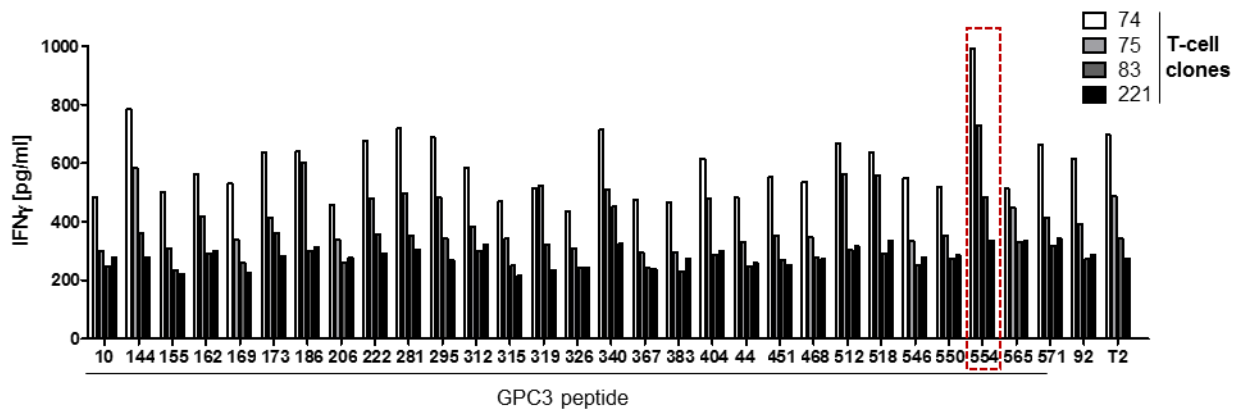


As explained above

CD137 sorted T-cell clones were isolated independent of prior knowledge of the specific epitopes they recognize. However the knowledge of the recognized epitope is essential for a

possible therapeutically application of a TCR in future. Therefore we investigated the GPC3 epitope specificity of CD137 sorted T-cell clones. T2 cells were loaded with 30 single GPC3 epitopes that have been chosen because of their high prediction score in different data bases (Table 24).

A



B

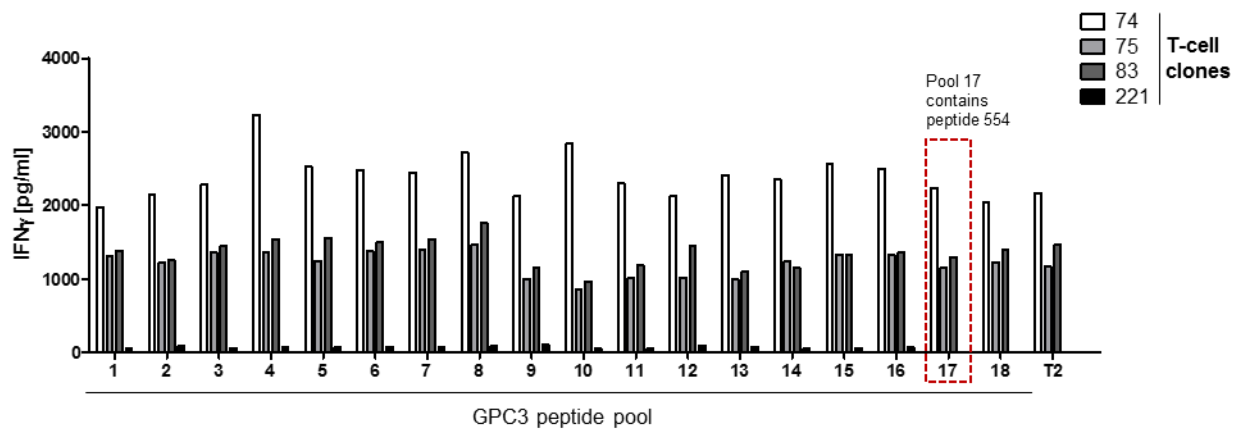


Figure 29 Peptide specificity of the CD137 sorted T-cell clones was investigated using T2 cells loaded with single GPC3 peptides (A) or GPC3 peptide pools (B). Supernatants were harvested after 24 h of co-culture and IFN γ levels were analysed by ELISA. E:T ratios of 1:1 were used. Responses to peptide 554 and pool 17 loaded target cells are highlighted with a red box.

Results for 4 pre-selected CD137 sorted T-cell clones are shown representatively for 19 clones that were assayed in this experiment (Figure 29 A). IFN γ secretion in response to T2 cells loaded with peptide GPC3₅₅₄ (red box) was increased in 7 clones, among them clone 74, 75 and 83 shown in Figure 29 A. To verify GPC3₅₅₄ specificity of those clones, T2 cells were loaded with GPC3 peptide pools consisting of 10 overlapping peptides each (96). IFN γ

secretion levels were independent of the peptide pools loaded to the target cells (Figure 29 B). Specificity against GPC3₅₅₄ or any other GPC3 epitope could therefore not be confirmed.

4.6 TCR Identification, Cloning, and Expression in Human T cells

After successful stimulation and isolation of GPC3-specific HLA-A2 restricted T-cell clones their corresponding TCR repertoire was analysed. Since TCR identification and evaluation of their functionality is costly and time consuming it was decided only to perform the investigation for T-cell clones with known specificities. The TCR repertoire of CD137 sorted T-cell clones was therefore not examined. Analysis of the TCR repertoire allows not only the identification of the TCR but also to draw conclusions about the clonality of the clones that were generated by limiting dilution cloning. Degenerated primers were used for the identification of α - and β -repertoire as described in 3.7.3. In brief RNA was isolated and transcribed into cDNA, which was then used to amplify the variable parts of the TCR α - and β -chains. PCR products were purified, sequenced and analysed with help of the data base IMGT/V-QUEST (Figure 30).

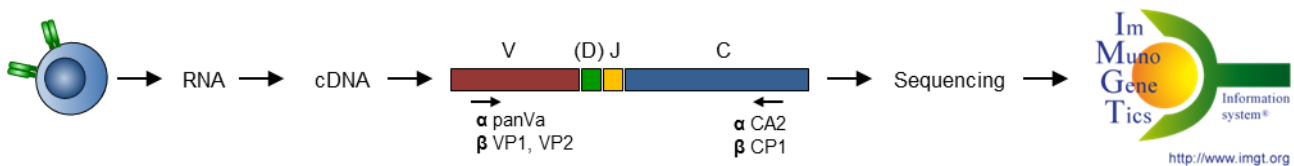


Figure 30 Schematic illustration of the TCR repertoire analysis of GPC3-specific T-cell clones. RNA was isolated from T-cell clones using Trizol and was transcribed into cDNA applying Invitrogen's superscript III kit. cDNA was used to amplify variable parts of α - and β -chains, which were gel purified, sequenced and analysed with IMGT/V-QUEST.

In Figure 31 (A and B), agarose gel electrophoresis of TRAV and TRBV PCR products are shown for one exemplary GPC3₃₆₇-specific T-cell clone. Expected PCR product size for TRAV and TRBV were 300-500 bp. Sequencing of gel-purified PCR products revealed one identical TCR sequence to be expressed in all GPC3₃₆₇-specific T-cell clones. The identified TCR consisted of TRBV30*01 and TRAV8-3*02 according to the IMGT nomenclature. These data suggests that all analysed GPC3₃₆₇-specific T-cell clones originated from the same clonal T cell.

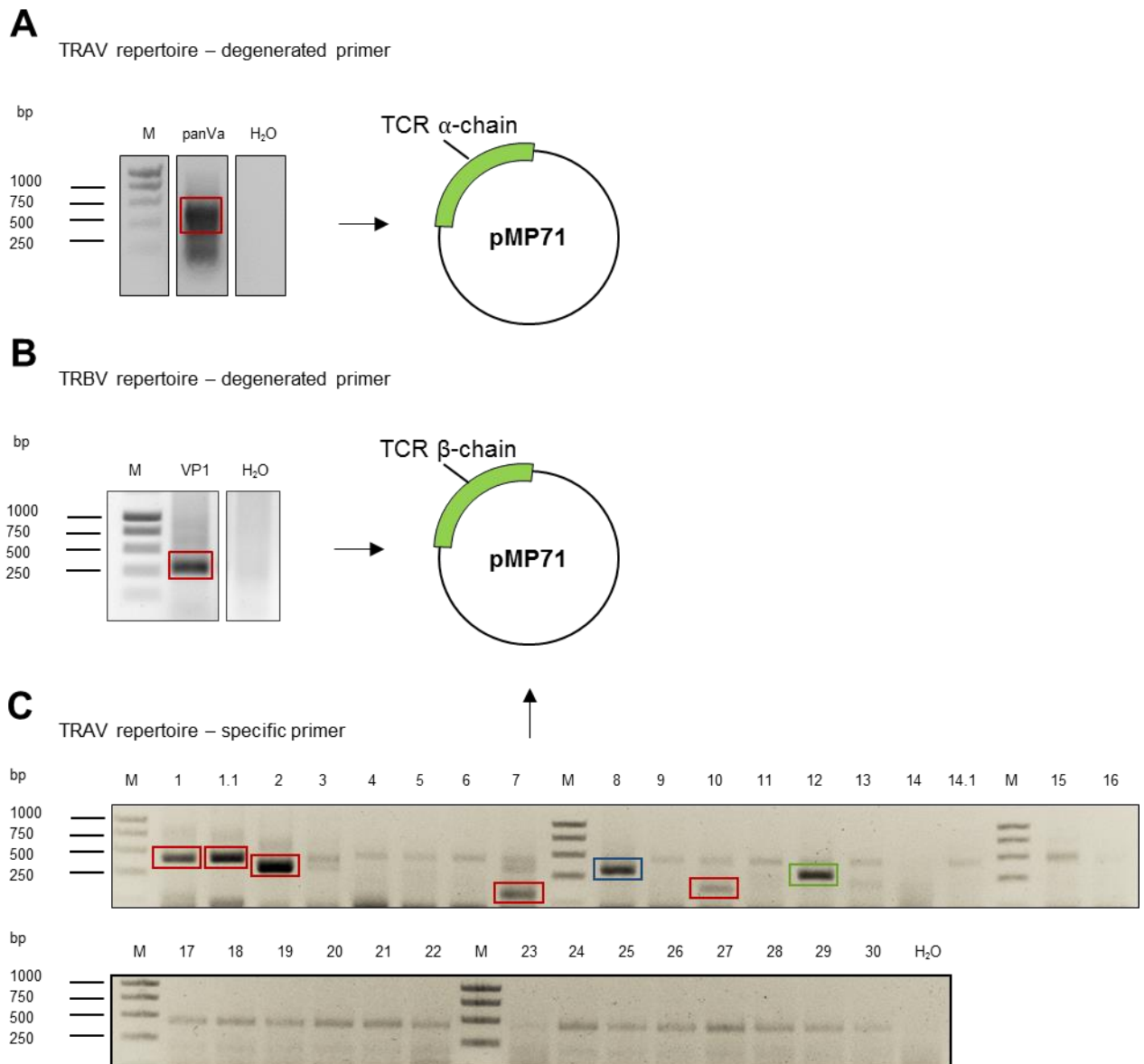


Figure 31 The TCR $\alpha\beta$ repertoire from functional T-cell clones was examined by PCR with degenerated primers. PCR products were purified by agarose gel electrophoresis and sequenced. Gel electrophoresis of TRAV (A) and TRBV (B) from one representative GPC₃₆₇-specific T-cell clone amplified by PCR with degenerated primers. (C) Gel electrophoresis of TRAV from one GPC₃₂₆-specific T-cell clone amplified by PCR with specific primers. PCR reactions with two primers pairs were performed. One amplifying the variable part of the α -chain the other amplifying a part of the constant domain, thereby serving as an internal control. Purified and analysed bands are indicated by boxes. Red: TRAV12-2*01, blue: TRAV13-1*02, green: TRAV19*01.

The TRBV sequence GPC₃₂₆-specific T-cell clones was assayed with degenerated primers as explained above. 5 out of 25 GPC₃₂₆-specific T-cell clones expressed one identical $\nu\beta$ -chain, namely TRBV9*01. Analysis of the TRAV repertoire of those GPC₃₂₆-specific T-cell clone was not possible using degenerated primers. Hence, a PCR with primers specific for one TRAV allele each was performed. Additionally an internal control, amplifying a part of the

constant region was run in each of that reactions. Expected PCR product size for TRAV and the internal control were 370-500 bp and 550 bp, respectively.

Analysis with specific primers revealed three different alpha chains to be expressed by GPC3₃₂₆-specific T-cell clones (Table 26). The remaining 20 GPC3₃₂₆-specific T-cell clones were oligoclonal and analysis of the TCR repertoire with the methods applied in this study was not possible.

Table 26 Identified TCR α - and β - chain sequences.

T-cell clones	IMGT			Arden	CDR3	
	V	D	J			
GPC3₃₆₇ (all clones)	α	TRAV8-3*02	-	TRAJ48*01	1S4	CAVGVLNFGNEKLTF
	β	TRBV30*01	TRBD1*01	TRBJ1-2*01	20S1	CAWSEDTAYYGTYF
GPC3₃₂₆ (5,7,20)		TRAV12-2*01	-	TRAJ45*01	2S1	CAGYSGGGADGLTF
	α	TRAV13-1*02 ¹	-	TRAJ54*01	8S1	CAASNGQGAQKLVF
		TRAV19*01	-	TRAJ6*01	12S1	CALSELASGGSYIPTF
	β	TRBV9*01	TRBD2*01	TRBJ2-7*01	1S1	CASSPGGIGYEQYF

¹ Identified together with Laura Hannemann

In Table 26 results of the TCR repertoire analysis of GPC3₃₂₆- and GPC3₃₆₇-specific T-cell clones are summarized. Taken together we identified one TCR consisting of defined α - and β - chains that were expressed by all GPC3₃₆₇-specific T-cell clones. From our GPC3₃₂₆-specific T-cell clones one β - and three α -chains were isolated. Experiments assessing the functionality of the different α - and β -chain pairs have been performed together with Laura Hannemann in her Master thesis. Here the combination TRBV9*01 and TRAV13-1*02 was identified to assemble to a GPC3₃₂₆-specific TCR, whereas combinations of TRBV9*01 with the other two α -chains showed no signs of functionality on GPC3₃₂₆ peptide loaded target cells or human hepatoma cells. Since those two TCRs represent the first GPC3₃₆₇- and GPC3₃₂₆-specific TCR isolated they are referred to as TCR P1-1 and TCR P2-1, with P1 coding for peptide GPC3₃₆₇

and P2 for GPC3₃₂₆. The α - and β -chains were amplified and cloned into pMP71 for expression in human T cells.

4.6.1 Expression and Functionality of TCRs Isolated from GPC3₃₂₆- and GPC3₃₆₇- specific T-cell clones

Before the TCRs were optimized and cloned into the final expression constructs their expression and functionality was assayed with precursor constructs, in which the isolated TCR α - and β -chain were cloned into the retroviral expression vector pMP71. As at this stage of the investigations the constructs are still preliminary. Therefore their precursor status is indicated in the nomenclature by an elevated pre in the end of their names.

To investigate whether the TCRs are expressed in donor cells, Jurkat cells were transduced (Figure 32 A). Expression of TCR P1-1^{pre} and TCR P2-1^{pre} was detected by staining with the IOTest TRBV staining kit. TCR P1-1^{pre} (TRBV30*01) and TCR P2-1^{pre} (TRBV9*01) were expressed in more than 90% of transduced Jurkat cells (Figure 32 B). In transduced T cells, TCR P1-1^{pre} was detected in 23.5% and TCR P2-1^{pre} in 20.3% of total T cells after staining with anti-TRBV. In addition to the TRBV staining, transduced T cells were stained with A2-GPC3 multimer. After TCR P1-1^{pre} transduction only 3.4% of T cells bound multimer A2-GPC3₃₆₇. In TCR P2-1^{pre} transduced cells no A2-GPC3₃₂₆ multimer binding was detected (Figure 32 B).

Assessment of the functionality revealed that the TCR P1-1^{pre} enables T cells to secrete IFN γ on target cells loaded with the specific GPC3 peptide (Figure 32 C) and to reduce viability of HepG2 cell by 10% after 24 h (Figure 32 D). Compared to that results obtained from TCR P2-1^{pre} transduced T cells were not convincing. No killing of HepG2 cells was observed, however secretion of IFN γ was higher on GPC3₃₂₆ loaded T2 cells compared to mock loaded targets. Since both expression and functionality was demonstrated for TCR P1-1^{pre} it was decided to further develop and investigate this receptor. Evaluation of the TCR P2-1^{pre} is currently performed in our laboratory and therefore not part of this thesis.

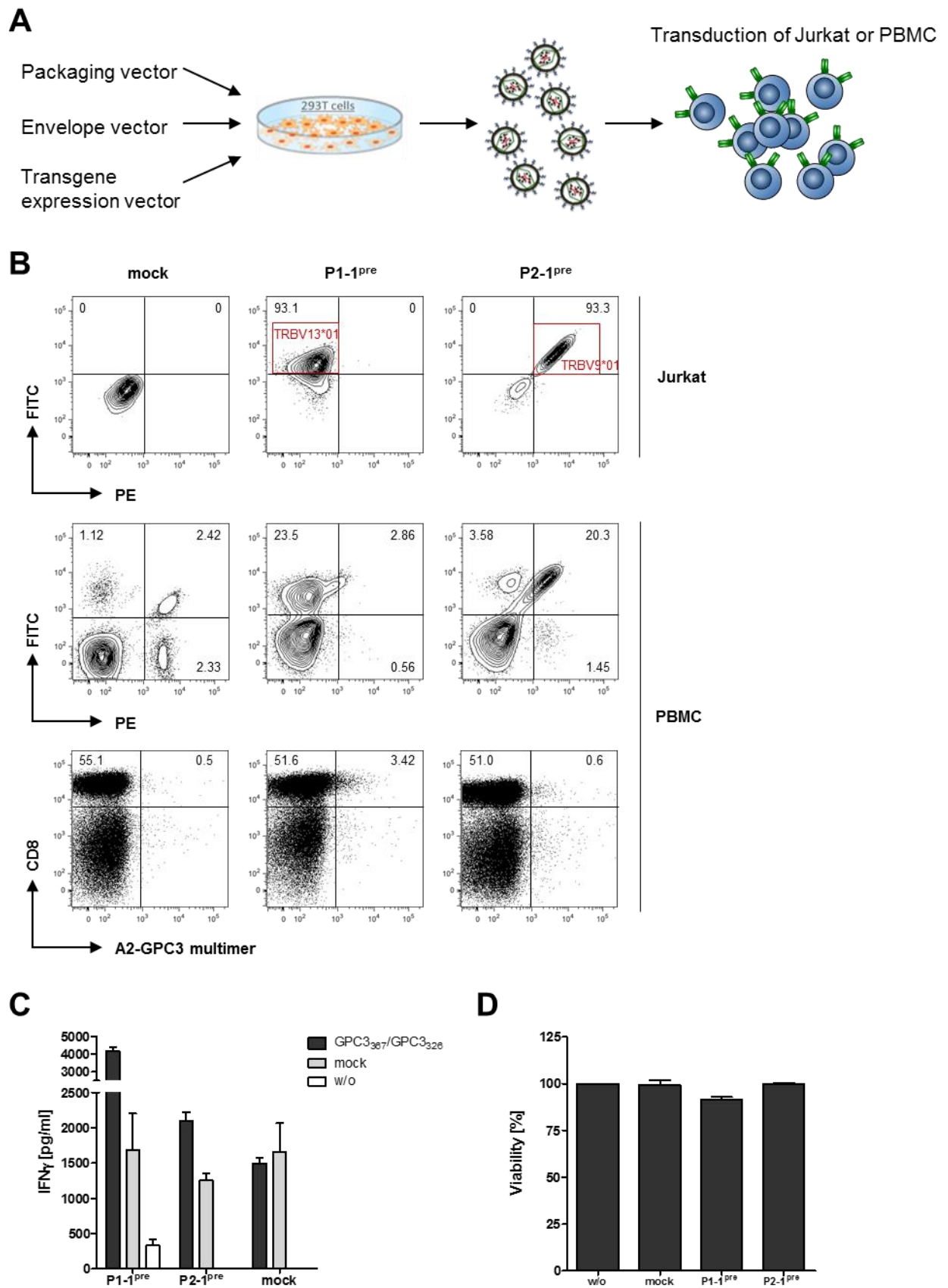


Figure 32 TCR P1-1^{pre} and TCR P2-1^{pre} were expressed in Jurkat cells and human T cells. (A) Schematic illustration of the transduction process. 293T cells were co-transfected with plasmids coding for the TCR α - and β -chains, packaging and envelope proteins. The retrovirus containing supernatant is used for transduction of human T cells. (B) Jurkat cells and T cells of healthy donors were transduced with TCR P1-1^{pre} and TCR P2-1^{pre}. Expression of the TCR in CD8⁺ T cells was analysed on day 4 post transduction by

flow cytometry after staining with A2-GPC3 multimer or anti-TRBV antibody. Anti-TRBV30*01 (TCR P1-1^{pre}) is FITC labelled. Anti-TRBV9*01 (TCR P2-1^{pre}) is FITC and PE labelled. Percentage of positive cells detected are shown in the upper right or left corner. T cells transduced with a mock TCR are shown as controls. (B) Functionality of TCR P1-1^{pre} and TCR P2-1^{pre} expressing T cells was assayed by co-incubation with peptide loaded T2 cells. IFN γ secretion was measured after 24 h of co-incubation. (C) Killing of HepG2 cells was detected via viability measurement after 24 h using the CellTiter-Blue[®] Cell Viability Assay. E:T ratios of 2:1 were used. SD of triplicates are shown.

4.6.2 Optimization of P1-1 for Expression in Human T cells

The TRAV and TRBV sequence of the identified TCR P1-1^{pre} were codon optimized for increased expression (Figure 33 A) and cloned into the retroviral vector pMP71 for transfer into human T cells connected by a P2A element to allow equimolar expression. The originated TCR is from now on referred to as TCR P1-1 (Figure 33 B).

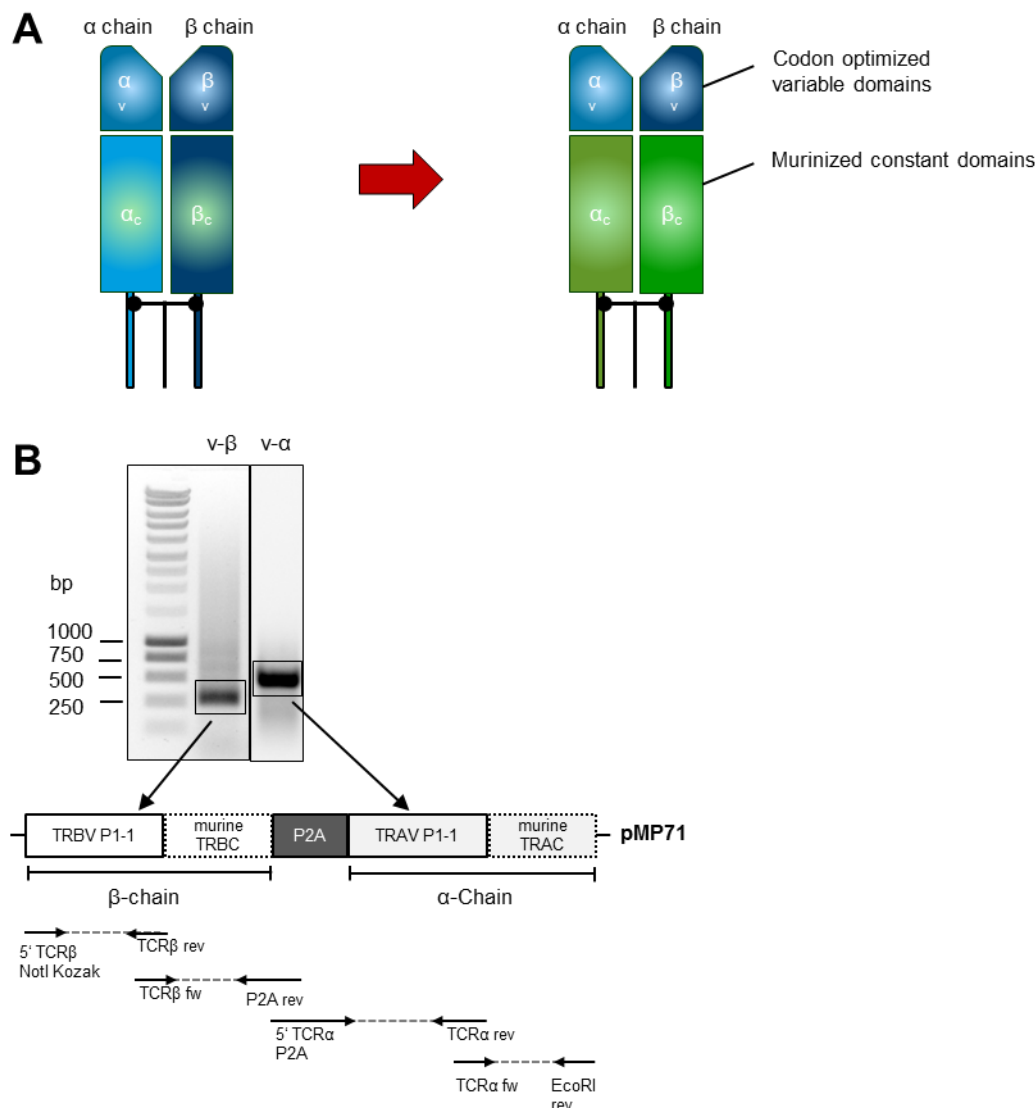


Figure 33 Optimization of P1-1 for expression in human T cells. (A) The $\nu\alpha\beta$ segments of TCR P1-1^{pre} were codon optimized for optimal expression in human cells. Constant domains were murinized to improve pairing of the two chains and avoid miss-pairing with endogenously expressed TCR chains. (B) Optimized TRAV and TRBV sequences and murinized constant domains were cloned into the retroviral expression vector pMP71. Complete α - and β -chains were linked by a P2A element. A schematic representation of the TCR-P1-1 expression construct and the cloning strategy involving 3 annealing PCR reactions is shown.

Figure 34 shows the optimized TCR sequence of P1-1. TRAV, TRAC, TRBV and TRBC gene segments and CDR regions are indicated.

```

ATG CTG TGT TCT CTG CTG GCT CTG CTG CTG GGC ACC TTC TTT GGA GTG CGG AGC CAG ACC TRBV P1-1
ATC CAC CAG TGG CCT GCT ACA CTG GTG CAG CCT GTG GGC AGC CCT CTG AGC CTG GAA TGT
ACC GTG GAA CDR1 GGC ACC AGC AAC CCC AAC CTG TAC TGG TAC AGA CAG GCC GCT GGC AGA GGC
CTG CAG CTG CTG TTT TAC CDR2 AGC GTG GGC ATC GGC CAG ATC AGC AGC GAG GTG CCC CAG AAT
CTG AGC GCC AGC AGA CCC CAG GAC CGG CAG TTT ATC CTG AGC AGC AAG AAG CTG CTG CTG
AGC GAC AGC GGC TTC TAC CTG TGC CDR3 GCT TGG AGC GAG GAC ACC GCC TAC TAC GGC TAC ACC
TTT GGC AGC GGC ACC CGG CTG ACA GTG GTG GAA GAA GAT CTG AGG AAC GTG ACC CCC CCC murine TRBC
F
AAG GTG TCC CTG TTC GAG CCC AGC AAG GCC GAG ATC GCC AAC AAG CAG AAA GCC ACC CTC
GTG TGC CTG GCC AGA GGC TTC TTC CCC GAC CAC GTG GAA CTG TCC TGG TGG GTC AAC GGC
AAA GAG GTG CAC AGC GGA GTC TGC ACC GAC CCC CAG GCT TAC AAA GAG AGC AAC TAC AGC
TAC TGC CTG TCC AGC AGA CTG CGG GTG TCC GCT ACC TTC TGG CAC AAC CCC CGG AAC CAC
TTC AGA TGC CAG GTG CAG TTC CAC GGC CTG AGC GAA GAG GAC AAG TGG CCC GAG GGC AGC
CCC AAG CCC GTG ACC CAG AAT ATC AGC GCC GAG GCC TGG GGC AGA GCC GAT TGT GGC ATC
ACC AGC GCC AGC TAC CAC CAG GGG GTG CTG AGC GCC ACC ATC CTG TAC GAG ATC CTG CTG
GGC AAG GCC ACC CTG TAC GCC GTG CTG GTG TCC GGA CTG GTG CTG ATG GCC ATG GTC AAG
AAG AAG AAC AGC GGC AGC GGC GCC ACC AAC TTC AGC CTG CTG AAG CAG GCC GGC GAC GTG P2A
GAA GAG AAC CCC GGG CCC ATG CTG CTG GAA CTG ATC CCT CTG CTG GGC ATC CAC TTC GTG TRAV P1-1
CTG AGA ACC GCC AGA GCC CAG AGC GTG ACC CAG CCC GAT ATC CAC ATC ACC GTG TCT GAG
GGC GCC AGC CTG GAA CTG CGG TGC AAC TAC AGC CDR1 TAC GGC GCC ACC CCC TAC CTG TTT TGG
TAC GTG CAG AGC CCC GGA CAG GGC CTG CAG CTG CTG CTG AAG CDR2 TAC TTT AGC GGC GAC ACC
CTG GTG CAG GGC ATC AAG GGA TTC GAG GCC GAG TTC AAG CGG AGC CAG AGC AGC TTC AAC
CTG CGG AAG CCC TCC GTG CAT TGG AGC GAC GCC GCC GAG TAC TTT TGT CDR3 GCC GTG GGC GTG
CTG AAC TTC GGC AAC GAG AAG CTG ACC TTT GGC ACC GGC ACC CGG CTG ACC ATC ATC CCT
L N F G N E K L T F C A V G V
ATC CAG AAC CCC GAG CCC GCC GTG TAC CAG CTG AAG GAC CCC AGA AGC CAG GAC AGC ACC murine TRAC
CTG TGT CTG TTC ACC GAC TTC GAC AGC CAG ATC AAC GTG CCC AAG ACC ATG GAA AGC GGC
ACC TTC ATC ACC GAT AAG TGC GTG CTG GAC ATG AAG GCC ATG GAC AGC AAG AGC AAC GGC
GCC ATT GCC TGG TCC AAC CAG ACC AGC TTC ACA TGC CAG G AC ATC TTC AAA GAG ACA AAC
GCC ACC TAC CCT TCC AGC GAC GTG CCC TGT GAC GCC ACC CTG ACC GAG AAG TCC TTC GAG
ACA GAC ATG AAT CTG AAT TTC CAG AAC CTG AGC GTG ATG GGC CTG CGG ATC CTG CTG CTG
AAA GTG GCC GGC TTC AAC CTG CTG ATG ACC CTG CGG CTG TGG TCC AGC TGA

```

Figure 34 Nucleic acid sequence of TCR P1-1. Gene segments are indicated with different colours and CDR regions are designated with black boxes. AA sequence of the TCR junctions are shown below the nucleotide sequence.

4.7 Functionality of TCR P1-1 *In Vitro* and *In Vivo*

Expression of TCR P1-1 was introduced into human T cells by retroviral transfer utilizing the envelope of MLV-10A1 (78). Surface expression of TCR P1-1 was detected by A2-GPC3₃₆₇ multimer staining in 9% of the total lymphocyte population and 46% of CD8⁺ T cells (Figure 35). The same expression levels were detected by staining with an anti-TRBV antibody. No multimer binding (0.03%) and anti-TRBV staining (0.15%) was detected in mock transduced T cells. No multimer staining in TCR P1-1 transduced T cells could be detected using the irrelevant multimer A2-AFP₃₂₅ (0.7%; data not shown). A2-GPC3₃₆₇ multimer staining was detected in CD8⁺ T cells, but not in the CD8⁻CD4⁺ T cell compartment. Nevertheless anti-TRBV staining showed expression of TCR P1-1 also in CD4⁺ T cells. This observation is analysed and discussed in more detail in section 4.7.3.

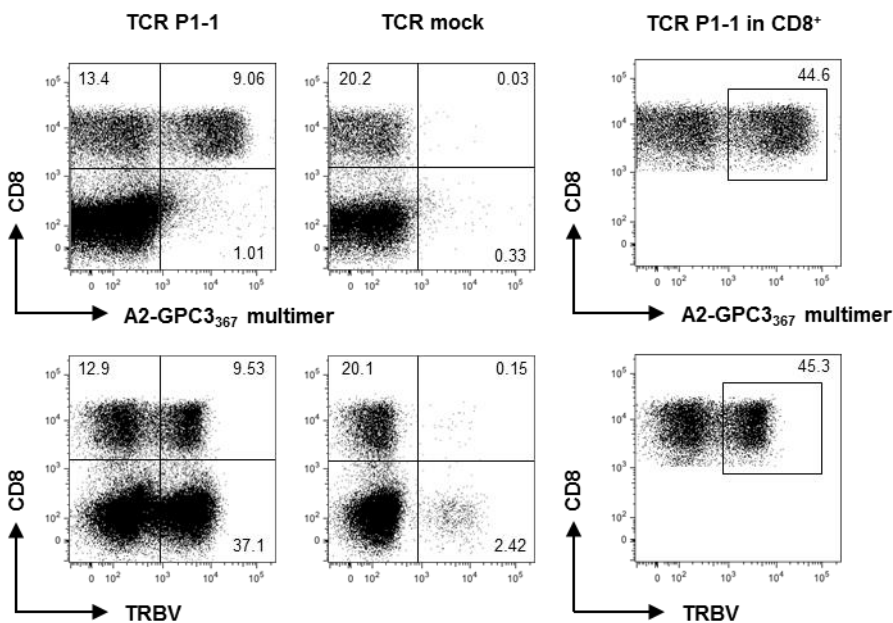


Figure 35 TCR P1-1 derived from GPC3₃₆₇-specific T-cell clones is expressed in donor T cells. T cells of healthy donors were transduced with TCR P1-1 or mock transduced. Expression of TCR P1-1 in CD8⁺ T cells was analysed on day 4 post transduction by flow cytometry after staining with A2-GPC3₃₆₇ multimer or and anti-TRBV antibody. Percentage of cells detected in each quadrant are shown.

4.7.1 Peptide Specificity and Cross-Reactivity of TCR P1-1 Grafted T cells

Peptide specificity of TCR P1-1 transduced T cells was first investigated by co-incubation of TCR P1-1⁺ T cells with peptide loaded T2 cells. High IFN γ secretion levels were observed after co-incubation with GPC3₃₆₇ loaded T2 cells but not with T2 cells loaded with an irrelevant

peptide or without peptide loading (Figure 36 A). Furthermore IFN γ secretion was assayed after co-culture with human hepatoma cells to verify recognition of endogenously processed peptides. IFN γ was secreted on HLA-A2⁺ GPC3⁺ HepG2 but not on Huh7 cells, which are GPC3⁺ but HLA-A2⁻ (Figure 36 A). Finally, IFN γ secretion after co-culture with human PBMC from HLA-A2 positive and HLA-A2 negative donors was analysed to exclude fratricide by TCR P1-1 transduced T cells. No IFN γ secretion above background level was detected (Figure 36 A).

To investigate the avidity of the TCR P1-1 we co-incubated TCR P1-1 transduced T cells with T2 cells loaded with titrated GPC3₃₆₇ peptide concentrations. Half maximal IFN γ secretion on peptide loaded T2 cells was observed with a peptide concentration of 0.1 μ M (Figure 36 B) indicating an intermediate functional avidity. IFN γ secretion on target cells with irrelevant or without peptide equalled IFN γ secretion levels detected with mock transduced T cells.

To evaluate the cross-reactivity of TCR P1-1 transduced T cells we analysed their IFN γ secretion after co-incubation with peptide loaded LCL that expressed different HLA allotypes. GPC3₃₆₇ presented on HLA-A*0201, 0202, 0207, 0216 and 0217 was recognized (Figure 36 C).

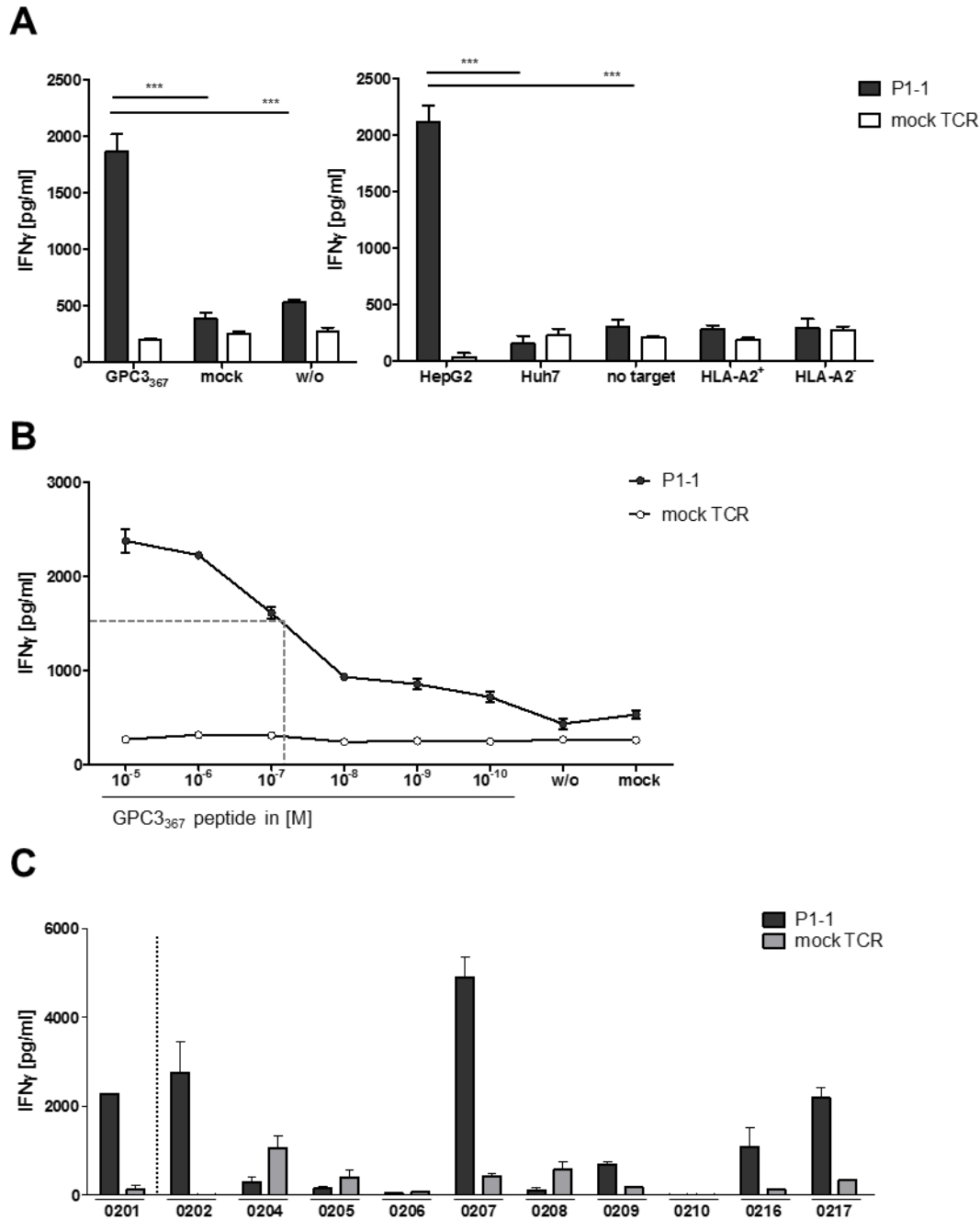


Figure 36 Peptide specificity and HLA-A2 dependency of TCR P1-1 expressing T cells. (A) To investigate peptide specificity of the TCR P1-1 we co-incubated TCR P1-1 and mock transduced T cells with T2 cells pulsed with 5 μ M GPC3₃₆₇ or irrelevant peptide or empty T2 cells. To evaluate recognition of endogenously processed peptide by TCR P1-1 transduced T cells the cells were co-cultured with human hepatoma cells HepG2 or Huh7. Co-culture with PBMC from HLA-A2⁺ or HLA-A2⁻ donors was performed to exclude fratricide by transduced T cells. IFN γ secretion was measured after 24 h of co-incubation from supernatants. (B) T2 cells were loaded with GPC3₃₆₇ peptide at titrated concentrations ranging from 10 μ M to 100 pM and used as target cells for TCR P1-1 and mock transduced T cells in an IFN γ secretion assay. (C) LCLs with different HLA-A2 subtypes were loaded with GPC3₃₆₇ and used as targets for TCR P1-1 or mock transduced T cells in an IFN γ secretion assay. E:T ratios of 1:1 were used. Error bars indicate SD of analysed triplicates. $P \leq 0.001$ (***)

4.7.2 Effective Killing of HLA-A2⁺ GPC3⁺ Human Hepatoma Cells by TCR P1-1 Grafted CD8⁺ T cells

TCR P1-1 transduced T cells were analysed with regard to their ability to recognize and kill GPC3⁺ HLA-A2⁺ human hepatoma cells in a co-culture assay with HepG2 cells. A rapid and significant killing of target cells was observed when E:T ratios of 0.6:1 or higher were used. After 16 h of co-incubation 80 to 100% of target cells were killed by GPC3₃₆₇ re-directed T cells. Significant killing of target cells after 6 h was already detected with E:T ratios as low as 0.15:1. Co-incubation with mock transduced T cells did not result in reduced viability of target cells, but rather strong proliferation was observed (Figure 37 A). Higher E:T ratios of 5:1 did not result in further optimization of specific cytotoxicity. No killing by P1-1 expressing T cells was observed after co-incubation with HLA-A2⁻ Huh7 cells (Figure 37 B).

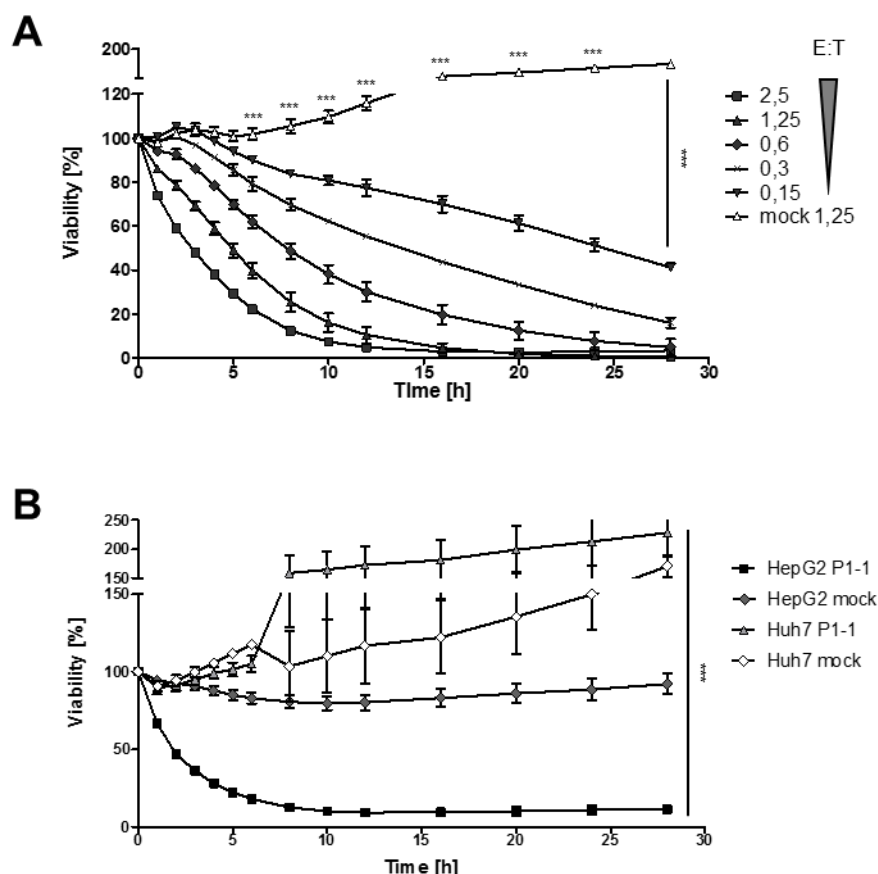


Figure 37 TCR P1-1 re-directs T cells to kill human hepatoma cells. (A) Functional activity of TCR P1-1 expressing T cells was assayed by co-incubation with HepG2 cells. E:T ratios ranging from 0.15:1 to 2.5:1 were used. (B) Unspecific killing was investigated by co-incubation with GPC3⁺ HLA-A2⁻ Huh7 cells. E:T ratios of 5:1 were used. Viability of target cells was analysed over time using the xCELLigence system. SD of triplicates are shown. P<0.001(***).

4.7.3 TCR P1-1 Can Retarget CD8⁺ but not CD4⁺ T cells Towards GPC3⁺ HLA-A2⁺ Tumour Cells

Since not only CD8⁺ T cells but also CD4⁺ T cells can be transduced with TAA-specific TCR and in some cases can be functional (97), we investigated the expression of the TCR P1-1 after transduction of total PBMC in CD8⁺ vs CD4⁺ T cells by flow cytometry. A2-GPC3₃₆₇ multimer binding was only detected in CD8⁺ T cells whereas staining with the TRBV antibody showed that around 50% of CD8⁺ and CD4⁺ T cells expressed the TCR after transduction (Figure 38 A). Lacking A2-GPC3₃₆₇ multimer binding indicated dependency on the co-receptor CD8, which argues for no or low functionality of the TCR P1-1 in CD4⁺ T cells.

In order to compare functionality of TCR P1-1⁺ CD8⁺ and CD4⁺ T cells, transduced PBMC were enriched for CD8⁺ or CD4⁺ T cells and co-incubated with HepG2 cells to analyse target cell viability over time. Only TCR P1-1⁺ CD8⁺ T cells killed HepG2 cells, while co-incubation with TCR P1-1⁺ CD4⁺ T cells and mock transduced T cells did not result in killing of target cells (Figure 38 B). T cell functionality was assayed by intracellular cytokine staining of IFN γ , IL-2 and TNF α secretion and LAMP-1 translocation after co-incubation with peptide loaded T2 cells. High percentage of TCR P1-1 equipped CD8⁺ (Figure 38 C) but not CD4⁺ (Figure 38 D) T cells secreted IFN γ , IL-2 and TNF α and mobilized LAMP-1 as a marker for degranulation on GPC3₃₆₇ peptide loaded T2 cells. No cytokine secretion was observed in CD8⁺ T cells after incubation with T2 cells loaded with irrelevant peptide. Furthermore we showed that the presence of TCR P1-1⁺ CD4⁺ T cells does not increase the ability of TCR P1-1⁺ CD8⁺ T cells to effectively kill HepG2 cells. The observed killing was time delayed but after 12 h a killing of 90% was reached by both, TCR P1-1⁺ CD8⁺ enriched T cells and TCR P1-1⁺ total T cells (Figure 38 E). This delayed killing of target cells is probably due to higher overall cell numbers in the well, since the number of applied cells was adjusted to identical numbers of TCR P1-1⁺ CD8⁺ T cells. Therefore target-effector cell interactions may be restrained. However, an inhibitory role of regulatory T cells can also not be excluded.

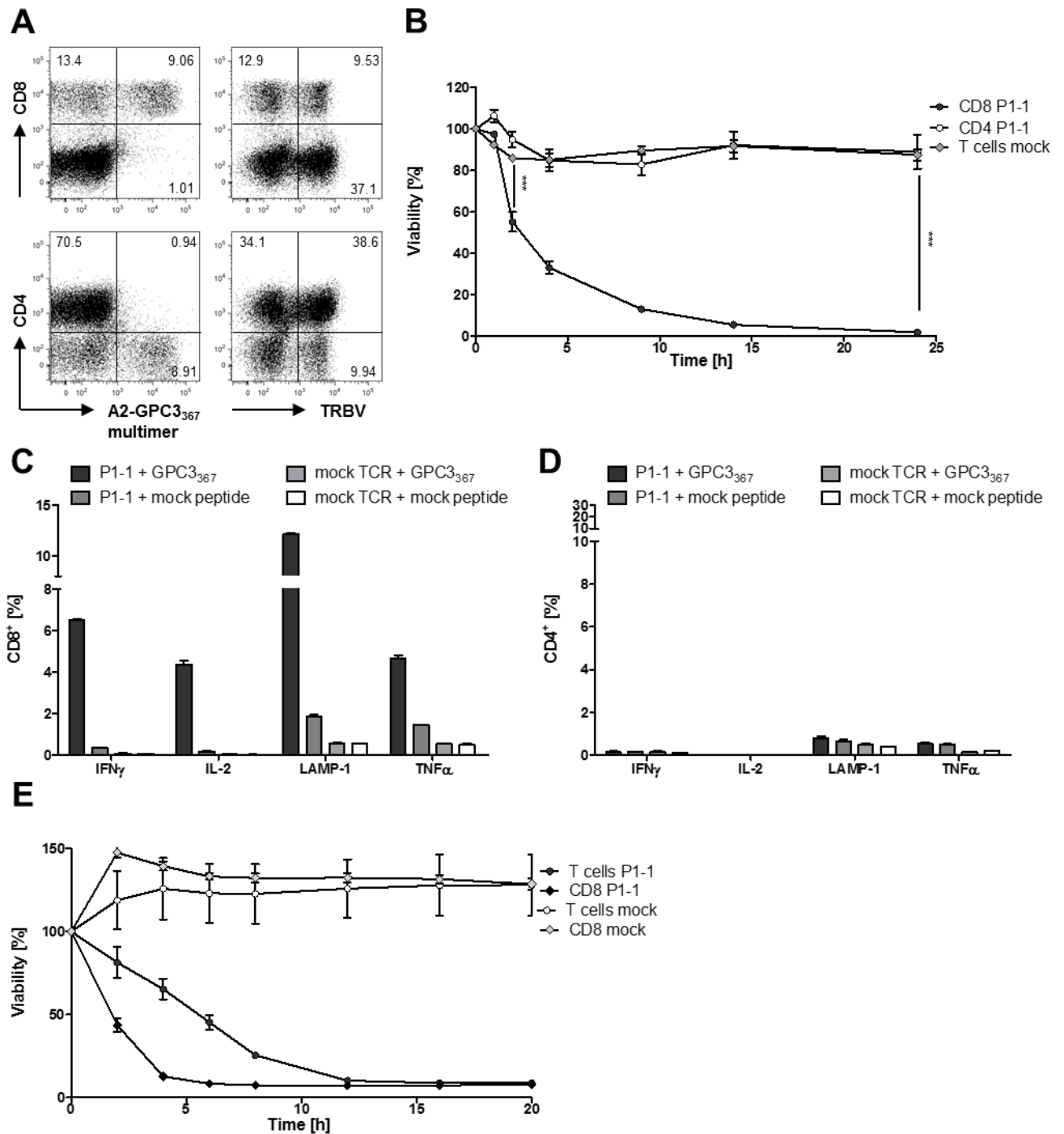


Figure 38 CD8⁺ but not CD4⁺ TCR P1-1⁺ T cells are re-directed to kill GPC3⁺ HLA-A2⁺ human hepatoma cells. (A) Expression of TCR P1-1 in transduced human CD8⁺ and CD4⁺ T cells was investigated by flow cytometry following A2-GPC3₃₆₇ multimer staining or anti-TRBV staining. Percentage of cells detected in each quadrant are shown. (B) Functional activity of TCR P1-1 expressing CD8⁺ or CD4⁺ T cells was assayed by co-incubation of enriched CD8⁺ or CD4⁺ with HepG2 cells. An E:T ratio of 2:1 was used. Viability of target cells was analysed over time using the xCELLigence system. Functionality of (C) CD8⁺ and (D) CD4⁺ T cells after co-incubation with GPC3₃₆₇ of mock peptide loaded T2 cells was examined. After 5 h of co-incubation T cells were harvested and an intracellular cytokine stain was performed before the cells were analysed by flow cytometry. (E) Functional activity of TCR P1-1 expressing CD8⁺ in presence or absence of CD4⁺ T cells was investigated by co-incubation of CD8⁺-enriched TCR P1-1⁺ or total TCR P1-1⁺ T cells with HepG2 cells. An E:T ratio of 2:1 was used. Viability of target cells was analysed over time using the xCELLigence system. SD of triplicates are shown. P \leq 0.001(***).

4.7.4 Adoptive Transfer of P1-1⁺ T cells Suppresses Tumour Growth in an *In Vivo* HCC Model

Eventually, killing of human hepatoma cells by P1-1⁺ T cells was confirmed *in vivo* using a murine transplantation models. Therefore SCID/Beige mice were transplanted with Gaussian luciferase expressing HepG2-luc cells before adoptive transfer of TCR P1-1 transduced human T cells.

HepG2 cells were stably transfected with Gaussian luciferase and luciferase activity was confirmed from cell lysates and living cells (Figure 39).

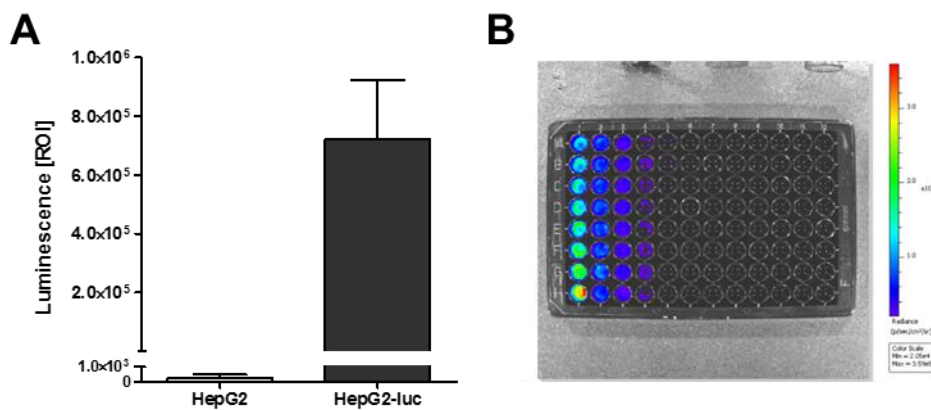


Figure 39 Generation of HepG2-luc cells for *in vivo* imaging. HepG2 cells were stably transfected with Gaussian luciferase. (A) Luciferase activity was determined from cell lysates using Tecan's Infinite™ F200. (B) Luciferase activity from living cells was measured by IVIS imaging of a HepG2-luc dilution series ranging from 10⁵ to 5 cells/ well in a 96-well plate.

An overview of the setup of the *in vivo* xenograft experiment is shown in Figure 40 A. 20 mice received HepG2-luc by intrasplenic injection on day -13/-12. In 7 out of 20 mice HepG2 derived tumours had established after 10 days. 4 animals were treated with TCR P1-1 transduced T cells, 3 were treated with mock transduced T cells. T cells were transferred on day 0. A quantification of the observed bioluminescence is shown in Figure 40 B. Growth of HepG2-luc-derived tumours in recipient animals was efficiently suppressed by i.p. injection of TCR P1-1⁺ T cells as compared to a control group receiving mock transduced T cells from the same donor. In control animals the tumour was steadily growing. Bioluminescence images taken of all 7 mice on day -3, 0 and 3 are shown in Figure 40 C.

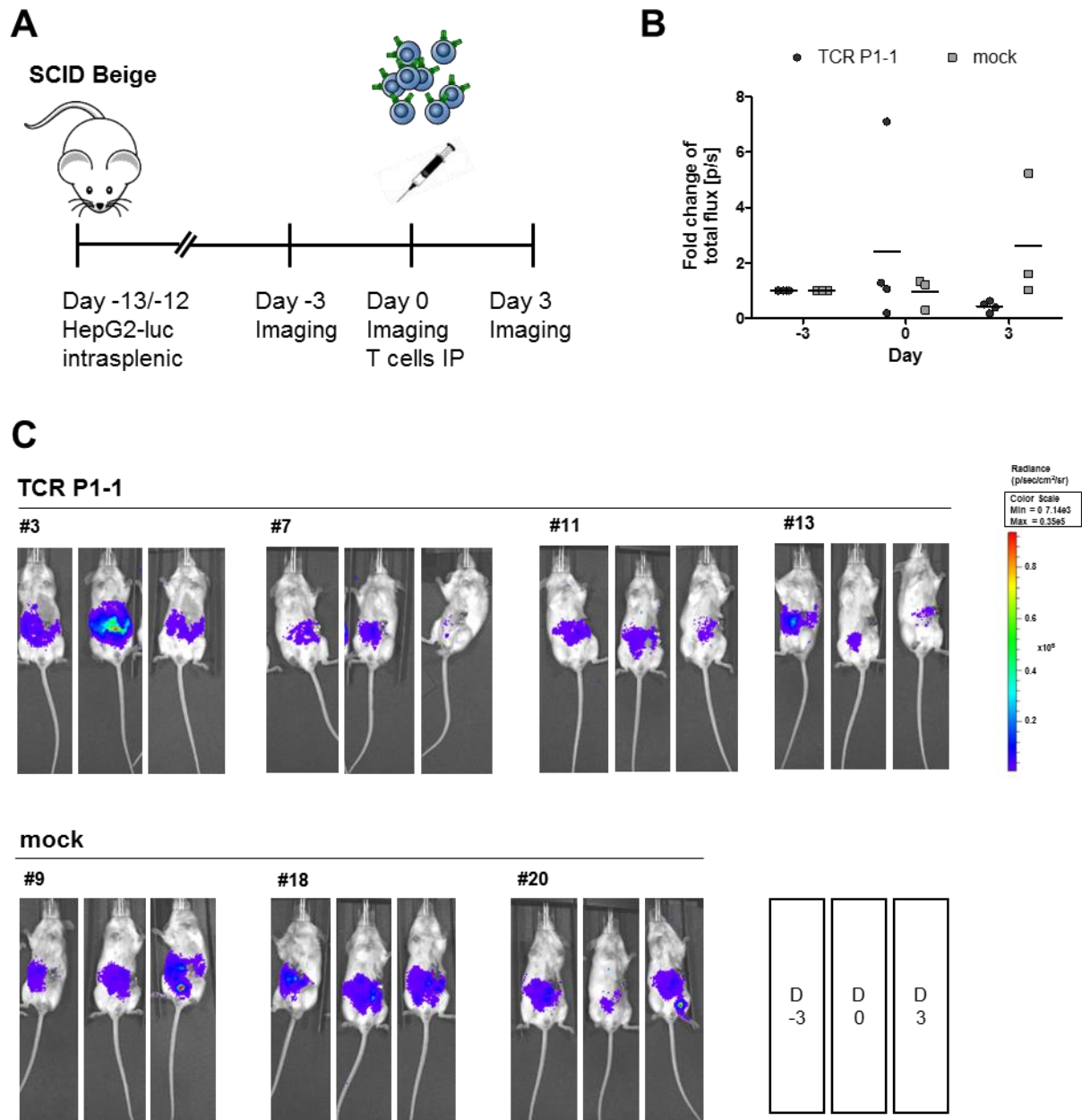


Figure 40 Adoptive transfer of TCR P1-1⁺ human T cells suppresses growth of human hepatoma cells in a xenograft *in vivo* model. (A) Schematic overview of the experimental setup. SCID/Beige mice were transplanted with HepG2-luc cells by intrasplenic injection resulting in tumorous growth in the liver. Based on the intensity of bioluminescence before treatment mice were assigned to treatment (TCR P1-1⁺ T cells) or control (T cells) group. T cells were injected i.p. on day 0, 13 days after tumour cell transplantation. Bioluminescence imaging was performed every 3 to 4 days. (B) Quantification of bioluminescence. The total flux is plotted as fold change of photon/s in relation to measurement on day -3. (C) Representative *in vivo* bioluminescence imaging of HepG2-luc xenografts treated with TCR P1-1⁺ T cells or mock T cells. Images were set at the same pseudocolor scale to show the relative bioluminescence changes over time.

5 Discussion

5.1 Selection of GPC3 as Target for Adoptive T-cell therapy of HCC

The selection of immunogenic target antigens is the first important step on the route to the development of an effective anti-cancer immunotherapy. For the present study we chose GPC3, because it is not expressed on healthy adult tissue but gets reactivated in 75% of all HCC patients (26-28). It is important to select a tumour antigen that is solely expressed on tumour tissue and furthermore cannot be lost by tumour cells through immunoediting. GPC3 drives carcinogenesis in HCC by inducing proliferation via Wnt signalling (24). Thus, it can be hypothesised that HCC cells rely on GPC3 expression in order to continue to grow.

O'Beirne et al. described that T cells can be stimulated to recognize the GPC3 epitope GPC3₅₂₂ (87). In order to identify other immunostimulatory epitopes within the GPC3 protein, we performed peptide predictions using three different prediction databases (SYFPEITHI, BIMAS and NetMHC). 24 GPC3 peptides were predicted to bind the HLA-A2 molecule with high affinity. However, using *in silico* prediction of peptide binding with computerized algorithms does not allow conclusions on proteasome cleavage patterns, transportation and peptide presentation on MHC I in tumour cells. Moreover SYFPEITHI, BIMAS and NetMHC employ different algorithms to predict peptide binding, which leads to significant differences in the predictions obtained from those databases (98). For instance peptide GPC3₃₆₇, which has been used for the T cell stimulation in this study, is predicted to bind HLA-A2 with strong affinity by SYFPEITHI and NetMHC. Nevertheless, a very short half time of dissociation, equivalent to only moderate binding affinity was predicted for GPC3₃₆₇ by BIMAS (Table 24). This disagreement within the results obtained by using different prediction tools has also been observed for several other GPC3 peptides in the analysis. Results obtained by peptide prediction should therefore be handled with care and additional methods for the validation of peptide binding strengths should always be performed. The major advantage of using computerized peptide binding prediction tools is the low expenditure of time (98).

In order to further select which epitopes may be useful for T cell stimulation, we performed a mass spectroscopic analysis of the HLA-A2 peptidome of an HLA-A2⁺ GPC3⁺ human hepatoma cell line (HepG2). Using this approach we were able to identify two GPC3 peptides, GPC3₃₆₇ and GPC3₃₂₆, which are processed and presented in context of HLA-A2 on hepatocellular carcinoma-derived cells. Both peptides were among the 30% most abundant peptides, with GPC3₃₆₇ being detected with slightly higher intensity in comparison to GPC3₃₂₆. The above mentioned peptide GPC3₅₂₂ was not discovered as potential target using this experimental approach; however, this might be due to peptide presentation in HepG2 cells below the detection limit of the method.

We were not able to verify our results obtained from the HLA-A2 peptidome analysis of HepG2 cells in patient-derived HCC lesions. Peptide processing and presentation may vary between individuals, but again, we cannot exclude that GPC3₃₆₇ and GPC3₃₂₆ were presented in concentrations below the detection limit.

To complete the peptide selection we investigated binding of the three chosen peptides, GPC3₅₂₂, GPC3₃₆₇ and GPC3₃₂₆, to HLA-A2 in a peptide competition assay. Therefore target cells were loaded with excess of GPC3 peptides, before the previously established HBV S₁₇₂ peptide was loaded and IFN γ secretion by HBV S₁₇₂ specific T cells was measured. HBV S₁₇₂ has been shown to be a potent target epitope for T cells by Karin Wisskirchen et al. (unpublished data). In comparison to peptide HBV S₁₇₂, GPC3₅₂₂ and GPC3₃₆₇ were found to bind stronger or at least comparably strong to the HLA-A2 molecule. Loading excess of peptide GPC3₃₂₆ to target cells before loading with HBV S₁₇₂ did not reduce IFN γ secretion by HBV S₁₇₂-specific T cells. Therefore it can be concluded that GPC3₃₂₆ binds HLA-A2 with lower affinity than HBV S₁₇₂. These results are in accordance with the results obtained by peptide prediction using SYFPEITHI. In BIMAS half time of dissociation of HBV S₁₇₂ is predicted to be 10-100 fold higher compared to our GPC3 peptides. NetMHC predicts stronger HLA-A2 binding strength of HBV S₁₇₂ in comparison to GPC3₃₆₇ and GPC3₃₂₆. HLA-A2 binding of GPC3₅₂₂ is predicted in a similar range as HBV S₁₇₂. These results underscore the varying outcome obtained by peptide binding prediction using different databases.

The combination of all three approaches employed in this study, pointed us to the selection of GPC3₅₂₂, GPC3₃₆₇ and GPC3₃₂₆ as targets for T cell stimulation. GPC3₅₂₂ obtained good prediction scores using all three databases and performed well in the peptide competition assay. Importantly GPC3₅₂₂ has been used for successful T cell stimulation before. GPC3₃₆₇ was identified to be processed and presented on HepG2 cells, obtained good scores from SYFPEITHI and NetMHC and performed well in the peptide competition assay. Finally GPC3₃₂₆ was also identified to be presented on HLA-A2 in HepG2 cells and was predicted to be a strong HLA-A2 binder by all three databases. In conclusion all three GPC3 peptides are potential candidates for T cell re-direction towards GPC3, but only GPC3₃₆₇ and GPC3₃₂₆ have been shown to be presented on human hepatoma cells, rendering those two into preferable targets for clinical applications.

5.2 Stimulation of Allorestricted GPC3-specific T cells

T cells can recognize peptides in context of foreign (allo) MHC I molecules, which can be utilized to isolate TAA-specific T cell by allorestricted stimulation (92). Choosing potent APCs to stimulate allorestricted TAA-specific T cells is essential for the success of this method.

HLA-A2⁺ T2 cells have been used to stimulate high avidity allorestricted peptide-specific T cells before (93, 99, 100) and have therefore been chosen as APCs in this study. The advantage in using T2 cells is that there is no or only negligible presentation of endogenous peptides, as a result of their TAP deficiency (80). Nevertheless they do present exogenously loaded peptides very well.

A recently developed approach to stimulate allorestricted T cells employs monocytic-derived mature dendritic cells and utilizes the pronounced capacity of DC to prime naïve T cells (101). In this system peptide presentation is not achieved by exogenous peptide loading but instead by *ivt*-RNA transfection. Accordingly, the complete target protein is translated and processed within the DC, which results in presentation of the complete range of peptides that are generated. Additionally this method ensures that peptides are only presented, if they are

naturally processed by the proteasome and thereby avoids stimulation of T cells towards artificial epitopes.

In the present study we first stimulated T cells with HLA-A2 *ivt*-RNA transfected moDC and loaded them with peptide GPC3₅₂₂. Transfection with GPC3 *ivt*-RNA was not yet successful during that time of the study and could therefore not be employed. The HLA-A2 peptidome analysis, which identified GPC3₃₇₆ and GPC3₃₂₆ as promising targets was performed at a later time point, which is why those two specificities were not included in stimulation 1. For T cell stimulation, DC and T cells were derived from the same HLA-A2 negative repertoire. Using an HLA-A2 negative background for stimulation of HLA-A2 restricted T cells towards TAA is essential as explained in detail above (see 0). Stimulation with GPC3₅₂₂ loaded HLA-A2 *ivt*-RNA transfected moDC was not successful. No A2-GPC3₅₂₂ multimer⁺ CD8⁺ T cells were detected at any time point and no T-cell clones originated from sorted T-cell lines. After restimulation with antigen pulsed moDC increased IFN γ secretion was detected only when HLA-A2 *ivt*-RNA transfected DC without GPC3₅₂₂ were used, indicating induction of alloreactive rather than peptide-specific T cell responses. Because no A2-GPC3₅₂₂ multimer⁺ T cells were detected, we decided to focus on the newly identified and not yet described peptides GPC3₃₇₆ and GPC3₃₂₆ in all further experiments.

Utilizing peptide loaded T2 cells in the second stimulation did also not result in successful isolation of GPC3-specific T cells. No A2-GPC3 multimer⁺ CD8⁺ T cells were detected in sorted T-cell lines or derived T-cell clones. Furthermore originated T-cell clones showed no signs of GPC3 specificity. The investigations were therefore not continued.

In the third stimulation, we were able to stimulate GPC3-specific HLA-A2 restricted T cells by using HLA-A2 *ivt*-RNA and GPC3 *ivt*-RNA transfected moDC as APCs. DC used in this stimulation were shown to obtain a typical mature phenotype and expression of HLA-A2 and GPC3 after *ivt*-RNA transfection was demonstrated. HLA-A2 expression levels reached its peak after 24 h, whereas GPC3 was only detectable shortly after electroporation. It can be assumed that GPC3 surface expression was instable and the protein was rapidly degraded by the proteasome after electroporation. For stimulation of HLA-A2 restricted GPC3-specific T

cells, stable HLA-A2 surface expression is essential, nevertheless GPC3 is only required in form of peptides that can be presented on HLA-A2. Therefore the generated moDC matched all criteria required for efficient T cell stimulation towards GPC3 in context of HLA-A2.

Stimulated T cells were detected using two different approaches. CD8⁺ T cells were either stained with A2-GPC3 multimer or CD137. A2-GPC3 multimer allows isolation of CD8⁺ T cells with distinct specificity whereas isolation of CD137⁺ CD8⁺ T cells offers the possibility to isolate antigen-specific CD8⁺ T cells independent of prior knowledge of the specific epitopes recognized (82). Since *inv*-RNA transfected DC can stimulate T cells with all possible GPC3 specificities, CD137 sorting is a valuable addition to multimer sorting. Both A2-GPC3 multimer⁺ and CD137⁺ CD8⁺ T cells were detected and could be expanded. Multiple T-cell clones originated from A2-GPC3₃₆₇ multimer⁺, A2-GPC3₃₂₆ multimer⁺ and CD137⁺ T-cell lines.

5.2.1 Specificity and Functionality of GPC3-specific T-cell clones

T-cell clones were analysed with regard to their ability to recognize GPC3 peptide and GPC3⁺ HLA-A2⁺ hepatoma cells (HepG2) in IFN γ secretion assays. As summarized in Table 27, a total of 482 T-cell clones originated from all three sortings and were screened in this study. 21 GPC3₃₆₇- and 25 GPC3₃₂₆-specific T-cell clones were identified. Furthermore 19 of the 318 CD137 sorted T-cell clones were GPC3-specific. GPC3 specificity was confirmed for most of the clones in an IFN γ secretion assays after co-culture with HepG2 cells.

Table 27 Summary of T-cell clones derived by multimer sorting or CD137 sorting. Numbers of T-cell clones originated from limiting dilution cloning, number of GPC3 peptide-specific clones and clones that recognized human hepatoma cells as well as A2-GPC3 multimer positive clones are shown.

	T-cell clones	Recognition of GPC3 peptide	Recognition of GPC3 ⁺ HepG2	Multimer ⁺
A2-GPC3₃₆₇	107	21	17	16
A2-GPC3₃₂₆	57	25	13	15
CD137	318	19	10	0

Many T-cell clones were not performing well when it came to proliferation and viability, therefore it can be assumed that lacking IFN γ secretion after co-incubation with HepG2 cells is most likely due to an anergic state of the T cells. T-cell clones were kept in culture for 8-10 weeks, before they stopped proliferating and cells died. Like most dividing cells, T cells die

after a certain number of divisions, because their telomeres progressively shorten (102). Moreover effector T cells are driven into apoptosis after activation and proliferation, a process called activation-induced cell death (AICD) (45). Also absence of antigen-specific stimulation can lead to apoptosis. Our T-cell clones were highly activated and moreover only unspecifically restimulated every two weeks, which can explain their poor viability. Staining for memory T cells within the T-cell clone populations could not be performed due to low cell numbers and because the material was required for RNA isolation and subsequent TCR identification at a later stage.

Sixteen A2-GPC3₃₆₇-sorted T-cell clones and 15 A2-GPC3₃₂₆-sorted clones bound A2-GPC3 multimer. Absent multimer binding in T-cell clones does not necessarily indicate a lack of GPC3 specificity. T-cell clones can be specific for their target although no multimer binding is detected.

GPC3 specificity of CD137 sorted T-cell clones was investigated on GPC3 *ivt*-RNA pulsed K562 cells, therefore the recognized epitopes were still unknown. Epitope specificity was analysed in two different experimental setups, using T2 cells loaded either with single GPC3 peptides (Table 24) or GPC3 peptide pools (96). Using the single peptides, peptide GPC3₅₅₄ was identified to be a potential candidate. Nevertheless this result could not be verified using the peptide pools and could also not be reproduced, because T-cell clones were not viable anymore. Because TCR gene therapy in the clinic is not feasible without knowledge of the epitope recognized and identification of the latter is time-consuming and costly, we decided to only analyse the TCR sequences from A2-GPC3 multimer sorted T-cell clones with defined specificities.

5.3 TCR Identification and Optimization

In order to transfer the specificity observed in these T-cell clones to other lymphocytes the TCR sequences had to be identified. First of all TCR transfer into donor T cells allows to further study the functionality of an identified TCR *in vitro* and *in vivo*. Secondly, the target antigen specificity can be transferred to donor cells and can thereby be connected to a certain TCR

sequence (103). Finally the TCR sequence can be used in therapeutic applications to treat cancer patients with adoptive T-cell therapy (52).

TCR analysis revealed one single TCR with identical CDR3 regions to be expressed in all GPC3₃₇₆-specific T-cell clones. This data suggests that all analysed GPC3₃₆₇-specific T-cell clones originate from the same clonal T cell. It can only be speculated whether or not these T-cell clones are derived from a cross-reactive reactivated memory T cell population. Reactivation of memory T cells could explain the dominant proliferation, which probably overgrew T-cell clones expressing other TCR, in case of presence.

RNA isolated from T-cell clones specific for GPC3₃₂₆ was unfortunately of poor quality. Many GPC3₃₂₆-specific T-cell clones were oligoclonal or possibly contaminated with feeder cells, which made it impossible to analyse their TCR sequences. Analysis of the TCR repertoire was possible for 5 clones. They expressed one single β -chain, but two or three α -chains. During T cell development in the thymus the TCR β -chain gene segments rearrange first. After successful synthesis of a rearranged β -chain a pre-TCR is produced, which then triggers inhibition of further β -chain rearrangement and ensures expression of only one distinct β -chain in every T cell. Also rearrangement of the TCR α -chain is induced at this stage of T cell development, which does not stop until positive selection of the TCR by a self-peptide:self-MHC complex occurs. This is why many T cells can produce two α -chains, although they have only a single functional specificity (45). However, detection of three different α -chains in one T-cell clone means that the clone was not monoclonal but consisted of at least two different T cell populations.

The TCR P1-1^{Pre} identified from GPC3₃₆₇-specific T cells was cloned into the retroviral expression vector pMP71 and expression and functionality was shown after genetic transfer into human T cells. Before the TCR functionality was further evaluated the sequence was codon optimized for improved expression in human cells and the constant domains were murinized. The use of enhanced translation of the transgenic TCR sequence by codon optimization has been demonstrated to increase expression and consequently functionality in human T cells (104, 105). Hybrid TCR with human viable and murinized constant domains

have been shown to elicit increased stability and improved function in comparison to fully human TCRs (106). Moreover miss-pairing with endogenous TCR chains is avoided by preferential pairing of the murine constant domains with themselves. A disadvantage of using murine constant domains is that the presence of non-human protein may induce an immune response against the murine peptides that can reduce the longevity of transduced T cells carrying this TCR *in vivo* (107). The recent identification of the few AA residues that are responsible for the improved function of the hybrid TCR can be utilized to use minimally murinized constant domains and may help to reduce this risk of immunogenicity (108). As a final modification an additional disulfide bond was introduced between the constant domains that further enhanced TCR stability and favoured pairing of the transferred TCR chains (109). The optimized and murinized TCR α - and β -chains were cloned into one retroviral vector, in order to improve equimolar translation of both chains. In pMP71, TCR P1-1 α - and β -chains are connected by a P2A element and under control of a sequence within the 5' LTR region, that acts as promoter in this construct (86).

Evaluation of the three different TCR α -chains identified from GPC3₃₂₆-specific T-cell clones was performed together with Laura Hannemann during the practical part of her Master thesis. The combination TRBV9*01 and TRAV13-1*02 showed the most promising results and the TCR P1-2 is currently codon optimized and murinized in our laboratory for further investigations.

Another way of how to identify TCRs from T cell populations with demonstrated specificity is the TCR single cell analysis method (TCR-SCAN) recently described by Dössinger et al. (110). Using this method, RNA is isolated from single cells immediately after multimer sorting of antigen-specific T cells. We have performed TCR-SCAN for A2-GPC3₃₂₆⁻ and A2-GPC3₃₇₆⁻ specific T-cell clones. RNA isolated from A2-GPC3₃₂₆⁻ was of poor quality and no sequence analysis was possible. TCR-SCAN of A2-GPC3₃₇₆⁻-sorted T cells showed that all cells expressed the already identified TCR P1-1 (data not shown). By excluding T cells that express TCR P1-1 with anti-TRBV staining, it may be possible to identify other TCRs that are expressed in a minority of T cells immediately after DC stimulation. Due to technical restrictions this

analysis could not be performed in the presented study, but may be a useful approach for the identification of additional GPC3-specific TCR sequences in future investigations.

5.4 Re-direction of Donor T cells towards GPC3 by TCR P1-1

The optimized GPC3₃₆₇-specific TCR P1-1 was successfully expressed in high frequencies (50%) of CD8⁺ T cells as shown by multimer as well as anti-TRBV staining. High surface expression of transduced TCR is correlated to functional activity of transduced T cells. Heemskerk et al. showed that surface expression of transferred TCRs can vary drastically depending on the endogenous TCR expressed by the cells (111). TCR chains with high inter-chain affinity are more likely to form a functional TCR complex than TCRs with low or intermediate inter-chain affinity. Inter-chain affinity is defined as the affinity of α - and β -chain among each other and depends mostly on the variable TCR regions (111). According to this assumption and our results TCR P1-1 exhibits high inter-chain affinity.

Although TCR P1-1 surface expression was very high in all donor T cells used for this study, its expression might vary in patients depending on the endogenous TCR repertoire expressed.

5.4.1 Peptide Specificity, Avidity and Cross-reactivity of TCR P1-1

TCR P1-1 equipped T cells specifically recognized GPC3₃₆₇ peptide loaded target cells in context of HLA-A2. Irrelevant peptides were not recognized. The mouse peptide GPC3₃₆₆, which is 89% homologous to human GPC3₃₆₇ was also not recognized (data not shown). Mouse GPC3₃₆₆ contains isoleucine instead of valine on position 6 within the AA sequence, which is the secondary anchor position of the peptide. Both AA are hydrophobic. Nevertheless recognition of mouse GPC3₃₆₆ was not observed. An important role of secondary positions for peptide binding has been demonstrated by Ruppert et al. before (112).

Naturally processed GPC3 peptide recognition in context of HLA-A2 has been demonstrated by detection of IFN γ secretion after co-incubation with HepG2 cells. HLA-A2 negative Huh7 cells were not recognized. HLA-A2 restricted fratricide because of alloreactivity of transduced T cells was excluded upon co-culture with HLA-A2⁺ and HLA-A2⁻ PBMC. No IFN γ secretion was detected in both groups.

Functional avidity of TCR P1-1 transduced T cells was detected as half maximal IFN γ secretion on target cells loaded with titrated GPC3 peptide concentrations. Half maximal secretion was detected on target cells loaded with 0.1 μ M GPC3₃₆₇, which is equivalent to an intermediate avidity. This is in accordance with the functional avidity that has been observed for TCRs specific for other tumour antigens (59). Since stimulated T cells were sorted via multimers, which represent the natural targets for their TCRs, high avidity T cells may have been strongly activated leading to AICD. It is controversially discussed, which functional avidity of TCRs is optimal for efficient anti-tumour immunotherapy and whether or not high avidity goes along with high tumour eradication at all. Previous studies have shown high (113) and no (114) functionality of high avidity TCR as well as high functionality of low avidity TCRs (115) *in vivo*. Using TCRs with high affinity can result in deletion of transferred T cells *in vivo*. Furthermore high avidity often goes along with substantial toxicity (63). Significant on-target cytotoxicity to normal melanocytes in the skin, eye and ear was observed in patients treated with a high avidity TCR recognizing MART-1 (52). Recognition of normal epithelial cells after transfer of a CEA-specific TCR in colorectal carcinoma patients lead to severe colitis and trials had to be stopped after only three patients (116). This indicates the need for precise surveillance of generated TCRs to avoid unwanted toxicity in future applications.

Cross-reactivity of TCR P1-1 transduced T cells was investigated using 10 HLA-A*0201 negative LCLs that express other HLA-A2 alleles and were loaded with GPC3 peptide. GPC3₃₆₇ was recognized in context of HLA-A*0202, 0207, 0216 and 0217 in addition to HLA-A*0201. GPC3 peptide recognition in context of other HLA-A2 alleles still needs to be investigated. Cross-reactivity of TCR specific for peptides in context of HLA-A2 has been demonstrated in several studies before (93, 117). In summary we demonstrated that the newly identified TCR P1-1 enables T cells to specifically recognize peptide with medium avidity in context of HLA-A*0201, but can furthermore recognize peptide presented on HLA-A*0202, 0207, 0216 and 0217.

In order to exclude cross-reactivity to other peptides than GPC3₃₆₇ that are presented on HLA-A2, a peptide array could be performed. The group of W. Uckert (Max Delbrück Centre for

108

Molecular Medicine, Berlin) processes such an array, including over 100 peptides derived from different healthy human tissues and will investigate cross-reactivity of our TCR P1-1 with this peptide library in the near future.

5.4.2 TCR P1-1 Re-directs CD8⁺ T cells to Kill Human Hepatoma Cells *In Vitro*

Efficient recognition and cytotoxic activity in response to natural target cells has been demonstrated in a killing assay with the GPC3 and HLA-A2 expressing human hepatocellular carcinoma derived cell line HepG2 (21). We observed rapid killing of HepG2 cells even with very low E:T ratios. TCR P1-1 transduced T cells used in an E:T ratio of 0.6:1 were sufficient to kill nearly 100% of target cells after 28 h. The observed cell-mediated cytotoxicity by TCR P1-1 expressing T cells was remarkably fast and efficient when compared to reports about other TAA-specific TCRs, which often only reach approximately 60% killing of target cells using E:T ratios above 1:1 (83, 106, 118). It can be assumed that incubation times longer than 28 h would result in killing of nearly 100% target cells also for E:T ratios below 0.6:1.

We could furthermore show that recognition of GPC3 peptide depends on presentation of HLA-A2, since HLA-A2 negative GPC3 expressing Huh7 cells were not recognized and killed by TCR P1-1⁺ T cells. Concluding from this results, TCR P1-1 enables T cells to specifically recognize and effectively kill GPC3⁺ HLA-A2⁺ target cells, but is not active on cells that are negative for HLA-A2.

5.4.3 TCR P1-1 in CD8⁺ and CD4⁺ T cells

In addition to CD8⁺ T cells, CD4⁺ T cells have been demonstrated to acquire cytotoxic capacities after adoptive transfer into patients (119). Even without direct cytotoxic activity, CD4⁺ T cells are often required in order to provide the necessary help for efficient CD8⁺ T cell function and to establish long-living memory T cell populations (120). To achieve complete immunological control over the tumour it is therefore likely that both, CD8⁺ and CD4⁺ T cells are required. Reduced activity and persistence of CD8⁺ T cells in absence of CD4⁺ T cells has been shown *in vivo* (50).

We demonstrated expression of TCR P1-1 in 50% of CD4⁺ T cells by anti-TRBV staining. However A2-GPC3 multimer binding by CD4⁺ T cells was not observed. It can be assumed that A2-GPC3₃₆₇ multimer binding depended strongly on the expression of the co-receptor CD8, which indicates that there might be no or low functionality of TCR P1-1⁺ CD4⁺ T cells. This assumption was verified in killing assays on HepG2 using TCR P1-1⁺ CD8⁺ or CD4⁺ T cells. Cell-mediated cytotoxicity was observed only when TCR P1-1⁺ CD8⁺ T cells were used. Moreover CD4⁺ T cells secreted no cytokines after peptide-specific stimulation, whereas CD8⁺ T cells exhibited a clear cytotoxic effector cell phenotype with increased IFN γ , TNF α and IL2 secretion and degranulation (LAMP-1 translocation) (45, 121).

CD8 dependency of a TCR correlates with the TCR avidity. It has been shown that TCR with high affinity can bind MHC I peptide complexes (in form of tetramers) independent of CD8 co-expression, whereas MHC I peptide complex binding of low affinity TCR depended on CD8 co-expression (122). In accordance with that observation, P1-1 has a medium avidity and strongly relies on CD8 co-expression for efficient MHC I peptide complex binding.

To answer the question if TCR P1-1⁺ CD4⁺ T cells provide essential help for CD8⁺ T cell mediated cytotoxicity we co-cultured HepG2 cells with transduced CD8⁺ T cells and transduced total T cells. When using total TCR P1-1⁺ T cells, killing of HepG2 cells was delayed for about 5 h, but eventually reached the same level in comparison to co-cultures with TCR P1-1⁺ CD8⁺ T cells. Therefore a benefit of CD4⁺ T cell help was not detected *in vitro*. On the contrary the observed time delay in killing of target cells might indicate a potential role of CD8⁺ T cell inhibition by T_{reg} cells. In preliminary experiments we did not detect enhanced expression of FoxP3 after TCR P1-1 transduction and peptide-specific stimulation, hence found no prove for this hypothesis so far. Most probably the delayed killing of target cells when using total TCR P1-1⁺ T cells was due to higher overall cell numbers in the well and therefore restrained target-effector cell interactions. Further investigation is needed to identify the potential role of TCR P1-1⁺ CD4⁺ T cells in adoptive transfer, but in our experiments TCR P1-1⁺ CD8⁺ T cells were clearly demonstrated to be the key players mediating cytotoxicity after re-direction towards GPC3 expressing target cells.

5.5 Functionality of TCR P1-1 *In Vivo*

Eventually, we could show that T cells transduced with TCR P1-1 are functional not only *in vitro* but also *in vivo* in a human xenograft mouse model using HepG2-luc transplanted SCID/beige mice. Efficient reduction of tumour mass was observed after treatment with TCR P1-1 transduced T cells. Control animals received mock transduced T cells and the tumour size was constantly increasing in those animals.

Numbers of transplanted HepG2-luc and transferred T cells were taken from literature (123) and previous studies performed in our laboratory. Due to restrictions in animal numbers and shortage of time it was not possible to titrate the applied cell numbers in advance. Therefore administered HepG2-luc numbers might have been too low. This assumption is supported by the fact that only 7 out of 20 transplanted animals established tumours. A repetition of this experiment with higher HepG2 and T cell numbers applied as well as monitoring of the animals over a longer period of time is planned and will show if the results can be verified.

Despite this promising *in vivo* data obtained in this experiment, further investigations are mandatory. The animal model used in the present study does not represent the disease model in an appropriate way. The advantage in using a xenograft mouse model is the comparably quick, inexpensive and easy realisation of *in vivo* experiments. Nevertheless a xenograft mouse models has major limitations when it comes to genetics and histology of the developed tumours that are not representative of the correspondent human tumour. Moreover xenografts have no functional immune system, which makes it impossible to study the effectivity of a therapeutic application in context of an environment comparable to the patient's. In conclusion xenograft models are not sufficient to predict therapeutic success, but nevertheless can be helpful to obtain first *in vivo* verification of the applied therapeutics. Until now there is a lack of an appropriate animal model to study the efficacy and safety of GPC3-specific TCR gene therapy *in vivo*. We therefore started to establish a HCC mouse model with human GPC3 expression in HHDII-HLA-DR1 mice that express human HLA-A2 and HLA-DR1. GPC3 expression and tumour cell formation will supposedly be introduced by *in vivo*-jetPEI® injection of a vector coding for SV40 large T antigen, which drives carcinogenesis, GPC3 and firefly

luciferase under control of a liver specific promoter. The readout will be performed using IVIS *in vivo* imaging.

5.6 Possible Therapeutic Applications of TCR P1-1

The goal of this study was to isolate GPC3-specific HLA-A2 restricted T cells and to identify their cognate TCRs as tool for adoptive T-cell therapies of HCC. Functionality and specificity of TCR P1-1 have been demonstrated *in vitro* and *in vivo* and will be further investigated. In the future the TCR P1-1 can be used to re-direct T cells from HCC patients towards GPC3⁺ tumour tissue before the TCR P1-1 equipped T cells are infused back into the patient.

In order to use TCR P1-1 for adoptive T-cell therapy of HLA-A2⁺ HCC patients with demonstrated GPC3 expression, it is important that peptide GPC3₃₆₇ is processed and presented on MHC I in HCC tissue. For successful clinical application it is fundamental that the epitope that is recognized by the TCR will be presented on HCC tissue. Since the peptide was identified from HepG2 cells, which is a hepatocellular carcinoma derived cell line, it is very likely that GPC3₃₆₇ will also be presented in HCC tissue. Nevertheless experimental verification is still required. We performed HLA-A2 peptidome analysis of 3 GPC3⁺ HLA-A2⁺ patient derived HCC lesions, but did not detect any GPC3 peptides (data not shown). Nevertheless it might be possible that GPC3₃₆₇ was presented at levels below the detection limit. Also the purification of HLA-A2 peptide complexes from HCC lesions has been newly developed and needs to be improved. Investigations are currently ongoing.

TCR P1-1 might not only be useful for adoptive T-cell therapy of HCC but also for patients with other GPC3 expressing tumours. Baumhoer et al. demonstrated GPC3 expression in several tumour entities next to HCC by immunohistochemistry (124). Squamous cell carcinoma of the lung, liposarcoma and testicular nonseminomatous germ cell tumour were found to express GPC3 in 50% of analysed cases. Also cervical intraepithelial neoplasia (40% GPC3⁺), malignant melanoma (30% GPC3⁺) and adenoma of the adrenal gland (30% GPC3⁺) might be potential targets (124). However, it was also observed by Baumhoer et al. that GPC3 is expressed in normal biliary tract mucosa in 3 out of 18 cases, which might give rise to potential

side effects of GPC3-specific TCR gene therapy. Further verification of this observation is still outstanding. Nevertheless due to the successful application of an anti-GPC3 monoclonal antibody (GC33) in clinical trials without occurrence of alarming safety issues, major limitations in clinical application can be excluded (38, 39).

By any means the safety of TCR gene therapy is a topic that is discussed extensively. One possibility to enhance safety of genetically transferred TCR is the incorporation of a suicide gene. One recently developed approach uses human caspase 9, which can be activated *in vivo* by administration of cell permeable small molecules (125). Another possibility is to co-express the TCR with epidermal growth factor receptor (EGFR) and use the FDA approved anti-EGFR antibody Cetuximab to shut down T cell responses (126).

Therapeutic usage of TCR P1-1 is conceivable as a combinational therapy. (I) TCR P1-1 gene therapy can be included in a combination with immune modulatory agents such as anti-PD1 or anti-CTLA-4. TAA-specific T cells are often exhausted in HCC as shown by elevated levels of PD-1 expression (19). (II) HCC has been shown to express several TAA next to GPC3 (see 1.1.1). Next to our GPC3-specific TCR P1-1, TCRs specific for MART-1 (52, 63) and NY-ESO-1 (64) have been developed and could be used in an individualized combination harmonized to each patient's TAA expression profile. 60% of all HCC cases follow chronic HBV infections (1, 5), therefore HCCs often express viral proteins rendering the cells a target for HBV-specific T-cell therapy (Wisskirchen et al., unpublished data) that can be used in combination with TCR P1-1. GPC3 expression is not always uniform in the complete tumour tissue, instead expression was detected in 1 to 100% of all cells within HCC tissues, which might induce selection of resistant variants under anti-GPC3 treatment (26). Using a combination of TCRs directed towards different TAA would avoid selection of resistant cells and thereby reduce the risk of tumour recurrence.

5.7 Bypassing HCC Induced Immune Tolerance

In contrast to other organs the liver comprises a unique immunosuppressive microenvironment. In addition to DC, other antigen presenting cells are present, such as liver

sinusoidal endothelial cells (LSEC) and Kupffer cells. Albeit efficient antigen-presentation, these cells provide insufficient co-stimulation and moreover an excess of co-inhibitory signals, such as PD-L1. Thereby they promote tolerance induction in CD8⁺ T cells (127). Furthermore, recognition of MHC on hepatocytes has been shown to induce T cell tolerance *in vivo* (128). In HCC patients elevated T_{reg} frequencies have been observed to correlate to CD8⁺ T cell dysfunction (129) and myeloid-derived suppressor cells (MDSC) inhibit appropriate functionality of NK cells and DC (130, 131). Furthermore HLA-I has been shown to be downregulated in HCC (132). Immunotherapeutic treatment might lead to further loss of MHC I expression. Rustifo et al. observed loss of β 2microglobulin in metastatic melanoma patients after immunotherapy (133). In a therapeutic context MHC I expression could be enhanced by application of IFN γ in order to overcome this problem, since IFN γ is known to promote MHC I surface expression in tumour cells (134).

In order to overcome local immunosuppression within the tumour microenvironment an approach utilizing IL12 has been developed. Expression of single chain IL12 in tumour-specific T cells has been shown to enhance efficacy (135) of T-cell therapy and eliminated the need of lymphodepletion (136) before T cell transfer *in vivo*.

5.8 Conclusion

In conclusion two novel immunodominant epitopes within the GPC3 protein were identified in this work. Those epitopes are not only useful to isolate T cells that specifically recognize GPC3 expressing cells for the development of an adoptive T-cell therapy but can also be used for peptide vaccinations of HCC patients.

In the present study GPC3-specific T cells were successfully stimulated with GPC3 *ivt*-RNA and HLA-A2 *ivt*-RNA pulsed moDC in an allorestricted approach. GPC3-specific HLA-A2 restricted T cells were isolated and their cognate TCRs were identified. Retroviral transfer of the identified GPC3-specific TCR P1-1 lead to stable surface expression in high frequencies of donor T cells. TCR P1-1 has been shown to specifically recognize GPC3₃₆₇ peptide in an HLA-A2 dependent manner. Peptide loaded target cells as well as endogenously processed

peptide in HepG2 cells has been recognized by TCR P1-1⁺ T cells and induced IFN γ secretion. Unspecific recognition was not observed, therefore no off-target reactivity in patients should be expected. Cross-reactivity to GPC3 peptide complexes with 4 other HLA-A2 alleles in addition to HLA-A*0201 was shown, which extends the group of patients susceptible to this therapy. Finally effective killing of GPC3⁺ HLA-A2⁺ human hepatoma cells by TCR P1-1⁺ CD8⁺ T cells has been demonstrated (Figure 41).

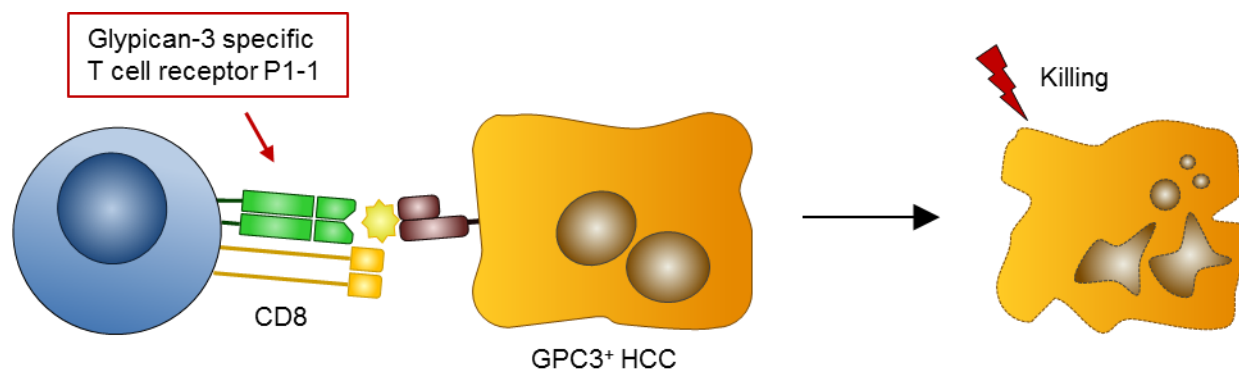


Figure 41 The TCR P1-1 re-directs CD8⁺ T cells to recognize and kill GPC3⁺ target cells in context of HLA-A2.

The hereby presented TCR P1-1 can serve as a potential tool for adoptive T-cell therapy of HCC patients. Until today no curative treatments are available for HCC patients, especially at late stage. Therefore adoptive T-cell therapy targeting GPC3 in HCC may have meaningful impact in clinics.

6 References

1. Jemal A, Bray F, Center MM, Ferlay J, Ward E, Forman D. Global cancer statistics. *CA: a cancer journal for clinicians*. 2011;61(2):69-90.
2. J. F, I. S, M. E, R. D, S. E, C. M, et al. GLOBOCAN 2012 v1.0, Cancer Incidence and Mortality Worldwide: IARC CancerBase No. 11 Lyon, France: International Agency for Research on Cancer; 2013 [31.08.2014]. Available from: <http://globocan.iarc.fr>.
3. Shin HR, Oh JK, Masuyer E, Curado MP, Bouvard V, Fang YY, et al. Epidemiology of cholangiocarcinoma: an update focusing on risk factors. *Cancer science*. 2010;101(3):579-85.
4. Ioannou GN, Splan MF, Weiss NS, McDonald GB, Beretta L, Lee SP. Incidence and predictors of hepatocellular carcinoma in patients with cirrhosis. *Clinical gastroenterology and hepatology : the official clinical practice journal of the American Gastroenterological Association*. 2007;5(8):938-45, 45.e1-4.
5. Parkin DM. The global health burden of infection-associated cancers in the year 2002. *International journal of cancer Journal international du cancer*. 2006;118(12):3030-44.
6. Bosetti C, Levi F, Boffetta P, Lucchini F, Negri E, La Vecchia C. Trends in mortality from hepatocellular carcinoma in Europe, 1980-2004. *Hepatology (Baltimore, Md)*. 2008;48(1):137-45.
7. Forner A, Llovet JM, Bruix J. Hepatocellular carcinoma. *Lancet*. 2012;379(9822):1245-55.
8. El-Serag HB. Hepatocellular carcinoma. *The New England journal of medicine*. 2011;365(12):1118-27.
9. Llovet JM, Ricci S, Mazzaferro V, Hilgard P, Gane E, Blanc JF, et al. Sorafenib in advanced hepatocellular carcinoma. *The New England journal of medicine*. 2008;359(4):378-90.
10. Cheng AL, Kang YK, Chen Z, Tsao CJ, Qin S, Kim JS, et al. Efficacy and safety of sorafenib in patients in the Asia-Pacific region with advanced hepatocellular carcinoma: a phase III randomised, double-blind, placebo-controlled trial. *The Lancet Oncology*. 2009;10(1):25-34.
11. Society AC. *Cancer Facts & Figures 2011*. Atlanta: American Cancer Society, 2011.
12. Wada Y, Nakashima O, Kutami R, Yamamoto O, Kojiro M. Clinicopathological study on hepatocellular carcinoma with lymphocytic infiltration. *Hepatology (Baltimore, Md)*. 1998;27(2):407-14.
13. Unitt E, Marshall A, Gelson W, Rushbrook SM, Davies S, Vowler SL, et al. Tumour lymphocytic infiltrate and recurrence of hepatocellular carcinoma following liver transplantation. *Journal of hepatology*. 2006;45(2):246-53.
14. Ikeguchi M, Oi K, Hirooka Y, Kaibara N. CD8+ lymphocyte infiltration and apoptosis in hepatocellular carcinoma. *European journal of surgical oncology : the journal of the European Society of Surgical Oncology and the British Association of Surgical Oncology*. 2004;30(1):53-7.
15. Hiroishi K, Eguchi J, Baba T, Shimazaki T, Ishii S, Hiraide A, et al. Strong CD8(+) T-cell responses against tumor-associated antigens prolong the recurrence-free interval after tumor treatment in patients with hepatocellular carcinoma. *Journal of gastroenterology*. 2010;45(4):451-8.

16. Chew V, Chen J, Lee D, Loh E, Lee J, Lim KH, et al. Chemokine-driven lymphocyte infiltration: an early intratumoural event determining long-term survival in resectable hepatocellular carcinoma. *Gut*. 2012;61(3):427-38.
17. Mizukoshi E, Nakamoto Y, Marukawa Y, Arai K, Yamashita T, Tsuji H, et al. Cytotoxic T cell responses to human telomerase reverse transcriptase in patients with hepatocellular carcinoma. *Hepatology (Baltimore, Md)*. 2006;43(6):1284-94.
18. Zerbini A, Pilli M, Soliani P, Ziegler S, Pelosi G, Orlandini A, et al. Ex vivo characterization of tumor-derived melanoma antigen encoding gene-specific CD8+ cells in patients with hepatocellular carcinoma. *Journal of hepatology*. 2004;40(1):102-9.
19. Gehring AJ, Ho ZZ, Tan AT, Aung MO, Lee KH, Tan KC, et al. Profile of tumor antigen-specific CD8 T cells in patients with hepatitis B virus-related hepatocellular carcinoma. *Gastroenterology*. 2009;137(2):682-90.
20. Butterfield LH, Meng WS, Koh A, Vollmer CM, Ribas A, Dissette VB, et al. T cell responses to HLA-A*0201-restricted peptides derived from human alpha fetoprotein. *Journal of immunology (Baltimore, Md : 1950)*. 2001;166(8):5300-8.
21. Komori H, Nakatsura T, Senju S, Yoshitake Y, Motomura Y, Ikuta Y, et al. Identification of HLA-A2- or HLA-A24-restricted CTL epitopes possibly useful for glypican-3-specific immunotherapy of hepatocellular carcinoma. *Clinical cancer research : an official journal of the American Association for Cancer Research*. 2006;12(9):2689-97.
22. Takayama T, Sekine T, Makuuchi M, Yamasaki S, Kosuge T, Yamamoto J, et al. Adoptive immunotherapy to lower postsurgical recurrence rates of hepatocellular carcinoma: a randomised trial. *Lancet*. 2000;356(9232):802-7.
23. Iglesias BV, Centeno G, Pascuccelli H, Ward F, Peters MG, Filmus J, et al. Expression pattern of glypican-3 (GPC3) during human embryonic and fetal development. *Histology and histopathology*. 2008;23(11):1333-40.
24. Capurro MI, Xiang YY, Lobe C, Filmus J. Glypican-3 promotes the growth of hepatocellular carcinoma by stimulating canonical Wnt signaling. *Cancer research*. 2005;65(14):6245-54.
25. Filmus J, Capurro M, Rast J. Glypicans. *Genome biology*. 2008;9(5):224.
26. Capurro M, Wanless IR, Sherman M, Deboer G, Shi W, Miyoshi E, et al. Glypican-3: a novel serum and histochemical marker for hepatocellular carcinoma. *Gastroenterology*. 2003;125(1):89-97.
27. Zhu ZW, Friess H, Wang L, Abou-Shady M, Zimmermann A, Lander AD, et al. Enhanced glypican-3 expression differentiates the majority of hepatocellular carcinomas from benign hepatic disorders. *Gut*. 2001;48(4):558-64.
28. Hsu HC, Cheng W, Lai PL. Cloning and expression of a developmentally regulated transcript MXR7 in hepatocellular carcinoma: biological significance and temporospatial distribution. *Cancer research*. 1997;57(22):5179-84.
29. Hippo Y, Watanabe K, Watanabe A, Midorikawa Y, Yamamoto S, Ihara S, et al. Identification of soluble NH2-terminal fragment of glypican-3 as a serological marker for early-stage hepatocellular carcinoma. *Cancer research*. 2004;64(7):2418-23.
30. Shirakawa H, Suzuki H, Shimomura M, Kojima M, Gotohda N, Takahashi S, et al. Glypican-3 expression is correlated with poor prognosis in hepatocellular carcinoma. *Cancer science*. 2009;100(8):1403-7.
31. Liang J, Ding T, Guo ZW, Yu XJ, Hu YZ, Zheng L, et al. Expression pattern of tumour-associated antigens in hepatocellular carcinoma: association with immune infiltration and disease progression. *British journal of cancer*. 2013;109(4):1031-9.

32. Tada Y, Yoshikawa T, Shimomura M, Sawada Y, Sakai M, Shirakawa H, et al. Analysis of cytotoxic T lymphocytes from a patient with hepatocellular carcinoma who showed a clinical response to vaccination with a glypican3-derived peptide. *International journal of oncology*. 2013;43(4):1019-26.
33. Ishiguro T, Sugimoto M, Kinoshita Y, Miyazaki Y, Nakano K, Tsunoda H, et al. Anti-glypican 3 antibody as a potential antitumor agent for human liver cancer. *Cancer research*. 2008;68(23):9832-8.
34. Nakano K, Orita T, Nezu J, Yoshino T, Ohizumi I, Sugimoto M, et al. Anti-glypican 3 antibodies cause ADCC against human hepatocellular carcinoma cells. *Biochemical and biophysical research communications*. 2009;378(2):279-84.
35. Li Y, Siegel DL, Scholler N, Kaplan DE. Validation of glypican-3-specific scFv isolated from paired display/secretory yeast display library. *BMC biotechnology*. 2012;12:23.
36. Kaplan D, inventor Glypican-3-specific antibody and uses thereof. 2013.
37. Sawada Y, Yoshikawa T, Nobuoka D, Shirakawa H, Kuronuma T, Motomura Y, et al. Phase I trial of a glypican-3-derived peptide vaccine for advanced hepatocellular carcinoma: immunologic evidence and potential for improving overall survival. *Clinical cancer research : an official journal of the American Association for Cancer Research*. 2012;18(13):3686-96.
38. Zhu AX, Gold PJ, El-Khoueiry AB, Abrams TA, Morikawa H, Ohishi N, et al. First-in-man phase I study of GC33, a novel recombinant humanized antibody against glypican-3, in patients with advanced hepatocellular carcinoma. *Clinical cancer research : an official journal of the American Association for Cancer Research*. 2013;19(4):920-8.
39. Ikeda M, Ohkawa S, Okusaka T, Mitsunaga S, Kobayashi S, Morizane C, et al. Japanese phase I study of GC33, a humanized antibody against glypican-3 for advanced hepatocellular carcinoma. *Cancer science*. 2014;105(4):455-62.
40. Wiemann B, Starnes CO. Coley's toxins, tumor necrosis factor and cancer research: a historical perspective. *Pharmacology & therapeutics*. 1994;64(3):529-64.
41. Burnet FM. The concept of immunological surveillance. *Progress in experimental tumor research*. 1970;13:1-27.
42. Urban JL, Schreiber H. Tumor antigens. *Annual review of immunology*. 1992;10:617-44.
43. van der Bruggen P, Traversari C, Chomez P, Lurquin C, De Plaen E, Van den Eynde B, et al. A gene encoding an antigen recognized by cytolytic T lymphocytes on a human melanoma. *Science (New York, NY)*. 1991;254(5038):1643-7.
44. Morris EC, Bendle GM, Stauss HJ. Prospects for immunotherapy of malignant disease. *Clinical and experimental immunology*. 2003;131(1):1-7.
45. Murphy K. TP, Walport M. *Janeway's immunobiology*. 7th edition ed. New York and Abingdon: Garland Science; 2008.
46. Rooney CM, Smith CA, Ng CY, Loftin S, Li C, Krance RA, et al. Use of gene-modified virus-specific T lymphocytes to control Epstein-Barr-virus-related lymphoproliferation. *Lancet*. 1995;345(8941):9-13.
47. Pule MA, Savoldo B, Myers GD, Rossig C, Russell HV, Dotti G, et al. Virus-specific T cells engineered to coexpress tumor-specific receptors: persistence and antitumor activity in individuals with neuroblastoma. *Nature medicine*. 2008;14(11):1264-70.
48. Riddell SR, Watanabe KS, Goodrich JM, Li CR, Agha ME, Greenberg PD. Restoration of viral immunity in immunodeficient humans by the adoptive transfer of T cell clones. *Science (New York, NY)*. 1992;257(5067):238-41.

49. Mackinnon S, Thomson K, Verfuert S, Peggs K, Lowdell M. Adoptive cellular therapy for cytomegalovirus infection following allogeneic stem cell transplantation using virus-specific T cells. *Blood cells, molecules & diseases*. 2008;40(1):63-7.
50. Rosenberg SA, Dudley ME. Cancer regression in patients with metastatic melanoma after the transfer of autologous antitumor lymphocytes. *Proceedings of the National Academy of Sciences of the United States of America*. 2004;101 Suppl 2:14639-45.
51. Dudley ME, Wunderlich JR, Robbins PF, Yang JC, Hwu P, Schwartzentruber DJ, et al. Cancer regression and autoimmunity in patients after clonal repopulation with antitumor lymphocytes. *Science (New York, NY)*. 2002;298(5594):850-4.
52. Morgan RA, Dudley ME, Wunderlich JR, Hughes MS, Yang JC, Sherry RM, et al. Cancer regression in patients after transfer of genetically engineered lymphocytes. *Science (New York, NY)*. 2006;314(5796):126-9.
53. Kawata A, Une Y, Hosokawa M, Uchino J, Kobayashi H. Tumor-infiltrating lymphocytes and prognosis of hepatocellular carcinoma. *Japanese journal of clinical oncology*. 1992;22(4):256-63.
54. Berger C, Turtle CJ, Jensen MC, Riddell SR. Adoptive transfer of virus-specific and tumor-specific T cell immunity. *Current opinion in immunology*. 2009;21(2):224-32.
55. Baron F, Maris MB, Sandmaier BM, Storer BE, Sorrow M, Diaconescu R, et al. Graft-versus-tumor effects after allogeneic hematopoietic cell transplantation with nonmyeloablative conditioning. *Journal of clinical oncology : official journal of the American Society of Clinical Oncology*. 2005;23(9):1993-2003.
56. Toze CL, Galal A, Barnett MJ, Shepherd JD, Conneally EA, Hogge DE, et al. Myeloablative allografting for chronic lymphocytic leukemia: evidence for a potent graft-versus-leukemia effect associated with graft-versus-host disease. *Bone marrow transplantation*. 2005;36(9):825-30.
57. Kolb HJ, Schmid C, Barrett AJ, Schendel DJ. Graft-versus-leukemia reactions in allogeneic chimeras. *Blood*. 2004;103(3):767-76.
58. Lindahl KF, Wilson DB. Histocompatibility antigen-activated cytotoxic T lymphocytes. II. Estimates of the frequency and specificity of precursors. *The Journal of experimental medicine*. 1977;145(3):508-22.
59. Felix NJ, Donermeyer DL, Horvath S, Walters JJ, Gross ML, Suri A, et al. Alloreactive T cells respond specifically to multiple distinct peptide-MHC complexes. *Nature immunology*. 2007;8(4):388-97.
60. Wilde S, Geiger C, Milosevic S, Mosetter B, Eichenlaub S, Schendel DJ. Generation of allo-restricted peptide-specific T cells using RNA-pulsed dendritic cells: A three phase experimental procedure. *Oncoimmunology*. 2012;1(2):129-40.
61. Li LP, Lampert JC, Chen X, Leitao C, Popovic J, Muller W, et al. Transgenic mice with a diverse human T cell antigen receptor repertoire. *Nature medicine*. 2010;16(9):1029-34.
62. Rosenberg SA, Restifo NP, Yang JC, Morgan RA, Dudley ME. Adoptive cell transfer: a clinical path to effective cancer immunotherapy. *Nature reviews Cancer*. 2008;8(4):299-308.
63. Johnson LA, Morgan RA, Dudley ME, Cassard L, Yang JC, Hughes MS, et al. Gene therapy with human and mouse T-cell receptors mediates cancer regression and targets normal tissues expressing cognate antigen. *Blood*. 2009;114(3):535-46.
64. Robbins PF, Morgan RA, Feldman SA, Yang JC, Sherry RM, Dudley ME, et al. Tumor regression in patients with metastatic synovial cell sarcoma and melanoma using genetically engineered lymphocytes reactive with NY-ESO-1. *Journal of clinical*

- oncology : official journal of the American Society of Clinical Oncology. 2011;29(7):917-24.
65. Carding SR, Egan PJ. Gammadelta T cells: functional plasticity and heterogeneity. *Nature reviews Immunology*. 2002;2(5):336-45.
 66. Wencker M, Turchinovich G, Di Marco Barros R, Deban L, Jandke A, Cope A, et al. Innate-like T cells straddle innate and adaptive immunity by altering antigen-receptor responsiveness. *Nature immunology*. 2014;15(1):80-7.
 67. Malissen B, Schmitt-Verhulst AM. Transmembrane signalling through the T-cell-receptor-CD3 complex. *Current opinion in immunology*. 1993;5(3):324-33.
 68. Rudolph MG, Stanfield RL, Wilson IA. How TCRs bind MHCs, peptides, and coreceptors. *Annual review of immunology*. 2006;24:419-66.
 69. Hogquist KA, Baldwin TA, Jameson SC. Central tolerance: learning self-control in the thymus. *Nature reviews Immunology*. 2005;5(10):772-82.
 70. Starr TK, Jameson SC, Hogquist KA. Positive and negative selection of T cells. *Annual review of immunology*. 2003;21:139-76.
 71. Srinivasan M, Frauwirth KA. Peripheral tolerance in CD8+ T cells. *Cytokine*. 2009;46(2):147-59.
 72. Knolle PA, Gerken G. Local control of the immune response in the liver. *Immunological reviews*. 2000;174:21-34.
 73. Wherry EJ, Teichgraber V, Becker TC, Masopust D, Kaech SM, Antia R, et al. Lineage relationship and protective immunity of memory CD8 T cell subsets. *Nature immunology*. 2003;4(3):225-34.
 74. Ibe S, Qin Z, Schuler T, Preiss S, Blankenstein T. Tumor rejection by disturbing tumor stroma cell interactions. *The Journal of experimental medicine*. 2001;194(11):1549-59.
 75. Shankaran V, Ikeda H, Bruce AT, White JM, Swanson PE, Old LJ, et al. IFN γ and lymphocytes prevent primary tumour development and shape tumour immunogenicity. *Nature*. 2001;410(6832):1107-11.
 76. Street SE, Cretney E, Smyth MJ. Perforin and interferon-gamma activities independently control tumor initiation, growth, and metastasis. *Blood*. 2001;97(1):192-7.
 77. FF G-G, S C, D M, AR J, . Allele frequency net: a database and online repository for immune gene frequencies in worldwide populations. Liverpool, U.K. [08.09.2014]. Available from: <http://www.allelefrequencienet/>.
 78. Uckert W, Becker C, Gladow M, Klein D, Kammertoens T, Pedersen L, et al. Efficient gene transfer into primary human CD8+ T lymphocytes by MuLV-10A1 retrovirus pseudotype. *Human gene therapy*. 2000;11(7):1005-14.
 79. Engels B, Cam H, Schuler T, Indraccolo S, Gladow M, Baum C, et al. Retroviral vectors for high-level transgene expression in T lymphocytes. *Human gene therapy*. 2003;14(12):1155-68.
 80. Salter RD, Howell DN, Cresswell P. Genes regulating HLA class I antigen expression in T-B lymphoblast hybrids. *Immunogenetics*. 1985;21(3):235-46.
 81. Broeren CP, Verjans GM, Van Eden W, Kusters JG, Lenstra JA, Logtenberg T. Conserved nucleotide sequences at the 5' end of T cell receptor variable genes facilitate polymerase chain reaction amplification. *European journal of immunology*. 1991;21(3):569-75.

82. Zhou D, Srivastava R, Grummel V, Cepok S, Hartung HP, Hemmer B. High throughput analysis of TCR-beta rearrangement and gene expression in single T cells. *Laboratory investigation; a journal of technical methods and pathology*. 2006;86(3):314-21.
83. Schuster I. Identifikation, Klonierung und retroviraler Transfer allorestingierter FMNL1-peptidspezifischer T-Zellrezeptoren für die Entwicklung adoptiver Immuntherapien gegen B-Zell-Non-Hodgkin-Lymphome. [Dissertation]. Munich: Ludwig-Maximilians-Universität; 2008.
84. Biolabs NE. Tm calculator 2014 [26.08.2014]. Available from: <https://www.neb.com/tools-and-resources/interactive-tools/tm-calculator>.
85. Sommermeyer D, Neudorfer J, Weinhold M, Leisegang M, Engels B, Noessner E, et al. Designer T cells by T cell receptor replacement. *European journal of immunology*. 2006;36(11):3052-9.
86. Szymczak AL, Workman CJ, Wang Y, Vignali KM, Dilioglou S, Vanin EF, et al. Correction of multi-gene deficiency in vivo using a single 'self-cleaving' 2A peptide-based retroviral vector. *Nature biotechnology*. 2004;22(5):589-94.
87. O'Beirne J, Farzaneh F, Harrison PM. Generation of functional CD8+ T cells by human dendritic cells expressing glypican-3 epitopes. *Journal of experimental & clinical cancer research : CR*. 2010;29:48.
88. Rammensee H, Bachmann J, Emmerich NP, Bachor OA, Stevanovic S. SYFPEITHI: database for MHC ligands and peptide motifs. *Immunogenetics*. 1999;50(3-4):213-9.
89. Parker KC, Bednarek MA, Coligan JE. Scheme for ranking potential HLA-A2 binding peptides based on independent binding of individual peptide side-chains. *Journal of immunology (Baltimore, Md : 1950)*. 1994;152(1):163-75.
90. Nielsen M, Lundegaard C, Worning P, Lauemoller SL, Lamberth K, Buus S, et al. Reliable prediction of T-cell epitopes using neural networks with novel sequence representations. *Protein science : a publication of the Protein Society*. 2003;12(5):1007-17.
91. Lundegaard C, Lamberth K, Harndahl M, Buus S, Lund O, Nielsen M. NetMHC-3.0: accurate web accessible predictions of human, mouse and monkey MHC class I affinities for peptides of length 8-11. *Nucleic acids research*. 2008;36(Web Server issue):W509-12.
92. Stauss HJ. Immunotherapy with CTLs restricted by nonself MHC. *Immunology today*. 1999;20(4):180-3.
93. Schuster IG, Busch DH, Eppinger E, Kremmer E, Milosevic S, Hennard C, et al. Allorestricted T cells with specificity for the FMNL1-derived peptide PP2 have potent antitumor activity against hematologic and other malignancies. *Blood*. 2007;110(8):2931-9.
94. Dauer M, Obermaier B, Hertel J, Haerle C, Pohl K, Rothenfusser S, et al. Mature dendritic cells derived from human monocytes within 48 hours: a novel strategy for dendritic cell differentiation from blood precursors. *Journal of immunology (Baltimore, Md : 1950)*. 2003;170(8):4069-76.
95. Wolf M, Kuball J, Ho WY, Nguyen H, Manley TJ, Bleakley M, et al. Activation-induced expression of CD137 permits detection, isolation, and expansion of the full repertoire of CD8+ T cells responding to antigen without requiring knowledge of epitope specificities. *Blood*. 2007;110(1):201-10.
96. Flecken T, Schmidt N, Hild S, Gostick E, Drognitz O, Zeiser R, et al. Immunodominance and functional alterations of tumor-associated antigen-specific CD8+ T-cell responses in hepatocellular carcinoma. *Hepatology (Baltimore, Md)*. 2014;59(4):1415-26.

97. Muranski P, Restifo NP. Adoptive immunotherapy of cancer using CD4(+) T cells. *Current opinion in immunology*. 2009;21(2):200-8.
98. Kessler JH, Melief CJ. Identification of T-cell epitopes for cancer immunotherapy. *Leukemia*. 2007;21(9):1859-74.
99. Visseren MJ, van Elsas A, van der Voort EI, Rensing ME, Kast WM, Schrier PI, et al. CTL specific for the tyrosinase autoantigen can be induced from healthy donor blood to lyse melanoma cells. *Journal of immunology (Baltimore, Md : 1950)*. 1995;154(8):3991-8.
100. Ho WY, Nguyen HN, Wolfi M, Kuball J, Greenberg PD. In vitro methods for generating CD8+ T-cell clones for immunotherapy from the naive repertoire. *Journal of immunological methods*. 2006;310(1-2):40-52.
101. Banchereau J, Steinman RM. Dendritic cells and the control of immunity. *Nature*. 1998;392(6673):245-52.
102. Shay JW, Wright WE. Senescence and immortalization: role of telomeres and telomerase. *Carcinogenesis*. 2005;26(5):867-74.
103. Heemskerk MH, Hoogeboom M, Hagedoorn R, Kester MG, Willemze R, Falkenburg JH. Reprogramming of virus-specific T cells into leukemia-reactive T cells using T cell receptor gene transfer. *The Journal of experimental medicine*. 2004;199(7):885-94.
104. Scholten KB, Kramer D, Kueter EW, Graf M, Schoedl T, Meijer CJ, et al. Codon modification of T cell receptors allows enhanced functional expression in transgenic human T cells. *Clinical immunology (Orlando, Fla)*. 2006;119(2):135-45.
105. Hart DP, Xue SA, Thomas S, Cesco-Gaspere M, Tranter A, Willcox B, et al. Retroviral transfer of a dominant TCR prevents surface expression of a large proportion of the endogenous TCR repertoire in human T cells. *Gene therapy*. 2008;15(8):625-31.
106. Cohen CJ, Zhao Y, Zheng Z, Rosenberg SA, Morgan RA. Enhanced antitumor activity of murine-human hybrid T-cell receptor (TCR) in human lymphocytes is associated with improved pairing and TCR/CD3 stability. *Cancer research*. 2006;66(17):8878-86.
107. Davis JL, Theoret MR, Zheng Z, Lamers CH, Rosenberg SA, Morgan RA. Development of human anti-murine T-cell receptor antibodies in both responding and nonresponding patients enrolled in TCR gene therapy trials. *Clinical cancer research : an official journal of the American Association for Cancer Research*. 2010;16(23):5852-61.
108. Sommermeyer D, Uckert W. Minimal amino acid exchange in human TCR constant regions fosters improved function of TCR gene-modified T cells. *Journal of immunology (Baltimore, Md : 1950)*. 2010;184(11):6223-31.
109. Kuball J, Dossett ML, Wolfi M, Ho WY, Voss RH, Fowler C, et al. Facilitating matched pairing and expression of TCR chains introduced into human T cells. *Blood*. 2007;109(6):2331-8.
110. Dossinger G, Bunse M, Bet J, Albrecht J, Paszkiewicz PJ, Weissbrich B, et al. MHC multimer-guided and cell culture-independent isolation of functional T cell receptors from single cells facilitates TCR identification for immunotherapy. *PloS one*. 2013;8(4):e61384.
111. Heemskerk MH, Hagedoorn RS, van der Hoorn MA, van der Veken LT, Hoogeboom M, Kester MG, et al. Efficiency of T-cell receptor expression in dual-specific T cells is controlled by the intrinsic qualities of the TCR chains within the TCR-CD3 complex. *Blood*. 2007;109(1):235-43.
112. Ruppert J, Sidney J, Celis E, Kubo RT, Grey HM, Sette A. Prominent role of secondary anchor residues in peptide binding to HLA-A2.1 molecules. *Cell*. 1993;74(5):929-37.

113. Alexander-Miller MA, Leggatt GR, Berzofsky JA. Selective expansion of high- or low-avidity cytotoxic T lymphocytes and efficacy for adoptive immunotherapy. *Proceedings of the National Academy of Sciences of the United States of America*. 1996;93(9):4102-7.
114. Bendle GM, Holler A, Pang LK, Hsu S, Krampera M, Simpson E, et al. Induction of unresponsiveness limits tumor protection by adoptively transferred MDM2-specific cytotoxic T lymphocytes. *Cancer research*. 2004;64(21):8052-6.
115. Lyman MA, Nugent CT, Marquardt KL, Biggs JA, Pamer EG, Sherman LA. The fate of low affinity tumor-specific CD8+ T cells in tumor-bearing mice. *Journal of immunology (Baltimore, Md : 1950)*. 2005;174(5):2563-72.
116. Parkhurst MR, Yang JC, Langan RC, Dudley ME, Nathan DA, Feldman SA, et al. T cells targeting carcinoembryonic antigen can mediate regression of metastatic colorectal cancer but induce severe transient colitis. *Molecular therapy : the journal of the American Society of Gene Therapy*. 2011;19(3):620-6.
117. Fleischhauer K, Tanzarella S, Wallny HJ, Bordignon C, Traversari C. Multiple HLA-A alleles can present an immunodominant peptide of the human melanoma antigen Melan-A/MART-1 to a peptide-specific HLA-A*0201+ cytotoxic T cell line. *Journal of immunology (Baltimore, Md : 1950)*. 1996;157(2):787-97.
118. Sadovnikova E, Stauss HJ. Peptide-specific cytotoxic T lymphocytes restricted by nonself major histocompatibility complex class I molecules: reagents for tumor immunotherapy. *Proceedings of the National Academy of Sciences of the United States of America*. 1996;93(23):13114-8.
119. Hunder NN, Wallen H, Cao J, Hendricks DW, Reilly JZ, Rodmyre R, et al. Treatment of metastatic melanoma with autologous CD4+ T cells against NY-ESO-1. *The New England journal of medicine*. 2008;358(25):2698-703.
120. Martin-Orozco N, Muranski P, Chung Y, Yang XO, Yamazaki T, Lu S, et al. T helper 17 cells promote cytotoxic T cell activation in tumor immunity. *Immunity*. 2009;31(5):787-98.
121. Hamann D, Baars PA, Rep MH, Hooibrink B, Kerkhof-Garde SR, Klein MR, et al. Phenotypic and functional separation of memory and effector human CD8+ T cells. *The Journal of experimental medicine*. 1997;186(9):1407-18.
122. Johnson LA, Heemskerk B, Powell DJ, Jr., Cohen CJ, Morgan RA, Dudley ME, et al. Gene transfer of tumor-reactive TCR confers both high avidity and tumor reactivity to nonreactive peripheral blood mononuclear cells and tumor-infiltrating lymphocytes. *Journal of immunology (Baltimore, Md : 1950)*. 2006;177(9):6548-59.
123. Lee YH, Andersen JB, Song HT, Judge AD, Seo D, Ishikawa T, et al. Definition of ubiquitination modulator COP1 as a novel therapeutic target in human hepatocellular carcinoma. *Cancer research*. 2010;70(21):8264-9.
124. Baumhoer D, Tornillo L, Stadlmann S, Roncalli M, Diamantis EK, Terracciano LM. Glypican 3 expression in human nonneoplastic, preneoplastic, and neoplastic tissues: a tissue microarray analysis of 4,387 tissue samples. *American journal of clinical pathology*. 2008;129(6):899-906.
125. Di Stasi A, Tey SK, Dotti G, Fujita Y, Kennedy-Nasser A, Martinez C, et al. Inducible apoptosis as a safety switch for adoptive cell therapy. *The New England journal of medicine*. 2011;365(18):1673-83.
126. Wang X, Chang WC, Wong CW, Colcher D, Sherman M, Ostberg JR, et al. A transgene-encoded cell surface polypeptide for selection, in vivo tracking, and ablation of engineered cells. *Blood*. 2011;118(5):1255-63.

127. Diehl L, Schurich A, Grochtmann R, Hegenbarth S, Chen L, Knolle PA. Tolerogenic maturation of liver sinusoidal endothelial cells promotes B7-homolog 1-dependent CD8+ T cell tolerance. *Hepatology (Baltimore, Md)*. 2008;47(1):296-305.
128. Holz LE, Benseler V, Bowen DG, Bouillet P, Strasser A, O'Reilly L, et al. Intrahepatic murine CD8 T-cell activation associates with a distinct phenotype leading to Bim-dependent death. *Gastroenterology*. 2008;135(3):989-97.
129. Fu J, Xu D, Liu Z, Shi M, Zhao P, Fu B, et al. Increased regulatory T cells correlate with CD8 T-cell impairment and poor survival in hepatocellular carcinoma patients. *Gastroenterology*. 2007;132(7):2328-39.
130. Hoechst B, Voigtlaender T, Ormandy L, Gamrekelashvili J, Zhao F, Wedemeyer H, et al. Myeloid derived suppressor cells inhibit natural killer cells in patients with hepatocellular carcinoma via the NKp30 receptor. *Hepatology (Baltimore, Md)*. 2009;50(3):799-807.
131. Hu CE, Gan J, Zhang RD, Cheng YR, Huang GJ. Up-regulated myeloid-derived suppressor cell contributes to hepatocellular carcinoma development by impairing dendritic cell function. *Scandinavian journal of gastroenterology*. 2011;46(2):156-64.
132. Huang J, Cai MY, Wei DP. HLA class I expression in primary hepatocellular carcinoma. *World journal of gastroenterology : WJG*. 2002;8(4):654-7.
133. Restifo NP, Marincola FM, Kawakami Y, Taubenberger J, Yannelli JR, Rosenberg SA. Loss of functional beta 2-microglobulin in metastatic melanomas from five patients receiving immunotherapy. *Journal of the National Cancer Institute*. 1996;88(2):100-8.
134. Svane IM, Engel AM, Nielsen M, Werdelin O. Interferon-gamma-induced MHC class I expression and defects in Jak/Stat signalling in methylcholanthrene-induced sarcomas. *Scandinavian journal of immunology*. 1997;46(4):379-87.
135. Kerkar SP, Goldszmid RS, Muranski P, Chinnasamy D, Yu Z, Reger RN, et al. IL-12 triggers a programmatic change in dysfunctional myeloid-derived cells within mouse tumors. *The Journal of clinical investigation*. 2011;121(12):4746-57.
136. Pegram HJ, Lee JC, Hayman EG, Imperato GH, Tedder TF, Sadelain M, et al. Tumor-targeted T cells modified to secrete IL-12 eradicate systemic tumors without need for prior conditioning. *Blood*. 2012;119(18):4133-41.

7 Acknowledgements

First of all I thank Ulrike Protzer for giving me the chance to work on this exciting project. Ulla always believed in me and supported me in every possible way. Just to mention a few of them, I could visit several inspiring conferences and participate at soft-skill courses that certainly helped me to achieve my goals and set important foundations for my future career.

I also thank Jörg Durner and Dirk Busch for their time and all their useful input during my thesis committee meetings.

I would like to thank the Konrad-Adenauer Foundation, not only for their financial but also for the ideational support and the opportunity to meet all these intriguing people.

I am very grateful to Theresa Asen, Kathrin Kappes, Christina Neff, Natalie Röder, Kerstin Ackermann, Daniel Kull and Lynette Henkel for their excellent technical assistance. Susanne Wilde, Karin Wisskirchen, Felix Bohne, Martin Sprinzl and Richard Klar were always there to discuss data or help with trouble shootings and shared a lot of protocols with me.

Thank you to Katrin Singethan, Almut Glinzer, Barbara Heidenreich, Nina Böttinger and Felix Bohne for proof reading my doctoral thesis and their helpful input.

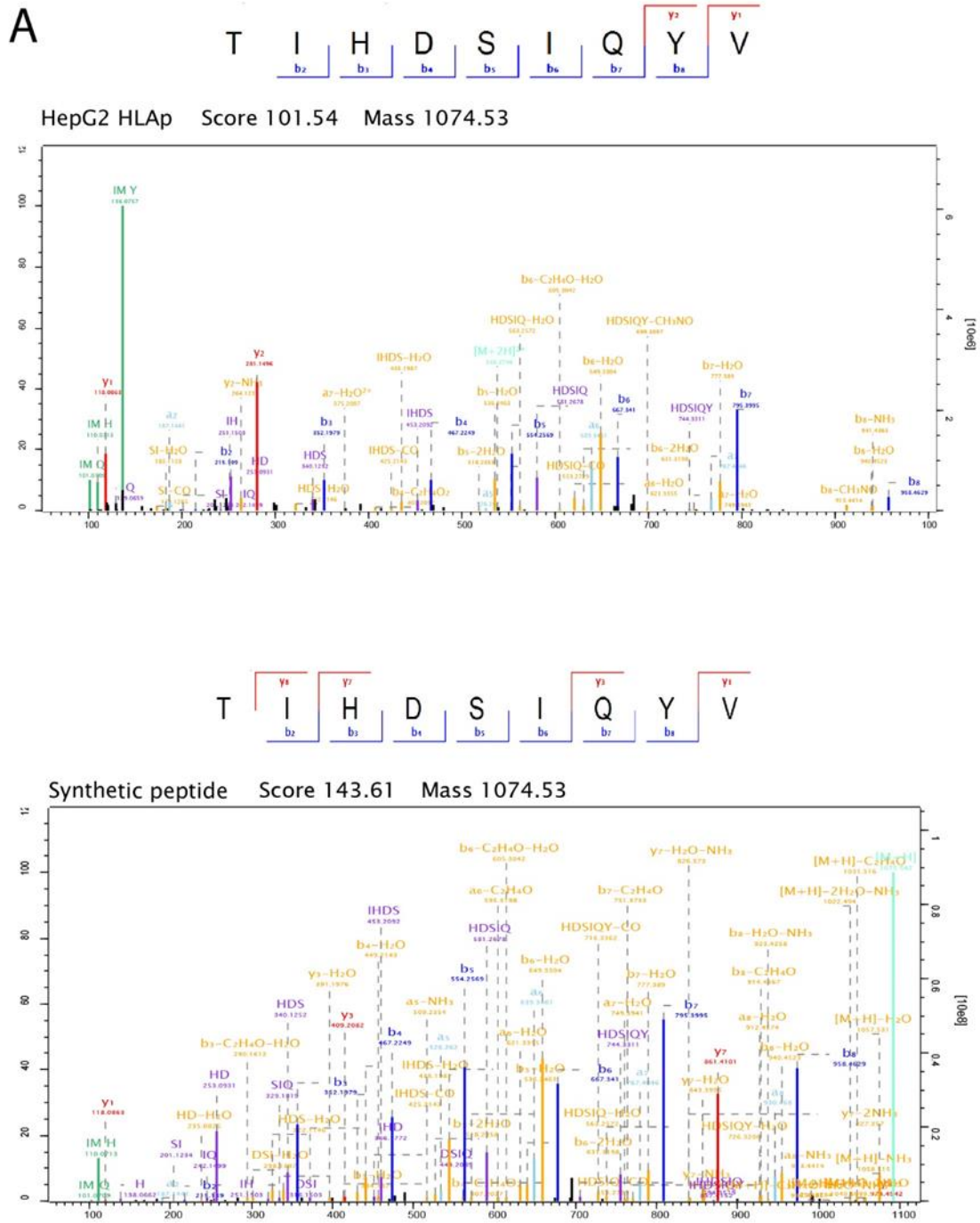
My time here in Munich in the Virology lab would not have been as great and successful without the wonderful working atmosphere in the lab. Special thanks for that to Stefanie Graf, Theresa Asen, Julia Hasreiter, Felix Bohne, Nina Böttinger, Clemens Jäger, Caro Russo, Antje Malo, Karin Wisskirchen, Katrin Singethan, Kerstin Ackermann, Jochen Wettengel, Knud Esser, Yuchen Xia, Xiaoming Chen, Oliver Quitt and everybody else of the group. It was a pleasure and lots of fun to work with you.

I want to thank my friends Almut and Barbara, Nils, my Family – especially my two sisters Anke and Britta, Steffi and Katrin, who were there when I needed someone to talk to.

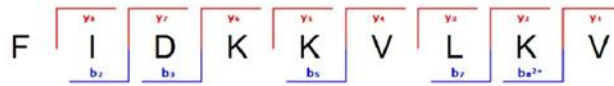
In the end I want to thank Nils with all my heart. He was always there to cheer me up when I was frustrated from lab work and offered more than welcome distractions during stressful times.

8 Appendix

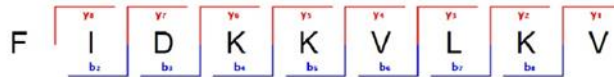
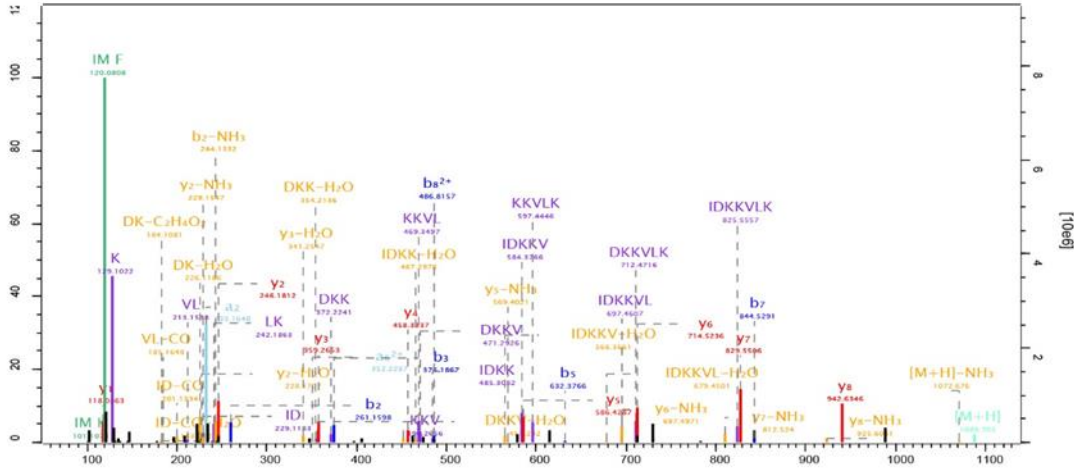
8.1 Mass spectra of GPC3₃₆₇ (TIHDSIQYV) and GPC3₃₂₆ (FIDKKVLKV)



B



HepG2 HLAp Score 113.71 Mass 1088.7



Synthetic peptide Score 147.75 Mass 1088.7

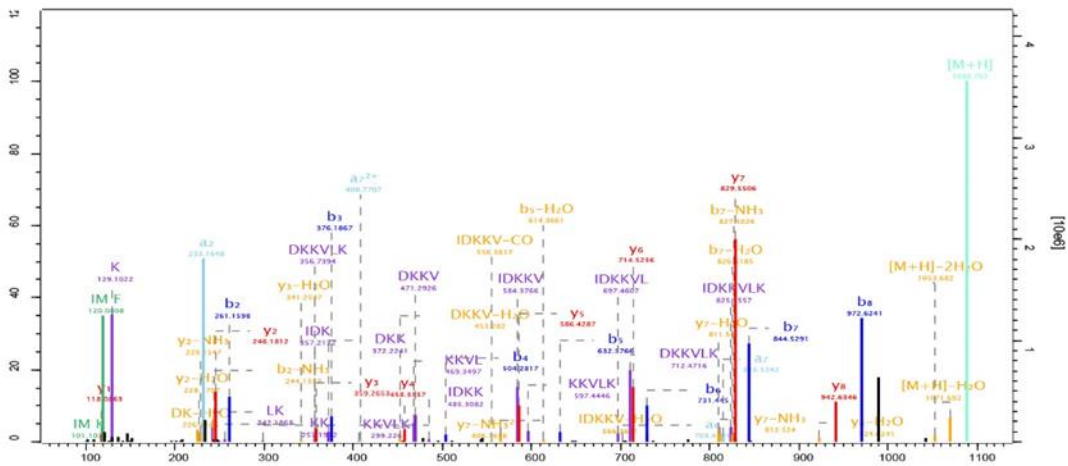


Figure 42 Mass spectra of (A) GPC3₃₆₇ (TIHDSIQYV) and (B) GPC3₃₂₆ (FIDKKVLKV). Mass spectra of the two purified peptides and their synthetic counterparts are shown.

8.2 Methods for mass spectroscopic analysis of immune-affinity purified HLA-I complexes

8.2.1 Affinity purification of HLA molecules

HLA-I complexes were purified from two biological replicates of 5x10⁸ HepG2 cells lysed with 0.25% sodium deoxycholate, 0.2 mM iodoacetamide, 1 mM EDTA, 1:200 Protease Inhibitors Cocktail (Sigma), 1 mM Phenylmethanesulfonyl fluoride (Sigma), 1% octyl- β -D glucopyranoside (Sigma) in PBS at 4 °C for 1 h. The lysates were cleared by 30 min centrifugation at 40,000 \times g. HLA-I molecules from cleared lysate were immunoaffinity purified with the W6/32 antibody, which was purified from the growth medium of HB-95 hybridoma cells, covalently bound to protein-A Sepharose beads (Invitrogen, CA). The affinity column was thoroughly washed first with 10 column volumes of 150 mM NaCl, 400 mM NaCl and 150 nM NaCl containing and pure 20 mM Tris HCl, pH 8.0, each. HLA-I molecules were eluted at room temperature in 7 fractions à 500 μ l of 0.1 N acetic acid and were analysed by 12% SDS-PAGE to evaluate yield and purity.

8.2.2 Purification and concentration of HLA-I peptides

Eluted HLA-I peptides and the subunits of the HLA complex were loaded on Sep-Pak tC18 (Waters) cartridges that were pre-washed with 80% acetonitril (ACN) in 0.1% trifluoroacetic acid (TFA) and with 0.1% TFA only. After loading, the cartridges were washed with 0.1% TFA. The peptides were separated from the HLA-I heavy chains on the C18 cartridges, based on their hydrophobicity. The peptides were eluted with 30% ACN in 0.1% TFA. HLA-I peptides were further purified using Silica C-18 column (Harvard Apparatus, MA) tips and eluted again with 30% ACN in 0.1% TFA. The peptides were concentrated and the volume was reduced to 15 μ l using vacuum centrifugation. For the mass spectrometry analysis 5 μ l of the highly enriched HLA peptides sample were used.

8.2.3 LC-MS/MS analysis of HLA peptides

HLA peptides were separated by a nanoflow HPLC (Proxeon Biosystems, now Thermo Fisher Scientific) and coupled on-line to a Q Exactive mass spectrometer (Thermo Fisher Scientific)

with a nanoelectrospray ion source (Proxeon Biosystems). The column (20 cm long, 75 μm inner diameter) is packed in-house with ReproSil-Pur C18-AQ 1.9 μm resin (Dr. Maisch GmbH, Ammerbuch-Entringen, Germany) in buffer a (0.5% acetic acid). Peptides were eluted with a linear gradient of 2–30% buffer B (80% ACN and 0.5% acetic acid) at a flow rate of 250 nl/min over 90 min. Data was acquired using a data-dependent ‘top 10’ in order to isolate them and fragment them by higher energy collisional dissociation (HCD). Full scan MS spectra were acquired at a resolution of 70,000 at 200 m/z with a target value of 3,000,000 ions. The ten most intense ions were sequentially isolated and accumulated to an AGC target value of 100,000 with a maximum injection time of 120 to increase signal of the fragments. Unassigned precursor ion charge states, as well as 4 and above charged species were rejected and peptide match was disabled. The fragmentation spectra of ions were acquired in the Orbitrap analyser with a resolution of 17,500 at 200 m/z.

8.2.4 Mass spectrometry data analysis of HLA peptides

MaxQuant computational proteomics platform (Cox and Mann, 2008) version 1.3.10.14 was used. Andromeda, a probabilistic search engine incorporated in the MaxQuant framework (Cox et al., 2011), was used to search the peak lists against the UniProt database (86,749 entries). N-terminal acetylation and methionine oxidation were set as variable modifications. The second peptide identification option in Andromeda was enabled. For statistical evaluation, the posterior error probability and false discovery rate were used. A false discovery rate of 0.01 was required for peptides and no false discovery rate was required for proteins, using a reverse database with no special AAs. The enzyme specificity was set as unspecific. A length restriction of 8 to 15 SS. was set, or a maximum peptides mass of maximum 1,500 Da. The initial mass deviation of the precursor ion was set up to 6 ppm and the fragment mass deviation was set up to 20 ppm. The ‘match between runs’ option was enabled, that allows matching of identifications across different replicates, in a time window of 0.5 min.

8.3 Vector maps

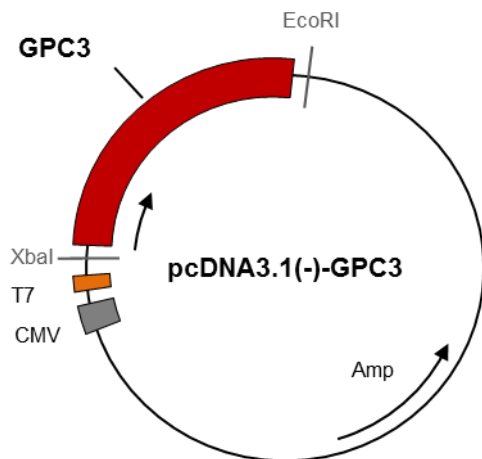


Figure 43 Vector map of pcDNA3.1(-)-GPC3. GPC3 was inserted into the vector by *XbaI* and *EcoRI* restriction sites. GPC3 transcription is induced by a CMV or T7 promoter. The plasmid contains an ampicillin resistance gene.

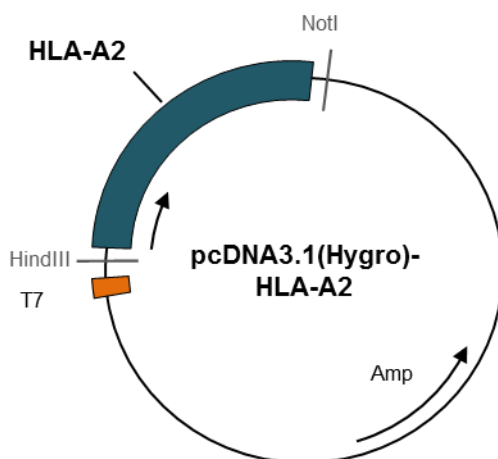


Figure 44 Vector map of pcDNA3.1(Hygro)-HLA-A2. HLA-A2 was inserted into the vector by *HindIII* and *NotI* restriction sites. HLA-A2 transcription is induced by a T7 promoter. The plasmid contains an ampicillin resistance gene.

8.4 Curriculum Vitae

Christina Dargel



Clara-Immerwahr-Weg 1
50933 Köln
Mobil: + 49 (0) 176 6150 6326
E-Mail: christina.dargel@web.de

Persönliche Daten

Geburtstag:	08. August 1986
Geburtsort:	Marl
Familienstand:	Ledig, keine Kinder

Akademischer Werdegang

09/2011-10/2014	Technische Universität München/Helmholtz Zentrum München, Institut für Virologie, Doktorandin <ul style="list-style-type: none"> ▪ Entwicklung einer T-Zell-basierten Immuntherapie zur Behandlung des Hepatozellulären Karzinoms ▪ Projektmanagement-, Konfliktmanagement- und BWL Grundkurse an der Graduate School HELENA (Helmholtz Environmental Health)/ TUM Medical Graduate School ▪ Vermittlung von Labormethoden und Herangehensweisen an wissenschaftliche Fragestellungen an studentische Mitarbeiter ▪ Präsentation der Forschungsergebnisse auf wissenschaftlichen Kongressen
10/2009-08/2011	Ludwig-Maximilians-Universität München Masterstudium Pharmaceutical Sciences Abschlussnote 1,5 Schwerpunkte: Pharmazeutische Biologie, Pharmakologie
01/2011-07/2011	Leiden University Medical Center, Institut für medizinische Mikrobiologie, Niederlande Masterarbeit: Charakterisierung der T-Antigene des Trichodysplasia-Spinulosa-assoziiertem Polyomavirus
10/2006-09/2009	Ludwig-Maximilians-Universität München Bachelorstudium Pharmaceutical Sciences Abschlussnote 1,7 Schwerpunkte: Pharmazeutische Biologie, Pharmakologie, Pharmazeutische Technologie und Pharmazeutische Chemie
03/2009-04/2009	Technische Universität München, Institut für Virologie Bachelorarbeit: Konstruktion und Charakterisierung rekombinanter MVA Impfstoffe zur Therapie chronischer Hepatitis B-Infektionen
10/2005-03/2006	Technische Universität München Bachelorstudium Biologie

Praktische Erfahrungen/Auslandsaufenthalte

09/2010-12/2010	University College London, Department for Infection and Immunity, Großbritannien Praktikantin mit eigenem Forschungsprojekt über Immunantworten bei Hepatitis B-Virus Infektionen
10/2009-08/2010	Technische Universität München, Institut für Virologie, Wissenschaftliche Hilfskraft
10/2006-10/2008	Bencard Allergie GmbH, München, Werksstudentin Unterstützung der Clinical Research Associates bei der Dokumentation zu durchgeführten klinischen Studien
08/2006-09/2006	Paracelsus-Klinik, Marl, Praktikum in der Krankenhausapotheke
06/2006-07/2006	Bencard Allergie GmbH, München, Praktikantin
04/2006-05/2006	Äskulap Apotheke, Marl, Praktikantin
04/2005-09/2005	Movie Park Germany, Bottrop, Animateurin

Schulischer Werdegang

08/1996-06/2005	Abitur am Gymnasium im Loekamp, Marl Abschlussnote 1,3
-----------------	---

Zusatzqualifikationen

Fremdsprachen:	<ul style="list-style-type: none"> ▪ Englisch – verhandlungssicher ▪ Niederländisch – Grundkenntnisse ▪ Französisch – Grundkenntnisse
EDV-Kenntnisse:	<ul style="list-style-type: none"> ▪ Sehr gute Kenntnisse in MS Word, MS Excel, MS Powerpoint ▪ Sehr gute Kenntnisse in FACS Diva, FlowJo, Prism Graphpad, Vector NTI
Seminare (unter anderem):	<ul style="list-style-type: none"> ▪ Rhetorik-Seminar, Konrad-Adenauer-Stiftung, Sankt Augustin ▪ BWL – Einführung in die Unternehmensplanung und Marketing, Graduate School HELENA, München ▪ Basics in Business and Administration, TUM Graduate School

Ehrenamtliches Engagement

05/2012-03/2013	Organisation der wissenschaftlichen Konferenz Interact 2013, München <ul style="list-style-type: none"> ▪ Selbstständige Planung und Durchführung als Teil des Logistik-Teams ▪ Enge Kooperation mit den Teams Marketing, Scientific Content und Finance
11/2011-11/2013	Doktorandensprecherin der Graduate School HELENA, München
12/2006-12/2008	Fachschaft Pharmazie LMU, München
2002-heute	Kinderbetreuung: Union-Sozial-Werk, Marl/Kinderbibelgarten St. Ursula, München

Stipendien/Auszeichnungen

12/2013-heute	Roche Stipendium für Naturwissenschaftler
05/2013	Auszeichnung für die beste Posterpräsentation der DGSV Tagung Berlin

05/2013-heute	Stipendiatin bei e-fellows
02/2008-heute	Stipendiatin der Konrad-Adenauer-Stiftung (Studien- und Promotionsförderung)

Interessen

| Bergsport in Verbindung mit Reisen ins Ausland, Fitnessstraining, abstrakte Malerei

München, 7. Mai 2015

Christina Dargatzis